

This is to certify that the

dissertation entitled

INCIDENT DETECTION ALGORITHM DEVELOPMENT ON SIGNALIZED  
URBAN ARTERIAL STREETS

presented by

Jung-Taek Lee

has been accepted towards fulfillment  
of the requirements for

Ph.D. degree in Civil Engineering

*William C. Taylor*  
Major professor

Date 4/3/97

PLACE IN RETURN BOX to remove this checkout from your record.  
TO AVOID FINES return on or before date due.

DATE DUE	DATE DUE	DATE DUE
APR 11 2000	_____	_____
APR 25 2000	_____	_____
_____	_____	_____
_____	_____	_____
_____	_____	_____
_____	_____	_____
_____	_____	_____

**INCIDENT DETECTION ALGORITHM DEVELOPMENT  
ON SIGNALIZED URBAN ARTERIAL STREETS**

By

Jung-Taek Lee

**A DISSERTATION**

Submitted to  
Michigan State University  
in partial fulfillment of the requirements  
for the degree of

**DOCTOR OF PHILOSOPHY**

Department of Civil and Environmental Engineering

1997

## **ABSTRACT**

### **INCIDENT DETECTION ALGORITHM DEVELOPMENT ON SIGNALIZED URBAN ARTERIAL STREETS**

By

Jung-Taek Lee

Congestion due to incidents on urban freeways and arterial streets is an important issue in urban mobility. It is also an area with potential for successful implementation of ITS (Intelligent Transportation Systems) technology. For many years, traffic engineers have studied techniques to detect an incident on urban freeways. However, since the traffic flow pattern on arterial streets is more dynamic than on freeways, algorithms to detect incidents on arterials have been more difficult to define.

Existing freeway and signalized arterial street incident detection algorithms have been investigated to determine the merits of each in their potential use on urban arterial streets. Based on the literature review, a Kalman Filtering Predictor Algorithm was modified and used to recursively filter and update aggregate traffic control variables and to eventually determine an incident state.

A test using non-incident arterial street data showed good tracking ability of selected traffic variables over time. A second test, using data from an incident on an arterial street, confirmed that the algorithm developed in this study has good potential for arterial street incident detection.

A simulation using TRAF-NETSIM was then conducted to test the algorithm for incident-free and various incident states. The algorithm performance measures were a false alarm rate (FAR) of 0.319 percent per hour per station, a detection rate (DR) of 100 percent with a mean detection time (MDT) of 4.93 minutes for one-lane blockages. For the high traffic volume direction, the FAR was reduced to 0.111 percent per hour per station. The MDT varied from 4.8 minutes for long links to 2.7 minutes for short links.

A discussion of the algorithm and recommendations for further research to improve incident detection on urban arterial streets is also included in this report.

## ACKNOWLEDGMENTS

I would like to express my sincere appreciation to my advisor, Dr. William C. Taylor, for his continuous advice, guidance and support. He is not only a teacher who helped me realize what “engineering” is but also an example of my life.

I want to thank my guidance committee: Dr. Thomas Maleck, Dr. Thomas Wolff and Dr. Martin Fox for their invaluable advice and suggestions that helped me complete this work. I would like to express my special gratitude to Dr. Thomas Maleck. This work would not be possible without his continuous support.

I would like to show my gratitude to my parents for their concerns and continuous support. Their support was a great help through my school years. My thanks to my brothers and sisters who encouraged and supported me to reach my goals. My mother-in-law and brothers-in-law are ones that I can not thank enough for their support.

My wife, Jeongrim, and my daughter, Jean, are a reason for me to have been able to finish this work. It was great luck for me to meet and have Jeongrim in my life.

My thanks also go to my colleagues at Michigan State University who helped and continuously supported me in my school years although I can not refer to them all here.

## TABLE OF CONTENTS

<b>LIST OF TABLES</b> .....	viii
<b>LIST OF FIGURES</b> .....	x
<b>CHAPTER 1 INTRODUCTION</b> .....	1
1.1 Statement of the Problem.....	1
1.2 Characteristics of an Incident.....	3
1.2.1 Definition of an Incident.....	3
1.2.2 Impact of Incident.....	4
1.2.3 Traffic Variable Changes During a Freeway Incident.....	5
1.3 Objective and Scope of the Research.....	8
1.4 Research Methodology.....	8
<b>CHAPTER 2 EXISTING INCIDENT DETECTION ALGORITHM REVIEW</b> .....	10
2.1 Existing Freeway Incident Detection Algorithms.....	10
2.1.1 Comparative Algorithms (Pattern Recognition Algorithms).....	12
2.1.2 Statistical Algorithms.....	14
2.1.3 Dynamic Model-Based Technique Algorithm.....	22
2.1.4 High Occupancy (HIOCC) Algorithm.....	23
2.1.5 McMaster Algorithm (Catastrophe Theory Algorithm).....	24
2.1.6 Advanced Technology-Based Algorithms.....	25
2.1.7 Video Image Processing Technique-Based Algorithms.....	26
2.1.8 VRC Sensor-Based Incident Detection Algorithm.....	28
2.2 Existing Urban Arterial Street Incident Detection Algorithms.....	29
2.2.1 Automatic Incident Detection (AID) within Urban Traffic Control System.....	29
2.2.2 A Dynamic Real-Time Incident Detection System for Urban Arterial System.....	30
2.2.3 Neural Networks for Real-Time Data Fusion Method.....	32
2.2.4 Video Image Processing Technique-Based Algorithm.....	33
2.2.5 Intersection Accident Detection Algorithm.....	34
2.2.6 Smart Corridor Arterial Incident Detection System.....	35
2.3 Summary of Existing Freeway and Urban Arterial Street Incident Detection Algorithms.....	36

<b>Chapter 3 INCIDENT DETECTION ALGORITHM DEVELOPMENT .....</b>	<b>40</b>
3.1 Kalman Filtering Theoretical Background.....	40
3.1.1 Optimal Estimate and Orthogonal Projection .....	40
3.1.2 Linear Optimal Filters .....	42
3.1.3 Kalman Filtering Algorithm.....	44
3.2 Incident Detection Algorithm Development using the Kalman Filtering.....	46
3.2.1 Considerations for Signalized Arterial Street Incident Detection.....	47
3.2.2 Linear State-Space Model .....	48
3.2.3 A Recursive Incident Detection Algorithm.....	50
3.2.4 Incident State Determination .....	51
<b>Chapter 4 INCIDENT DETECTION ALGORITHM TESTS ON ARTERIAL STREET FIELD DATA .....</b>	<b>54</b>
4.1 Application to Incident-Free Field Data .....	55
4.1.1 Linear State-Space Model for the Data.....	55
4.1.2 Linear Measurement Model for the Data .....	56
4.1.3 Initialization .....	58
4.1.4 Results of Incident-Free Field Data Application .....	59
4.2 Application to Incident Data Set.....	68
<b>Chapter 5 TRAF-NETSIM SIMULATION TEST.....</b>	<b>74</b>
5.1 Simulation Test for the Algorithm.....	74
5.2 Description of the Arterial Street Network .....	74
5.3 Measures of Effectiveness .....	75
5.4 Incident-Free Data Set Description.....	77
5.5 Incident Data Set Description .....	78
5.5.1 Link Selection for Incident Generation.....	78
5.5.2 Incident Generation in TRAF-NETSIM .....	84
5.5.3 Various Incident Generation .....	85
5.6 Results of the Incident-Free Test .....	90
5.7 Results of the Incident Test.....	95
5.7.1 Results of One-Lane Blockage in Link 34.....	95
5.7.2 Results of Full-Link Blockage in Link 34.....	96
5.7.3 Results of One-Lane Blockage in Link 45 .....	97
5.7.4 Results of Full-Link Blockage in Link 45.....	97
5.8 A Sensitivity Test for Various Confidence Limits.....	97
5.8.1 False Alarm Changes over Different Limits .....	98
5.8.2 Detection Rate and Mean Detection Time Changes over Different Limits .....	99
5.8.3 A Detailed Sensitivity Test for Link 34 .....	102
5.8.4 Determination of Recommended Limits.....	115
5.9 Parameter Estimation for Different Conditions .....	119

5.10 Summary of TRAF-NETSIM Simulation Results .....	125
5.10.1 A Test at 95 Confidence Limits (2.0 $\sigma$ Limit).....	125
5.10.2 A Sensitivity Test for Various Confidence Limits.....	126
5.10.3 Parameter Estimation for Different Conditions .....	127
<b>Chapter 6 CONCLUSIONS AND DISCUSSION</b> .....	<b>128</b>
6.1 Conclusions.....	128
6.1.1 Summary of the Research .....	128
6.1.2 Comparisons with Previous Studies .....	132
6.1.3 Conclusions of the Research.....	135
6.2 Discussion of the Research and Further Research .....	135
<b>APPENDICES</b>	
APPENDIX A. DESCRIPTIONS OF TRAFFIC VOLUME FOR EACH NODE IN THE NETWORK.....	139
APPENDIX B. DESCRIPTION OF GEOMETRIC CONFIGURATIONS FOR NETWORK LINKS.....	140
APPENDIX C. DESCRIPTION OF SURFACE STREET TURNING MOVEMENTS .....	141
APPENDIX D. DESCRIPTION OF PRETIMED SIGNAL INTERVAL FOR EACH NODE .....	143
<b>LIST OF REFERENCES</b> .....	<b>144</b>

## LIST OF TABLES

Table 4.1 MSEs for Flow and Speed in Lane 1 and Lane 2.....	59
Table 5.1 LOS in Node 3, 4, and 5 .....	79
Table 5.2 Incidents in Link 34 Description.....	87
Table 5.3 Incidents in Link 45 Description.....	89
Table 5.4 Results of Incident Free Test for 95 Percent Confidence Limits .....	91
Table 5.5 Distribution of False Alarms over Detector Stations .....	92
Table 5.6 One-Hour Traffic Statistics at Detector Station 20.....	93
Table 5.7 One-Hour Traffic Statistics at Detector Station 5.....	94
Table 5.8 False Alarm Statistics Changes for 2.0, 2.5, and 3.0 $\sigma_{\hat{x}_k}$ .....	98
Table 5.9 Detection Rates of One-Lane Blockage over 2.0, 2.5, and 3.0 $\sigma_{\hat{x}_k}$ Changes (percent) .....	100
Table 5.10 Detection Rates of Full-Link Blockage over 2.0, 2.5, and 3.0 $\sigma_{\hat{x}_k}$ Changes (percent) .....	100
Table 5.11 Mean Detection Time of One-Lane Blockage over 2.0, 2.5, and 3.0 $\sigma_{\hat{x}_k}$ Changes (minutes) .....	101
Table 5.12 Mean Detection Time of Full-Link Blockage over 2.0, 2.5, and 3.0 $\sigma_{\hat{x}_k}$ Changes (minutes) .....	101
Table 5.13 False Alarm Changes over Different Intervals.....	105
Table 5.14 Detection Rate Changes for One-Lane Blockage in Link 34 over Different Intervals (percent) .....	106
Table 5.15 Mean Detection Time Changes for One-Lane Blockage in Link 34 over Different Intervals (minutes).....	106

Table 5.16 Detection Rate Changes for Full-Link Blockage in Link 34 over Different Intervals (percent) .....	107
Table 5.17 Mean Detection Time Change for Full-Link Blockage in Link 34 over Different Intervals (minutes).....	107
Table 5.18 Slope Changes of False Alarms over Different Intervals.....	117
Table 5.19 Slope Changes of DR and MDT for One-Lane Blockages over Different Intervals (Both Stations) .....	117
Table 5.20 Slope Changes of DR and MDT for Full-Link Blockages over Different Intervals (Both Stations) .....	118
Table 5.21 Results of Incident Detection Performance at Recommended Intervals.....	118
Table 5.22 Characteristics of Selected Links .....	119
Table A Description of Traffic Volume for Each Node in the Network .....	139
Table B Description of Geometric Configurations for Network Links .....	140
Table C Description of Surface Street Turning Movements.....	141
Table D Description of Pretimed Signal Interval for Each Node .....	143

Fi

Fi

Fi

Pr

Fi

Fi

C

Fi

L

Fi

## LIST OF FIGURES

Figure 1.1 Freeway Traffic Flow Changes due to an Incident .....	7
Figure 3.1 Recursive Kalman Filtering Steps .....	46
Figure 3.2 Incident Detection Algorithm using the Kalman Filtering Recursive Procedure .....	53
Figure 4.1 Data Fitting for True and Observed Flow and Speed .....	61
Figure 4.2 Predicted and Filtered Estimates of Flow and Speed in Lane 1, and 2 and 95 Confidence Intervals .....	62
Figure 4.3 Scatter Plots of Residuals for Traffic Flow and Average Speed in Lane 1 and Lane 2.....	64
Figure 4.4 $\Phi(i, i)$ Changes over Time .....	66
Figure 4.5 $Q(i, i)$ Changes over Time .....	67
Figure 4.6 A Priori Error Covariance Changes over Time .....	67
Figure 4.7 Incident Detection Procedure on Field Data.....	70
Figure 5.1 Simulation Network.....	80
Figure 5.2 Node 3 Geometric and Hourly Traffic Volume.....	81
Figure 5.3 Node 4 Geometric and Hourly Traffic Volume.....	82
Figure 5.4 Node 5 Geometric and Hourly Traffic Volume.....	83
Figure 5.5 Number of False Alarms for the Network over $\sigma_{\hat{x}_k}$ Changes.....	108
Figure 5.6 Number of False Alarms per Station for the Network over $\sigma_{\hat{x}_k}$ Changes.....	108
Figure 5.7 False Alarm Rate per Station for the Network over $\sigma_{\hat{x}_k}$ Changes .....	109

Figure 5.8 Number of False Alarms for High Traffic Direction over $\sigma_{\hat{x}_k}$ Changes.....	109
Figure 5.9 Number of False Alarms per Station for High Traffic Direction over $\sigma_{\hat{x}_k}$ Changes.....	110
Figure 5.10 Number of False Alarms per Station for High Traffic Direction over $\sigma_{\hat{x}_k}$ Changes.....	110
Figure 5.11 Detection Rate Changes for One-Lane Blockage in Link 34 over Interval Changes.....	111
Figure 5.12 Mean Detection Time (minutes) for One-Lane Blockage in Link 34 with Bars of One Standard Deviation (Upstream Station) .....	111
Figure 5.13 Mean Detection Time (minutes) for One-Lane Blockage in Link 34 with Bars of One Standard Deviation (Downstream Station) .....	112
Figure 5.14 Mean Detection Time (minutes) for One-Lane Blockage in Link 34 with Bars of One Standard Deviation (Both Upstream and Downstream Stations).....	112
Figure 5.15 Detection Rate Changes for Full-Link Blockage in Link 34 over Interval Changes.....	113
Figure 5.16 Mean Detection Time (minutes) for Full-Link Blockage in Link 34 with Bars of One Standard Deviation (Upstream Station) .....	113
Figure 5.17 Mean Detection Time (minutes) for Full-Link Blockage in Link 34 with Bars of One Standard Deviation (Downstream Station) .....	114
Figure 5.18 Mean Detection Time (minutes) for Full-Link Blockage in Link 34 with Bars of One Standard Deviation (Both Stations) .....	114
Figure 5.19 Parameter ( $\Phi$ ) Patterns in Different Geometric and Traffic Conditions .....	121

## **Chapter 1**

### **INTRODUCTION**

#### **1.1 Statement of the Problem**

The congestion on urban freeways and arterial streets is an important issue in urban mobility. It is also an area with potential for successful implementation of ITS (Intelligent Transportation Systems). A large component of ITS is directed toward congestion detection and management.

The traditional way to resolve the congestion problem is through new road construction and road-widening programs. In Oakland County, Michigan, for instance, over one billion dollars was identified for road construction needs during the next decade. Almost seventy percent of that investment was for improving mobility in congested areas (Barbaresso 1993). However, this type of solution is very expensive and can not always resolve the problem.

For many years, traffic engineers have studied techniques to reduce the impact of incidents on urban freeways. They have also developed automatic incident detection algorithms and responsive control systems. However, they were all developed for freeways. The traffic flow pattern in urban arterial streets is different from that of freeways.

The geometric and functional aspects of arterial streets are quite different from freeways. From an incident detection perspective, the traffic flow pattern on arterial streets makes it difficult to implement an incident detection program. While the traffic flow on freeways is continuous and uninterrupted, the traffic flow on arterial streets is often interrupted due to various external sources such as side street traffic, slow moving vehicles, on-street parking, etc. Above all, turning vehicles prevent the direct comparison of the upstream and the downstream condition, which is a commonly used incident detection method on freeways. A signal system also prevents the construction of a short-time data aggregating time interval because of stop-and-go patterns in a signal cycle.

A few recent studies have attempted to develop an incident detection algorithm for urban arterial streets. These efforts are, however, still in the conceptual stage. Most of the algorithms have not yet been applied to real field operations.

Some of these studies approach the problem similar to the way it is done in freeway incident detection applications. They detect abrupt changes in traffic features to identify an incident.

The other approach to incident detection on an arterial street is through using new technologies. However, not all the existing arterial streets are equipped with probe vehicles and video cameras required to obtain the necessary information.

There are aspects of freeway models and methodologies that may be applicable to detecting incidents on arterial streets. In this study, existing freeway and arterial street incident detection algorithms are reviewed to establish the usefulness of freeway based algorithm aspects for arterial streets.

A real-time adaptive linear Kalman filtering approach was selected for this study because it is simple, and operates in real-time to reflect dynamic arterial street traffic flow. The use of flexible thresholds by using prediction intervals constructed by a priori error covariance and the use of raw data from a single detector station are also advantages of this approach.

Field collected arterial data and simulated data are used to validate the algorithm. TRAF-NETSIM simulation is used to generate incident data sets due to the absence of sufficient arterial incident data.

## **1.2 Characteristics of an Incident**

In this section, characteristics of an incident are investigated. A definition of an incident is postulated. Impacts on roadways are investigated and traffic variable changes resulting from an incident are investigated since they are primary clues to the presence of an incident.

### **1.2.1 Definition of an Incident**

An incident is a relative term since some may consider a specific event an incident, and some may not. There is also no absolute quantitative definition of an incident in terms of incident duration and roadway capacity reduction. Traditionally an incident is defined as “*an accident, breakdown, spilled load or other random event that reduces the capacity of the roadway* (Judycki, and Robinson 1991: 359).” Other definitions are “*any occurrence that affects roadway capacity, either by obstructing travel lanes or by causing gawkers block* (Giuliano 1989: 387)” and “*a spill, breakdown, accident, or any other extraordinary event that causes congestion and delay by restricting normal traffic flow* (Urbanek, and

Rogers 1978: 1).” A red signal light and a slow truck in a no passing zone were also defined as “simple incidents” (Wirasinghe 1978). As can be understood by these definitions, an incident can be any event on a highway that negatively affects the traffic flow. However, it is worthy to note what “event” should be considered as an incident. As Han (1995) argued, an incident should be detectable and worth detecting. This is true especially in arterial street conditions since there are many “incident-like” events. On-street parking vehicles and slow buses could obstruct traffic flow but they are not incidents. A temporary stop to load or unload a passenger may block traffic flow but it would not be long enough to affect traffic flow significantly. A signalized intersection interrupts traffic flow regularly but is not an incident. Therefore, it is advantageous to define an incident as any event on a highway that lasts long enough to reduce roadway capacity over an extended time period.

### **1.2.2 Impacts of Incidents**

The impact of an incident can be viewed in various perspectives: the traffic operation perspective, the economic perspective, and the safety perspective.

In operations, the capacity reduction is more than the physical reduction in the available lanes. For instance, in a three lane section, an accident in one lane reduces physical capacity by 33 percent, but operational capacity is reduced by 47 to 48 percent or 50 percent. The two lane-blocking accident in the three lane section reduces 79 percent of operational capacity. In a two lane section, one lane blocking resulted in operational capacity reductions of 60 percent to 79 percent while the physical reduction was 50 percent (Goolsby 1971).

In economic terms, a recent FHWA study shows that incidents account for 60 percent of all freeway congestion in the 37 largest urban areas. Accordingly, user costs exceed five

billion dollars a year in delay and wasted fuel, based on 1984 data. The FHWA study also shows that 70 percent of urban freeway congestion is accounted for by incidents, and will cost users in excess of 35 billion dollars a year by the year 2005 in the absence of significant improvements (Judycki, and Robinson 1991).

From the perspective of safety, pedestrian accidents and accidents involving striking a parked vehicle resulted in 19 to 20 percent of all interstate system fatalities, almost 800 fatalities each year, during the years 1983-1985 (Judycki, and Robinson 1991). Other studies indicated that 13 percent of accidents (106 out of 812 accidents) were secondary accidents (Lari, Christianson and Porter 1982).

### **1.2.3 Traffic Variable Changes During a Freeway Incident**

Traffic flow associated with an incident can be quantitatively expressed by traffic features. These traffic features are used as control variables in automatic incident detection algorithms and the abrupt change in these variables are used to activate these algorithms. These features are usually traffic volume (flow), occupancy, density, speed, and travel time. During a freeway incident, the traffic flow features can be categorized in four regions as shown in Figure 1.1 (Hughes Aircraft and JHK & Associates 1992).

**Flow region A** is far upstream from the incident where traffic moves at normal speeds with normal density.

**Flow region B** is the area located immediately behind the incident where vehicles are queuing. In this region, low speed occurs and higher density is experienced.

**Flow region C** is the region immediately downstream of the incident, where traffic is flowing at a metered rate due to the restricted capacity caused by the incident. The density of region C is lower than the normal density and the speed may be slightly greater. However, the speed of the downstream immediately behind the incident is not necessarily higher since drivers slow down to look at the incident in some cases.

**Flow region D** is far downstream from the incident where traffic is not disturbed any more by the incident. Like region A, traffic in region D is flowing at normal density and speed.

Although not shown in Figure 1.1, occupancy is the traffic flow variable used in most incident detection algorithms rather than density. Occupancy is defined as the percentage of time a detector is occupied by a vehicle (or vehicles) during the reporting interval. Since occupancy is raw data and most properly corresponds to the point measures of speed and volume that are available, the use of this variable is beneficial. The use of density requires the measurement over a section of a roadway in order to calculate the number of vehicles per mile, and the converting of measured occupancy to density results in an unnecessary degree of uncertainty. In addition, associated with speed, travel time can be used as the indication of the onset of congestion as it is inversely related with the speed.

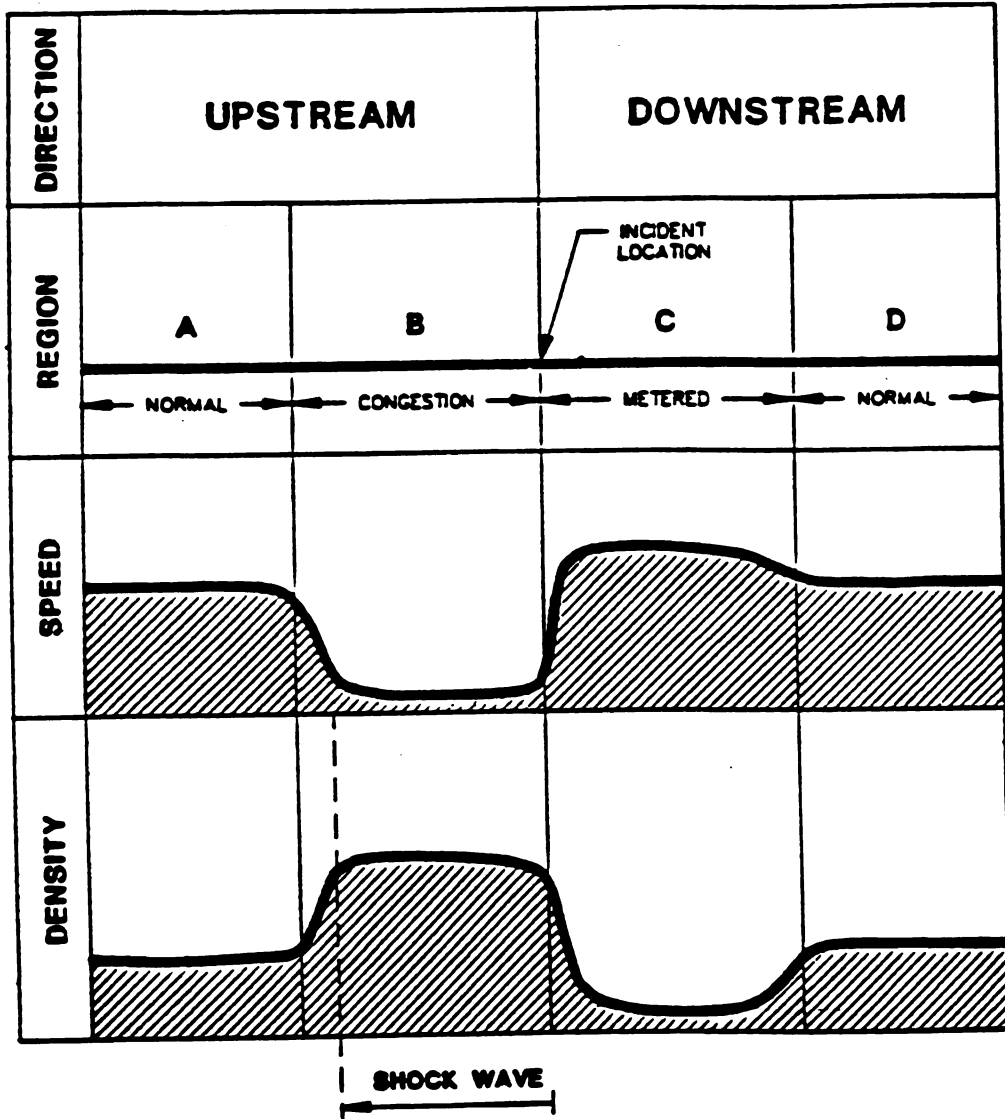


**Figure 1.1 Freeway Traffic Flow Changes due to an Incident**

### **1.3 Objective and Scope of the Research**

The objective of this research is to develop an incident detection algorithm for urban arterial streets and test it with field data and simulated data. The scope of the research includes:

- Reviews of existing freeway and arterial street incident detection algorithms to determine advantages and disadvantages for this research;
- Development of an incident detection algorithm based on the reviews and arterial street characteristics;
- Tests of the algorithm with field collected incident-free and incident data to show the potential as an incident detection algorithm;
- Tests of the algorithm with TRAF-NETSIM simulated data on an existing network to determine the performance of the algorithm;
- A search for best criteria in terms of evaluation metrics (the false alarm rate, the detection rate, and the mean detection time); and
- Tests for parameter changes for different geometric and traffic condition.

### **1.4 Research Methodology**

The development of an incident detection algorithm for arterial streets was based on the freeway and arterial street incident literature reviews. The original Kalman filtering algorithm was modified and programmed in FORTRAN 77.

The evaluation of the incident detection algorithm was conducted with field collected data and TRAF-NETSIM simulated data.

Incidents were identified by using flexible prediction intervals (limits) of a priori covariance estimates of the traffic control variables. If the filtered estimates were out of intervals, then an incident is alarmed.

Field collected data included incident-free data and incident data. Field incident data were collected by installing experimental detectors on arterial streets. Incident-free data were used to validate the algorithm and test for false alarms. A representative set of incident data used to show how the algorithm determines an incident.

The TRAF-NETSIM model was selected for generating incident data. The simulation program reflects the surface street traffic and drivers characteristics realistically. Simulated data were generated based on the geometric and traffic conditions of an existing arterial street, Washtenaw Avenue in Ann Arbor, Michigan.

Three metrics were used to evaluate the algorithm performance. They are the false alarm rate, the detection rate, and the mean detection time. Incident-free data were used to check the false alarm rate.

Two typical links were selected, representing large and small signal spacing, to generate various types of incidents. The incident data were then tested for the detection rate and the mean detection time.

By using different prediction intervals, an best incident detection criterion was found. The inverse relationship between false alarm rate and detection rate are considered in reaching an best point for these two metrics. Additionally, the mean detection time was also considered.

## **Chapter 2**

### **EXISTING INCIDENT DETECTION ALGORITHM REVIEW**

Since the Emergency Traffic Patrol (the "Minutemen") was established in 1961 in Chicago (the first efforts to deal with incident problems), various incident management systems and automated incident detection systems have been proposed and implemented (Dudek and Ullman 1992; Roper 1990). Popular methods of detecting incidents vary from observations and reporting by motorists or the police to closed-circuit television and cellular phone hotlines. These methods are based on direct observations. The alternative is to use indirect methods. This type of detection is usually accomplished by using sensors (e.g., loop detectors) placed along the roadway to obtain and process traffic flow data. This section will describe the current freeway and arterial street incident detection algorithms, and their performance characteristics.

#### **2.1 Existing Freeway Incident Detection Algorithms**

Current freeway incident detection algorithms have been placed in categories based on their theoretical aspects and operating characteristics (Balke 1993; Chen, and Chang 1992; Hughes Aircraft, and JHK & Associates 1992; Stephanedes, Chassiakos, and Michalopoulos 1992). They can be classified as follows.

**1. Comparative Algorithms (Pattern Recognition Algorithms)**

- California Algorithm
- Stream Discontinuity Model Algorithm
- Pattern Recognition (PATREG) Algorithm
- All Purpose Incident Detection (APID) Algorithm

**2. Statistical Approach Algorithms**

- Standard Normal Deviate (SND) Model
- Bayesian Approach Algorithm
- Exponential Smoothing Algorithm
- Dynamic Model Algorithm (Sakasita et al. 1975)
- Box-Jenkins Technique-Based Algorithm
- Filtering Technique-Based Algorithm
- Kalman Predictor Algorithm

**3. Dynamic Model-Based Algorithm (Willsky 1980)****4. HIOCC Algorithm (TRRL Algorithm)****5. McMaster Algorithm (Catastrophe Theory Algorithm)****6. Advanced Technology-Based Algorithms****7. Video Image Processing Technique-Based Algorithm****8. VRC Sensor Incident Detection Algorithm**

- Headway Algorithm
- Lane Switch Algorithm
- Lane-Monitoring Algorithm

### **2.1.1 Comparative Algorithms (Pattern Recognition Algorithms)**

The comparative algorithms or the pattern recognition algorithms are based on the assumption that there is some recognizable continuity in the traffic pattern at two consecutive sites under steady incident-free conditions. These algorithms detect an inconsistency in a selective traffic flow variable between adjacent detectors to activate the incident warning message.

The basic approach of the California algorithm to detect incident is by comparing the traffic flow data at one detector station and the data from an adjacent downstream station. The threshold values are pre-determined by a trial-and-error process. This algorithm is executed for each adjacent pair of sensor stations at regular intervals (e.g., 20 seconds, 30 seconds, or 1 minute). The generalized form of the algorithm is a binary decision tree, which includes a tree-like arrangement of binary decisions. Traffic features commonly used for the California algorithms are temporal and spatial average occupancy difference and relative average difference (Knobel, and Helfenbein 1976; Levin, and Kraus 1979a,b,c; Masters, Lam, and Wong 1991; Payne, Helfenbein, and Knobel 1976; Payne, and Tigor 1978; Tignor, and Payne 1977). Ten more extended versions of the California algorithm were developed to provide for more accurate incident detection under various traffic conditions. Algorithm 7 is the California Algorithm with a check for persistence. Algorithm 8 is the California Algorithm with a check for a compression wave and persistence, especially for “stop and go” traffic (Payne, Helfenbein, and Knobel 1976). Since the effectiveness of these types of algorithms is dependent on the thresholds chosen, a program, called CALB, was developed, which uses a random number generator that produces increments to be added to the current threshold vector to produce a new

threshold vector for evaluation (Knobel, and Helfenbein 1976; Leven, and Krause 1979a). Also, an optimal threshold calibration tool, called DAISI (Detection Automatique d'Incidents par Seuillage Iteratif - Automatic Incident Detection by Iterative Thresholding), for automatic incident detection algorithms including the California algorithm was developed. This tool uses usual performance criteria such as the false alarm rate and the detection rate. The optimization of a threshold is achieved by minimizing the false alarm rate, subject to a detection rate or by maximizing the detection rate, subject to a false alarm rate (Cohen 1994; Cohen, and Ketselidou *Unknown Date*).

In the Stream Discontinuity Model Algorithm, it is assumed that the occurrence of an incident creates a large difference in traffic measurements at an upstream and downstream detector. Occupancies at the upstream and downstream detectors are obtained and two parameters are determined, (1) the temporal difference of upstream and downstream occupancy by time interval  $t$ , and (2) the temporal ratio of downstream occupancy and upstream occupancy by time interval  $t$ . These two parameters are compared with pre-determined thresholds. The time interval  $t$  is estimated from downstream information such as detector spacing, the length of vehicle and detector, and number of vehicles counted at the downstream detector (Sakasita et al. 1975).

As an algorithm to test the feasibility of estimating the average journey time between measuring sites, the Pattern Recognition (PATREG) algorithm was also considered as an incident detection algorithm (Collins 1977; Collins, Hopkins, and Martin 1979). The incident is detected when a significant change in the speed (calculated at every 40 seconds by using a cross-correlation procedure) occurs and exceeds pre-determined lower and upper thresholds for a pre-set number of consecutive seconds.

The All Purpose Incident Detection (APID) algorithm is based on the California algorithm but is characterized by handling different traffic patterns (e.g., light/medium traffic conditions need a particular algorithm suited for these conditions). A compression wave test and persistent test are added to reduce false alarm rate in this algorithm as well (Lam and Tritter 1994; Masters, Lam, and Wong 1991).

The advantage of the comparative algorithm is a simple process to detect an incident. Complicated calibration is not required to interpret the data from detectors. Rather, raw data (occupancy) is used to identify an abrupt change in traffic flow between adjacent detectors. However, the simplicity does not explain dynamic traffic patterns between adjacent detector stations so the probability of false alarms is high. This could be a fatal flow on urban arterial streets because the traffic patterns in these roadways are more complex between detector stations. The use of threshold values between adjacent detectors is not flexible either. Since these values are obtained by historical observed data on particular conditions, they need to be re-calibrated under different conditions. The comparative algorithms is not an adequate strategy to be used on arterial streets.

### **2.1.2 Statistical Algorithms**

Statistical algorithms include the Standard Normal Deviate (SND) Model, the Bayesian Approach, the Exponential Smoothing Algorithm, the Dynamic Model Algorithm (Sakasita et al. 1975), the Box-Jenkins Technique Algorithm, the Filtering Technique Algorithm, and the Kalman Predictor Algorithm.

The Standard Normal Deviate (SND) Model algorithm was developed to circumvent the weakness of other models, the requirement of each different frequency distribution for

the measured traffic variable for defining threshold values for each different traffic operating conditions and detector stations (Dudek, Messer, and Nuckles 1974). This algorithm considers the rate of change of the control traffic variable (e.g., occupancy and kinetic energy that is computed from volume and speed for 3 and 5 min) rather than an absolute threshold values. The standard normal deviate (SND) reflects the degree to which the control variable has changed in relationship to the average trends measured during previous intervals. That is, a large SND value would reflect a major change in operating conditions on the freeway. This model was also used for a stoppage-wave-detection algorithm previously studied which detects queues or stoppage waves in the freeway to alert on-coming motorists (Dudek and Messer 1973).

The Bayesian Approach Algorithm assumes that the normal traffic flow follows its historical trend (Levin and Krause 1978; Levin and Krause 1979a,d). This algorithm obtains the frequency distribution functions of certain traffic feature ( $Z$ ) during incident ( $U_1$ ) and incident free ( $U_2$ ) situations for a certain geometric and traffic conditions. These traffic features are measured at either the upstream or downstream detector or at both located on one of the freeway lanes. If  $Z$  is greater than a threshold ( $Z_1$ ), a possible incident state is signaled and if  $Z$  is less than  $Z_1$ , and incident-free state is signaled. The probabilities of an incident,  $P(U_1)$ , occurring based on the history of capacity-reducing incidents on that freeway then is used to obtain the probability of incident state,  $P(1)$ , and the probability of an incident-free state,  $P(0)$ . The Bayesian consideration is applied to obtain the probability of having an incident given an incident signal (1) and the probability of incident-free given a non-incident signal (0). The optimal threshold  $Z_1$  is obtained by maximizing the sum of  $P(\text{incident}|1)$  and  $P(\text{no-incident}|0)$ . The signal can be

extended  $n$  successive time intervals to provide more reliable information. These conditional probabilities could be calibrated for any particular freeway section and specific traffic and environmental conditions, utilizing historical incident data.

The Exponential Smoothing Algorithm uses a short-term forecasting technique for detecting irregularities of a traffic variable (Cook and Cleveland 1974; Masters, Lam, and Wong 1991). The variables used are usually volume, occupancy and speed. An incident is signaled if the tracking signal deviates significantly from a pre-defined threshold value (zero). The tracking signal is defined as the algebraic sum to the present minute of all the previous estimate errors divided by the current estimate of the standard deviation. The estimate of the standard deviation is estimated by the mean absolute deviation, which is obtained by single (or double) exponential smoothing method. The output of the algorithm is two incident states: confirmed incident, and incident free.

In the Dynamic Model Algorithm, it is assumed that the arrival pattern of vehicles on a freeway lane remains essentially unchanged under non-incident conditions. A longitudinal pair of upstream and downstream detectors in a freeway lane was considered for input and output traffic information and linearly related in travel time period ( $\tau$ ) between two detectors. Parameters ( $v_i$ ) for this linear model can be summed to the steady-state gain ( $g$ ), which is the ratio of the mean values of traffic information at the upstream and downstream detectors. Under non-incident conditions,  $g$  is assumed to come very close to 1, and  $g$  becomes much smaller than 1 under incident conditions. Then, the incident detection criterion is a small value of the summation of estimated  $v_i$  (i.e.,  $\alpha$ ) and a large value of the temporal ratio of input and output in travel time period (i.e.,  $\beta$ ). Precisely, an incident is determined if an observed  $\alpha$ , and  $\beta$  point is in the critical region

in two dimensional space. This two dimensional region is determined empirically (Sakasita et al. 1975).

Based on past observations of traffic variables (i.e., volume and occupancy), a forecast can be made and compared with the next observation of the traffic variable. The difference of the forecast and the observation signals a possible change in the traffic stream behavior. The Box-Jenkins approach uses this idea to construct a prediction model for traffic variable (Ahmed and Cook 1979; Ahmed and Cook 1980; Ahmed and Cook 1982; Ahmed 1983). There is an assumption in this theory. A non-seasonable time series of freeway traffic observation (e.g., occupancy) taken at equally spaced time intervals is assumed to be stationary or can be reducible to a stationary form. Then, the dynamics of this observations (e.g., occupancy) is represented in the general class of linear models in the form of autoregressive integrated moving-average models of order  $p, d, q$  (i.e.,  $ARIMA(p,d,q)$ ). The ARIMA models are obtained by a three-stage iterative procedure. They are preliminary identification, estimation, and diagnostic check stages. In preliminary identification stage, the values of  $p, d$ , and  $q$  are determined by inspecting the autocorrelations and partial autocorrelations of the series or its differences, or both, and by comparing them with those of some basic stochastic processes. In the estimation stage, the autoregressive and moving average parameters are estimated by using non-linear least squares techniques after the values of  $p, d$ , and  $q$  have been obtained. Finally, in the diagnostic check stage, the goodness of the model fit is checked. If the model is satisfactory, then the resulting residuals should be uncorrelated random deviations.

Once an ARIMA model is obtained, a short-term forecast can be made by an operational expression for updating the forecasts of the model that is expressed in terms

of forecast errors. An incident is detected if the observed value of the control variable lies outside the confidence interval (e.g., 95 percent) for the corresponding point forecast.

In the Filtering Technique-Based Algorithm, a short-term averaging (low-pass filter) is employed to reduce the adverse effects of short-term traffic fluctuations and high-magnitude impulses in volume/occupancy measurement from a loop detector (Chassiakos 1992; Chassiakos and Stephanedes 1993; Stephanedes, and Chassiakos 1993a,b; Stephanedes, Chassiakos, and Michalopoulos 1992). The performance is based on the spatial occupancy difference between adjacent stations. Three smoothing techniques are considered in the detection algorithm: the Moving Average (linear transformation), the Median (non-linear transformation), and the Exponential Smoothing. The Moving Average technique is first formulated and built into the algorithm as the spatial difference of 30 second-occupancy outputs at time  $t$ . Given the hypothesis of an incident occurrence at time  $t$ , this algorithm uses 3-minute averages of the spatial occupancy difference after time  $t$  between adjacent stations to provide an indication of the traffic condition (traffic congestion). Then, the temporal change in the 5-minute average of the spatial occupancy difference past time  $t$  seeks the cause of the traffic congestion (incident or bottleneck). Therefore, the significant difference of 3-minute average of the spatial occupancy difference after time  $t$  and 5-minute average of the spatial occupancy difference past time  $t$  indicates a temporal change to distinguish incident related congestion from recurrent congestion. The transferability across stations and the time of day is achieved by the normalization obtained by the maximum of upstream and downstream station occupancy averaged over the most recent 5-minute period before the incident.

The Predictor Algorithm utilizes well known Kalman Filtering to detect anomalies which may arise from a loop detector system malfunction or traffic incidents. To reflect freeway traffic dynamics, the transition matrix of state equations was developed. Also the number of standard deviations over time from the prediction is used to determine threshold values to be compared with traffic flow observations. An incident is alarmed if the difference of the predicted and the observed parameters is significantly different from the number of standard deviations (Dailey 1993).

This method suggests very good potential for general application to various traffic conditions. Since the model is adaptive, it reflects freeway traffic flow over time. Also, the dynamic thresholds is another good positive feature.

These models contributed to the state-of the art in incident detection on freeways. Some of features of these algorithms are worth of comment.

***SND Model:*** This algorithm takes advantage of the rate of change of the control traffic variable instead of an absolute threshold value (Dudek, Messer, and Nuckles 1974). Also this method is very simple and efficient. However, assigning equal weights to the previous  $n$  sampling period for the mean in SND model will contaminate the most recent information by obscuring unusual outlying observation (Montgomery, Johnson, and Gradiner 1990). The determination of time span for the average value is also important because the sensitivity of the SND model is dependent on that span.

***Bayesian Approach Algorithm:*** The advantage of this algorithm comes from the simplicity based on Bayesian theory. In addition, since an operator is given the likelihood

of an incident, he or she is not in the decision of the limited possibilities (incident or no-incident). However, this algorithm is heavily dependent on historical incident and incident-free data to obtain the control variable's frequency distribution. It is not always easy to obtain such a large data set to calibrate the probability of an incident. These data sets are also heavily dependent on a particular location and time for the threshold. Because of this attribute, this model is not operational in different location and time condition with the once-determined threshold. Also the higher probability of correct detection of an incident requires longer mean time to detect. For example, it took 1 minute for  $P(\text{incident})=0.00305$  and 4 minutes for  $P(\text{incident})=0.81662$  (Levin and Krause 1978; Levin and Krause 1979; Levin and Krause 1979a, d).

***Exponential Smoothing Algorithm:*** This exponential smoothing method is the procedure that adjusts the smoothed statistic by an amount that is proportional to the most recent forecast error. This reflects the most recent data sets unlike the simple moving average. Theoretically, the exponential smoothing application needs to specify a value for the smoothing constant. A widely used technique is to conduct trials of various values on a set of historical data. Therefore, the smoothing constant for a particular data set could not be directly used for other data. Large data are also needed to establish the standard deviation of the tracking signal to determine an incident. The pre-defined threshold value that is based on a particular data sets results in wild fluctuation in the number of false alarms from day to day and from station to station (Masters, Lam, and Wong 1991).

**Dynamic Model Algorithm:** This algorithm includes a noise term in the linear model to account for lane changes and speed changes between adjacent detectors. The upstream and downstream information (occupancy and speed) is correlated, but the determination of an incident is basically static. The terms  $\alpha_0$ , and  $\beta_0$  are obtained empirically and take on different values depending on the type of incident and prevailing conditions. Therefore, the more flexible the algorithm, the more historical incident data required.

**Box-Jenkins Technique-Based Algorithm:** This algorithm is based on the assumption that the ARIMA model fits freeway traffic flow well. Theoretically this time series analysis requires a large historical data set to develop an acceptable ARIMA model (Mongomery, Johnson, and Gardiner 1990). In the ARIMA(0,1,3) model obtained from freeway data, the values of the moving average parameters vary from one detector station to another and over time due to variations in surrounding conditions (Ahmed and Cook 1982). These parameters are not changed automatically and requires manual examinations (Mongomery, Johnson, and Gardiner 1990). This fact will result in less flexibility in operation for different conditions.

**Filtering Technique Algorithm:** The idea of smoothing short-term traffic inhomogeneities is beneficial to get rid of corrupting impulsive noises that may impair detection performance. The consideration of the transferability across the various data sets is good as well. In addition, adoption of functions to identify incident-caused and recurrent traffic congestion based on the effects of an incident is a positive attribute of the algorithm. However, basically the DELOS algorithm uses the filtered spatial occupancy

difference between adjacent detector stations through time, which may not be valid method in areas where the traffic pattern is varying between adjacent detector stations as described in the comparative algorithms. Furthermore, the structure of the algorithm requires time delay (3 minutes) as the smoothing time, which brings slower detection response time in freeway detection algorithms. Although the moving average is simple and effective, it possibly obscures information contents by applying the same weights to averaged data.

### **2.1.3 Dynamic Model-Based Technique Algorithm**

This technique for an incident detection is based on the use of a macroscopic dynamic model describing the evolution of spatial-average traffic variables (velocity, flows, and density) over sections of the freeway (Willsky 1976; Willsky et al. 1980). The authors used the dynamic traffic flow model suggested by Payne for traffic flow and developed incident detection systems using two different hypothesis testing techniques, the Multiple Model (MM) and the Generalized Likelihood Ratio (GLR) algorithms. The dynamic freeway traffic flow is based on the basic aspects of both the fluid flow and car-following models of traffic dynamics that yields a spatial discretized set of coupled highly non-linear equations. Specifically three types of events for each link of the freeway were modeled. They are a capacity-reducing incident, a pulse of traffic that is lasting for a specified duration, and sensor failure. Based on the model, incident detection algorithms, MM (Multiple Model) and GLR (Generalized Likelihood Ratio) techniques, were developed.

That the inter-relation between principal traffic is directly modeled by the algorithms and the parameters are changed over time is a good aspect of the algorithm (Willsky, 1976). This algorithm, however, is among the more complex of the methods, and it has large data requirements, in terms of types of variables (density, space mean speed) and short time-space discretization (Stephanedes, Chassiakos, and Michalopoulos 1992). In addition, as the authors of the algorithms indicated, the use of the nominal-linearized Kalman filter is suspicious for a dynamic system. The literature indicated that such a use naturally introduces bias into the model, and thus limits the performance of the MM method and the GLR method (Willsky 1976; Willsky et al. 1980).

#### **2.1.4 High Occupancy (HIOCC) Algorithm**

The purpose of this algorithm is to detect an incident by looking for the presence of stationary or slow moving vehicles over a detector. This can be achieved by examining the one second instantaneous occupancy values (the occupancy outputs are scanned at 0.1 second intervals for the presence or absence of vehicles) for all detectors and looking for a short sequence (2 or 3 second long) of 100 percent occupancy. Once this occurs, an incident alarm is given. To continue the alarm during an incident, allowance is made for the situation where vehicles may be stopped clear of the detector for a certain time period (i.e., 8 seconds) (Collins 1977; Collins 1983).

The HIOCC algorithm is beneficial in that it does not require the complex calibration because the incident was detected by the occurrence of 100 percent values of instantaneous occupancy. It uses 1-second consecutive occupancy data (scanned in 0.1 second interval) to detect stationary or slowing moving vehicles. This method is simple to

execute and uses the direct observations (occupancy) from the detectors. However, such data (1 sec occupancy data) is not always available all the time with existing surveillance system (Stephanedes, Chassiakos, and Michalopoulos 1992). Especially in urban signalized arterial streets, one second data is meaningless since vehicles would stop over detectors for at least the red phase duration of the signal at intersections.

### **2.1.5 McMaster Algorithm (Catastrophe Theory Algorithm)**

This algorithm is based on the previous works on the freeway flow-density relationships (Hall 1987; Hall, Allen, and Gunter 1986; Hall, Shi, and Atala 1993; Persaud and Hall 1989). The application of catastrophe theory (especially the cusp catastrophe) on the relationships between speed, flow and occupancy is introduced from these works. The fact that the sudden drop in speed is obvious in traffic flow when congestion occurs is the basis for catastrophe theory. This idea led to the McMaster incident detection algorithm. A basic version of this algorithm uses the flow-occupancy data that is separated into four traffic states (the uncongested state and several types of congested states). The cause of congestion or a drop in speed makes the data change from the uncongested state to one of the congested states. If either or both of these continued for P consecutive periods, congestion is declared. In addition, the modified McMaster algorithm provides the capability to discern if the congestion is incident-related or recurrent-related (Gall, and Hall 1989; Persaud, Hall, and Hall 1990).

In this algorithm, the major advantages are the simplicity of design and a potential for improved detection performance (Stephanedes, Chassiakos, and Michalopoulos 1992). However, the use of particular data in defining the boundaries of congestion free and

congestion (incident-caused and recurrent-caused) have limitations in use for particular traffic and surrounding conditions.

### **2.1.6 Advanced Technology-Based Algorithms**

The neural network approach has been studied in combination with other incident algorithms since 1991 (Abdulhai and Ritchie 1995; Chang 1992; Chang and Huarng 1993; Cheu, Ritche, and Recker 1991; Ritchie and Cheu 1993). The basic concept of the neural network is to simulate the knowledge reasoning of the human brain, organizing massive amounts of information, and presenting this information in various forms. Information transmission is achieved by cells called neurons through nerve connection. Connection adjustment results in so called intelligent behavior. In freeway incident detection aspects, neural networks can be trained by the data to recognize volume patterns on freeways and to detect incidents. After being trained, the neural networks can be used to assist controllers in freeway management systems.

The basic idea of fuzzy logic is that it provides formal reasoning schemes that are approximate rather than exact as opposed to crisp logic. In the incident detection aspect, the fuzzy logic approach allows imprecision in data received. Perfect information is very expensive to obtain and not always available. In addition, the data needed for the detection process is usually accompanied with noise, resulting in false alarm problems. The fuzzy approach deals with imperfect data to get approximate results (Chang and Huarng 1993; Tarko, Tsai, and Roupail 1993).

There are some features that should be noted for these methods. The problem in providing all the data for the neural network is that information should include all

operational characteristics such as learning data and possible solutions. If the level of information is insufficient, the training results may not cover all cases (Chang and Huarng 1993). A particular data set for a self-learning mechanism to recognize traffic pattern uses only one data set. For different traffic or geometric conditions, additional data must be input to train the system. Although the PNN was recognized by the authors for transferability and flexibility for different traffic conditions, the longer time in recall without a parallel hardware implementation and the reliance on Euclidean distance between the patterns, which is inaccurate in cases of correlated input variables and input variables with very different variances were suggested as disadvantages (Abdulhai and Ritchie 1995).

Although the Fuzzy approach takes advantage of interpreting uncertain data to approximate results, it has computation problems. Since the fuzzy approach needs to compute for all the nodes to draw conclusions, more computations and comparisons are needed, which would result in detection time delay (Chang and Huarng 1993).

### **2.1.7 Video Image Processing Technique-Base Algorithms**

A computer image processing technique, the IMPACTS, was also developed for automatic incident detection (Hoose 1994; Kelly 1991). The strategy is to mimic the way in which a human observer might describe the pattern of traffic when viewing a CCTV monitor. A state of “cells” are used to identify a scene. A cell represents an area of the roadway within a video image. They are arranged along traffic lanes and are sized so as to convert an area of road approximately 1 lane wide by approximately 1 car length long. Three states are defined for a cell: None, Moving, and Stop. These cells are then grouped

along each traffic lane to form “objects”. These objects correspond to groups of adjacent cells that have a common “state”. Sampling time interval and image processing operations are conducted in 5-second cycles. An incident “alarm level” is generated when two or more stop cells are detected within three cycles and that the alarm level would be turned off when the above condition is not detected.

Another video detector system, AUTOSCOPE was also used in incident detection on freeways. However, this system uses raw data (e.g., speed or occupancy) from AUTOSCOPE detectors instead of using image processing methods. Two incident detection algorithms were developed. First, Speed Profile Incident Evaluation System (SPIES) employs two speed-traps placed in each lane of traffic. Then, volume-smoothed basis at roughly 15 second intervals and also 15-minute time intervals (for historical data) are generated. Incidents are then detected by comparing the difference from the volume smoothed speeds of adjacent detectors and historical data with an incident alarm threshold. The second method is AUTOSCOPE Incident Detection Algorithm (AIDA), combining the strength of McMaster and SPIES, but taking advantage of temporal variations of the traffic parameters in addition to spatial ones. Rapid breakdowns in traffic (e.g., sharp speed-drops or occupancy increases) is compared with speed thresholds for determining the congestion level (Michalopoulos and Jacobson 1992; Michalopoulos et al. 1993).

Fast incident detection is a favorable aspect of the technique. However, misclassification of stationary (a stop cell when there is no stationary traffic in the field of view), camera position problems and fixed threshold problems due to lighting conditions must be overcome (Kelly 1991). Traffic detection itself is also a problem for video

detection. Leading headlight reflections at night on wet pavement and strong shadows were found to cause a false detection of vehicles, which eventually results in false alarm in incident detection (Michalopoulos and Jacobson 1992; Michalopoulos et al. 1993).

### **2.1.8 VRC Sensor-Based Incident Detection Algorithms**

The VRC (Vehicle-to-Road Communication) or the AVI (Automatic Vehicle Identification) consists of a transponder or “tag” on the vehicle and a reader along or over the road and the communications link between the two. VRC readers can obtain at least the individual vehicle identification number from each transponder-equipped vehicle that passes. With this information, the system can obtain the car’s travel time, lane specific and station-specific headways, the volume of tagged vehicles on a section, their lane switching, and etc. Incident detection is implemented using this information. Three algorithms were suggested using the data from new traffic sensor VRC (Parkany, and Bernstein 1993; Parkany, and Bernstein 1995). They are the Headway Algorithm, the Lane Switches Algorithm, and the Lane-Monitoring Algorithm.

In the Headway Algorithm, both temporal and spatial comparisons of travel times and headways are used. A significant temporal difference in travel time from a pre-determined threshold brings up a temporal difference of headways. A signal difference of headways from a pre-determined thresholds then brings up spatial difference of headways. An incident is alarmed if all three conditions were satisfied.

The Lane Switches Algorithm counts the number of vehicles that have switched between readers. If the percentage of vehicles that have switched lanes exceeds a certain threshold, an incident alarm is declared.

In the Lane-Monitoring Algorithm, the lane average number of vehicles for two time intervals in lanes are obtained. If this average value of one of lanes is less than the pre-determined low threshold, then another lane average is compared with pre-determined high threshold. If any of the other volumes exceed the high threshold, then an incident is declared.

Even though, a new technology is used, these three algorithms are classical methods as they approach the problem similarly to the comparative algorithms. They are simple, easy to understand, and show potential for a freeway incident detection. However, even though the data sets that can be obtained from this type of sensors are valuable, they are not available on all freeways. Since this system depends on vehicles which are equipped with the “tag”, if there are not many equipped vehicles, then, there is less chance of success. In addition, the threshold values should be more dynamic than static for the algorithms to be applied under other conditions.

## **2.2 Existing Urban Arterial Street Incident Detection Algorithms**

Recently, the issue of automatic incident detection in signalized arterial streets has attracted traffic engineers. They include new approaches such as neural network and computer image processing as well as conventional ways that have been studied on freeways.

### **2.2.1 Automatic Incident Detection (AID) within Urban Traffic Control System**

As a pilot study, Bell and Thancanamootoo (1988) developed an automatic incident detection (AID) within an urban traffic control system. Basic exponential smoothing was

used for updating a traffic control variable, cyclic occupancy, aggregated in a signal cycle time interval. Occupancy variance was also exponentially smoothed and used to determine an incident if the newly obtained cyclic occupancy was out-of-bounds of a certain confidence limits. If the upper bound is infringed, an incident is suspected, and the lower bound is infringed at the next downstream detector, the incident is confirmed. The smoothing factors for exponential smoothing cyclic occupancy were 0.8 and 0.2. Also 0.9 and 0.1 were used for exponential smoothing occupancy variance parameters. The MONICA (Monitoring Incidents and Congestion Automatically) is the extended version of this work by Bretherton and Bowen (1991). While Bell and Thancanamootoo used information from only two links, which resulted in unacceptable false alarms, MONICA (Monitoring Incidents and Congestion Automatically) used surrounding links as well.

This algorithm uses the simple exponential smoothing method. The use of signal cycle length as data aggregation is also realistic for signal controlled streets. However, the determination of parameters for the exponential smoothing functions varies site by site. Also, the incident confirmation method by checking adjacent detector stations turned out to be impractical because some incidents were not even detected at adjacent detector stations.

### **2.2.2 A Dynamic Real-Time Incident Detection System for Urban Arterial System**

A dynamic real-time incident detection system for urban arterials were proposed recently (Chen, and Chang 1993; Chen 1994). This system consists of three major parts: 1) a dynamic traffic flow prediction model, 2) an incident identification, and 3) an incident monitoring process. Associated with the incident detection scheme, the

occurrence of an incident is alarmed by the discrepancy between the projected and detected traffic conditions. Time evolving traffic conditions are modeled with three traffic variables (flow, occupancy, and speed). This model considers the time-spatial dynamics of traffic information from upstream and downstream detectors. Exogenous effects in urban arterial streets (lane-changes, spilled-back queues, buses, parking vehicles, illegal pedestrians, green time of traffic signal, and uncontrolled access in the middle of a road sections) are involved in the time-space models. The Kalman Filtering technique was used to update model parameters at each time-step in real-time based to execute its self-learning mechanism.

By using Kalman filtering technique, the strength of this algorithm appears in dynamic parameter changes at each time step. The inclusion of various exogenous traffic flow disturbance factors between upstream and downstream detector stations is also another good consideration if the prediction model uses adjacent detector information. However, the use of two detector stations within a link is not realistic. In most streets there is only one detector station placed usually at the downstream end of a link. If the above dynamic prediction model is applied to a one detector station street, more complicated traffic interaction models within an intersection should be included. Also the method of data aggregating time interval is not general if the network has varying cycle time and link length. For example, a link that is 2000 feet long would need data aggregating time interval much greater than 30 seconds (probably 80 seconds if travel time is assumed to increase linearly with the length of a link). Different data aggregating time intervals are required for each different-length link, resulting in loss of generality over the network and longer detection time if the time interval is long.

### **2.2.3 Neural Networks for Real-Time Data Fusion Method**

This method uses information that is provided and preprocessed from three data sources (i.e., fixed detectors, probe vehicles, and anecdotal sources) to determine an incident after integrated in a data fusion process (Ivan et al. 1993; Ivan et al. 1995; Bhandari et al. 1995; Ivan 1996). Fixed detector algorithm preprocesses occupancy and volume data averaged over a fixed time interval (e.g., 5 or 7 minutes). Probe vehicles report link travel times by radio, and anecdotal information provides particular events affecting traffic flow. Fixed detector algorithm compares current and historical volume and occupancy data from fixed detectors at the end of every period. A discriminant score is then computed which determines incident state in the proximity of each detector. The probe vehicle algorithm uses current and historical (non-incident) probe travel time data. Average travel times are computed by aggregating individual probe reports at the end of each period in the first stage. Travel time ratio and speed ratio are computed using the observed travel time on the links and the corresponding historical travel times stored in a database. Incident determination is done by computing the discriminant score. The anecdotal information algorithm utilizes a qualitative description of incidents reported by field observers, both trained and untrained, to detect incidents in real time. These separate algorithm outputs are then combined for a neural network.

As discussed in the freeway section, neural networks require enough information which should include all operational characteristics and possible solutions. Practically it is hard to obtain sufficient valued data sets. Bad data sets such as malfunctioning of fixed detectors also may mislead the model. Especially in arterial streets applications, the data

aggregation time interval should be reconsidered. Aggregation time intervals of 7 minutes (Ivan et al. 1995) may be good to reduce fluctuations of traffic volume but long to detect an incident.

#### **2.2.4 Video Image Processing Technique-Based Algorithm**

Hoose, Vicencio, and Zhang (1992), and Martinez and et al. (1944) suggested video image processing as an incident detection system for urban roads. This method is similar to that used in freeway incident section. Video images of traffic scenes obtained from a video surveillance camera is used to determine an incident. The information by analyzing video images is a periodic description of the pattern of the traffic along the length of road and an intersection under surveillance. Information extraction is made from both urban links and intersections. Information for urban links is obtained in a basis of the traffic lane. Each lane has data set of spatial occupancy, number of objects (groups of adjacent cells that have a common state), and speed and errors in objects. Intersection information provides spatial occupancy, motion occupancy, static occupancy, number of groups (moving or stationary), and associated information in groups (motion and errors.) An incident is detected based on the data presented to it by the computer vision process, combined with external data (e.g., data from existing loop detector). The threshold values to be compared with the time length for vehicles to stop at stop bar for a red phase of a signal was also suggested. Sellam, and Boulmakoul (1994) also presented an automatic incident detection methodology at intersections. The method is based on several technologies such as object-oriented design, real-time knowledge-based systems and a video image processing. To differentiate incident-related stops of vehicles from non-

incident-related stops due to traffic red-light or parking, they characterized pre-defined (associated with area classes) punctual incidents and incidents of a functional type (shortcoming movements, overload of a phase or cycle etc.).

The system is useful for fast detection of incidents (although the qualitative value was not shown) (Martinez et al. 1994). However, high false alarms (24.23 percent on two field tests) is a problem for practical use over a larger network. Further research problems relate to variations in camera position and stability or extremes of weather and lighting condition (Hoose, Vicencio, and Zhang 1992).

### **2.2.5 Intersection Accident Detection Algorithm**

An accident detection method in an intersection is based on observing an intersection under accident and accident-free conditions (Stephanedes, and Vasilakis 1995). It is assumed, under accident-free condition, that traffic volume is evenly distributed across all main moving lanes and the probability that a driver chooses one of  $N$  lanes is normally distributed. Under accident conditions, severe lane change by drivers occurs and shows significant differences in comparison to normal traffic parameters (traffic volume), prior to and after the accident. A lane is defined as blocked if the detector transmits a 100 percent occupancy value at that location. These differences are compared with pre-determined threshold values. Significant deviation from the historical average indicates the occurrence of an accident.

This method uses abrupt change of traffic parameters such as volume and occupancy to detect an accident in an intersection. Basically this is true to some extent for accident cases. However, incidents at mid-block are not clearly supported by this method because

an incident at mid-block (if the link is long) would not affect traffic inter-actions easily at an intersection. Drivers who notice a stalled car in one of lanes would simply change lane for the block and switch again to then original lane, especially if they are turning at the intersection. This method also should consider data sampling collection time-interval and detector locations.

### **2.2.6 Smart Corridor Arterial Incident Detection System**

As a part of the Santa Monica Freeway Smart Corridor Demonstration Project, an automated incident surveillance system was developed (Roseman, and Skehan 1995). The methodology is based on a method of time weighted data analysis. Volume and occupancy data from each system detector are gathered from the real-time traffic control system on a minute-by-minute basis. They are then transmitted to the Smart Corridor system. The detector data is then combined into link data which is smoothed with data from the previous four minutes to obtain a sliding five minute average link value. That is then compared to a matrix which represents the normal, congested and maximum traffic values expected on this particular link. From the comparison, data values within range are given a persistence value. If traffic conditions warrants over time, the persistence value will increase, and ultimately an incident will be identified. Links in the system are assigned to a particular group based on their roadway conditions, which may change by time of day. Within each group, there is a table of threshold values which the system uses to compare current data to determine a persistence value. These threshold tables are selected by time of day, and day of week based on historic traffic flow conditions. The

Smart Corridor system uses a total of 144 persistence matrices (16 groups, each of which contains nine time-of-day threshold tables).

This methodology is simple and flexible to allow non-programmers to change the database for performance adjustments. But this simplicity comes at the expense of manually creating, fine-tuning, and maintaining the large link specific database. A significant effort is required to develop database for a particular location such as assigning detector and link parameters, assigning link group numbers, and developing the threshold values for the persistence matrices (Roseman, and Skehan 1995). The pre-determined threshold values are still static, which does not reflect dynamic traffic flows.

### **2.3 Summary of Existing Freeway and Urban Arterial Street Incident Detection Algorithms**

Existing incident detection algorithms for freeways and signalized arterial streets were reviewed. For freeway incident detection, many studies have been conducted over 20 years. From the conventional California Algorithms to emerging new technology-based algorithms such as neural network and video image processing methods, they have given valuable contributions. It is hard to say which model or algorithm is better than others since their direct comparisons were unavailable for all the different conditions. Each of these algorithms or models has shown superior results for a certain condition. However, by reviewing previous freeway studies, some commonly found issues should be recognized. Chen (1994) also presented these issues in his work. Some of these issues are inter-related.

**Data Dependency:** Usually models or algorithms that use fixed thresholds require comprehensive historical data for a particular condition. The comparative algorithms, some of the statistical approaches such as the Bayesian model, the Exponential Smoothing Algorithms, the Dynamic Model Algorithm, and the Box-Jenkins Technique-Based Algorithms need heavy historical data to obtain fixed thresholds or model constructions. This is also true for the McMaster Algorithm, the Neural Network-Based Algorithms.

**Transferability:** Transferability is inter-related with the data dependence problem. Although many studies showed good performance on a particular condition, they lack general application to other conditions. For example, the California Algorithm Family uses pre-determined thresholds that are obtained by trial and error from a particular traffic condition and geometry. These thresholds are not directly applicable to other conditions. Some of the statistical approaches such as the Bayesian-Based Algorithm, the Dynamic-Model Algorithm (Sakasita et al. 1975), and the Box-Jenkins Technique-Based Algorithm are also limited by heavy data dependence, preventing from being easily transferable to other conditions. This is true for the McMaster Algorithm since it uses the boundaries of flow-occupancy data of a particular geometric and traffic condition to determine an incident. The Neural Network-Based Algorithm needs a comprehensive descent data for training itself. This algorithm is not applicable for other conditions, unless corresponding data was provided. The VRC Sensor-Based algorithm still has this limitation since the incident approach is dependent on pre-determined thresholds.

**Adaptability (Real-Time Operation):** This issue is also inter-related with the transferability problem. Since many algorithms use pre-determined thresholds or models with fixed parameters, they are also limited in transferring to other conditions. Some of models such as the SND model, the Filtering models, and the Dynamic Model-Based Algorithm (Willsky et al. 1980) are prominent in this context. They take advantage of flexible thresholds and parameters to system changes. This adaptability is also an issue with the computing efficiency for the real-time operation of models. For the model to be implemented in real-time, these two factors should be satisfactory. The Kalman Predictor Algorithm and the Dynamic Model-Based Algorithm is superior in adaptability due to the Kalman filtering method. However, the complexity and long computing time of the Dynamic Model-Based Algorithm would not satisfy the real-time operation requirements (Chen 1994).

**Availability:** Newly emerging techniques such as video image processing and VRC sensor-based methods demonstrated the potential in incident detection. However, not all the freeways, streets, and cars are equipped with these systems. Penetration rate of these equipment, especially VRC sensor and “tags”, is an important issue to be studied.

The above issues are also applicable to the existing arterial street incident detection methodologies. Although newly developed methods show potential, these algorithms do not meet all the requirements. The AID study is limited with fixed smoothing parameters in transferability and adaptability. The Dynamic Real-Time Incident Detection System

meets above requirements, but failed in the availability due to existing detector configurations in arterial streets. The neural network for data fusion study also is restricted in the transferability and the adaptability due to heavy data dependence from various sources. The video image processing method is still in the study stage and not available on all the streets. The incident detection in intersections method should be generalized to cover the mid-block incidents. The Smart Corridor study also does not meet the adaptability and the transferability criteria due to heavy geometric and traffic flow data dependence.

## **Chapter 3**

### **INCIDENT DETECTION ALGORITHM DEVELOPMENT**

#### **3.1 Kalman Filtering Theoretical Background**

The Kalman filter was derived as the solution to the Wiener problems (i.e., the prediction of random signal, the separation of random signals from random noise, and the detection of signals of known form in the presence of random noise). In Kalman filtering, Wiener's problem is approached from the point of view of conditional distribution and expectations. It also uses the state-space model for the linear dynamic and random process to control system. It is not always possible or desirable to measure every variable to be controlled, and the Kalman filter provides a means for inferring the missing information from noisy measurements. A brief theoretical background is contained in the following sections (Kalman 1960; Grewal and Andrews 1993).

##### **3.1.1 Optimal Estimate and Orthogonal Projection**

In Kalman filtering, as in Wiener's problem, the estimation (predicted, filtered, and smoothed estimates) problem belongs to the realm of probability theory and statistics. The conditional probability distribution function of random variables, signal, noise and their linear function (random process), represents the basic idea of the estimation. For

example, any statistical estimate,  $X_1(t_1|t)$ ,  $X_1(t_1)$ , or simply  $X_1$ , of the random variable  $x_1(t)$  is some function of the conditional distribution,

$$\Pr[x_1(t_1) \leq \xi_1 | y(t_0) = \eta(t_0), \dots, y(t) = \eta(t)] = F(\xi_1) \quad (3.1)$$

and therefore a (non-random) function of the random variables  $y(t_0), \dots, y(t)$ . This conditional distribution represents the probability of the occurrence of variables values  $\xi_1(t)$  of the random variable  $x_1(t_1)$  given the set of measured values  $\eta(t_0), \dots, \eta(t)$  of the random variable  $y(t)$ .

Since there is, in general, a difference between the estimate  $X_1(t_1|t)$  and (unknown) true value  $x_1(t_1)$ , a *penalty* or *loss* for an incorrect estimate is assigned. The loss should be a positive and nondecreasing function of the *estimation error*  $\varepsilon = x_1(t_1) - X_1(t_1)$ . The loss function is, therefore, defined by

$$\begin{aligned} L(0) &= 0 \\ L(\varepsilon_2) &\geq L(\varepsilon_1) \geq 0 \text{ when } \varepsilon_2 \geq \varepsilon_1 \geq 0 \\ L(\varepsilon) &= L(-\varepsilon) \end{aligned} \quad (3.2)$$

Some common loss functions are  $L(\varepsilon) = a\varepsilon^2$ ,  $a\varepsilon^4$ ,  $a|\varepsilon|$ ,  $a[1 - \exp(-\varepsilon^2)]$ , etc., where  $a$  is a positive constant.

A way to choose  $X_1(t_1)$  may be derived, then, by minimizing risk (average loss)

$$E\{L[x_1(t) - X_1(t_1)]\} = E[E\{L[x(t_1) - X_1(t_1)] | y(t_0), \dots, y(t)\}] \quad (3.3)$$

The theorem (Kalman 1960: 37) shows that assuming that  $L$  satisfies (3.2) loss function type and the conditional distribution function  $F(\xi)$  defined in equation (3.1) is symmetric about the mean  $\bar{\xi}$  and convex for  $\xi \leq \bar{\xi}$ , the optimal estimate of  $x_1(t_1)$  which minimizes the risk is the conditional expectation

$$x_1^*(t_1|t) = E[x_1(t_1)|y(t_0), \dots, y(t)] \quad (3.4)$$

Especially, if  $L(\varepsilon) = \varepsilon^2$ , the assumption that  $F(\xi)$  is symmetry is unnecessary for the optimal estimate. For vector valued random variables, when  $L(\varepsilon) = \|\varepsilon\|^2$ , this theorem is still true.

This optimal estimate can be obtained from the orthogonality theory under a certain condition. If the optimal estimate is restricted to be a linear function of the observed random variables and  $L(\varepsilon) = \varepsilon^2$ , then

$$\begin{aligned} x_1^*(t_1|t) &= \text{optimal estimate of } x(t_1) \text{ given } y(t_0), \dots, y(t) \\ &= \text{orthogonal projection } \bar{x}(t_1|t) \text{ of } x(t_1) \text{ on } Y(t) \end{aligned} \quad (3.5)$$

where  $\bar{x}$  denotes the orthogonal projection of random variable  $x$ , and  $Y(t)$  a vector space (linear manifold) that is formed by  $y(t_0), \dots, y(t)$ .

### 3.1.2 Linear Optimal Filters

A stochastic process (or random process) is the evolution of the state of the system if the possible states of a non-deterministic system at any time can be represented by a random variable. It is supposed that stochastic linear systems associated with the Kalman filter can be represented and estimated by the types of plant (or state) and measurement models. These models can be described as

#### System Dynamic Model (State Space Equation)

$$\mathbf{x}_k = \Phi_{k-1} \mathbf{x}_{k-1} + \mathbf{w}_{k-1}, \quad \mathbf{w}_{k-1} \cong N(0, \mathbf{Q}_{k-1}) \quad (3.6)$$

#### Measurement Model (Observation Equation)

$$\mathbf{z}_k = \mathbf{H}_k \mathbf{x}_k + \mathbf{v}_k, \quad \mathbf{v}_k \cong N(0, \mathbf{R}_k) \quad (3.7)$$

where

$\mathbf{x}_k$  is a  $n \times 1$  state vector

$\mathbf{z}_k = l \times 1$  measurement vector

$\Phi_k = n \times n$  time-varying dynamic coefficient matrix

$\mathbf{H}_k = l \times n$  time-varying measurement sensitivity matrix

$\mathbf{w}_k = n \times 1$  zero-mean uncorrelated Gaussian “state noise” process

$\mathbf{v}_k = l \times 1$  zero-mean uncorrelated Gaussian “measurement noise” process

$\mathbf{Q}_k = n \times n$  time varying matrix

$\mathbf{R}_k = l \times l$  time-varying matrix

These models satisfy the following conditions.

$$\begin{aligned}
 \mathbf{E}(\mathbf{w}_k) &= \mathbf{E}(\mathbf{v}_k) = 0 \\
 \mathbf{E}(\mathbf{w}_k \mathbf{w}_j^T) &= \begin{cases} \mathbf{Q}_k, & k = j \\ 0, & k \neq j \end{cases} \\
 \mathbf{E}(\mathbf{v}_k \mathbf{v}_j^T) &= \begin{cases} \mathbf{R}_k, & k = j \\ 0, & k \neq j \end{cases} \\
 \mathbf{E}(\mathbf{w}_k \mathbf{v}_j^T) &= 0 \\
 \text{and} \\
 \mathbf{E}(\mathbf{x}_k \mathbf{w}_k^T) &= 0
 \end{aligned} \tag{3.8}$$

The state variable represents the variable to be controlled. They can not generally be measured directly, but are inferred from what can be measured. The future state of a dynamic system is uniquely determined by its current state and its future inputs. The dynamic behavior of each state variable of the system must be a known function of the instantaneous values of other state variables and the system inputs for the future state of a system to be determined. The state-space model represents these functional dependencies in terms of first-order differential equations (in continuous time) or difference equations (in discrete time).

In a linear dynamic system we can estimate the state of a linear stochastic system in three ways.

**Predictors** use observations strictly prior to the time that the state of the dynamic system is to be estimated ( $t_{\text{obs.}} < t_{\text{est.}}$ )

**Filters** use observations up to and including the time that the state of the dynamic system is to be estimated ( $t_{\text{obs.}} \leq t_{\text{est.}}$ )

**Smoothers** use observations beyond the time that the state of the dynamic system is to be estimated ( $t_{\text{obs.}} > t_{\text{est.}}$ )

Predicted estimates will be used to predict traffic variables. The predicted estimates are the dynamic changes of filtered estimates.

### 3.1.3 Kalman Filtering Algorithm

Kalman filtering is an algorithm used to estimate the state of a linear or non-linear dynamic system by assuming the state-space model and the measurement model. The typical procedure to estimate the state of a linear system is as follows.

1. Initialize the state and its error covariance, that is

$$\begin{aligned} \mathbf{E}(\mathbf{x}_0) &= \hat{\mathbf{x}}_0 \\ \mathbf{E}(\tilde{\mathbf{x}}_0 \tilde{\mathbf{x}}_0^T) &= \mathbf{P}_0 \end{aligned} \tag{3.9}$$

where  $\tilde{\mathbf{x}}_k = \hat{\mathbf{x}}_k - \mathbf{x}_k$ .

2. Compute  $\mathbf{P}_k(-)$  using  $\mathbf{P}_{k-1}(+)$ ,  $\Phi_{k-1}$ , and  $\mathbf{Q}_{k-1}$ . That is,

$$\mathbf{P}_k(-) = \Phi_{k-1} \mathbf{P}_{k-1}(+) \Phi_{k-1}^T + \mathbf{Q}_{k-1} \tag{3.10}$$

where  $\mathbf{P}_k(-)$  is the a priori covariance (the error covariance matrix before the measurement), which is

$$\begin{aligned}\mathbf{P}_k(-) &= \mathbf{E}[(\mathbf{x}_k - \hat{\mathbf{x}}_k(-))(\mathbf{x}_k - \hat{\mathbf{x}}_k(-))^T] \\ &= \mathbf{E}(\tilde{\mathbf{x}}_k^- \tilde{\mathbf{x}}_k^{-T})\end{aligned}\quad (3.11)$$

where  $\tilde{\mathbf{x}}_k^- = \mathbf{x}_k - \hat{\mathbf{x}}_k(-)$ .

3. Compute  $\bar{\mathbf{K}}_k$  using  $\mathbf{P}_k(-)$  (computed in step 2),  $\mathbf{H}_k$  and  $\mathbf{R}_k$ , that is,

$$\bar{\mathbf{K}}_k = \mathbf{P}_k(-)\mathbf{H}_k^T[\mathbf{H}_k\mathbf{P}_k(-)\mathbf{H}_k^T + \mathbf{R}_k]^{-1}\quad (3.12)$$

where  $\bar{\mathbf{K}}_k$  is the Kalman gain matrix.

4. Compute  $\mathbf{P}_k(+)$  using  $\bar{\mathbf{K}}_k$  (computed in step 3) and  $\mathbf{P}_k(-)$  (from step 2). That is,

$$\mathbf{P}_k(+) = [\mathbf{I} - \bar{\mathbf{K}}_k\mathbf{H}_k]\mathbf{P}_k(-)\quad (3.13)$$

where  $\mathbf{P}_k(+)$  is the a posteriori covariance matrix (the error covariance matrix after update), which is

$$\begin{aligned}\mathbf{P}_k(+) &= \mathbf{E}[(\mathbf{x}_k - \hat{\mathbf{x}}_k(+))(\mathbf{x}_k - \hat{\mathbf{x}}_k(+))^T] \\ &= \mathbf{E}(\tilde{\mathbf{x}}_k^+ \tilde{\mathbf{x}}_k^{+T})\end{aligned}\quad (3.14)$$

where  $\tilde{\mathbf{x}}_k^+ = \mathbf{x}_k - \hat{\mathbf{x}}_k(+)$ .

5. Compute the value of  $\hat{\mathbf{x}}_k(+)$ , a filtered estimate, using the computed values of  $\bar{\mathbf{K}}_k$  (from step 4), and measurement  $\mathbf{z}_k$ . That is,

$$\begin{aligned}\hat{\mathbf{x}}_k(+) &= \hat{\mathbf{x}}_k(-) + \bar{\mathbf{K}}_k[\mathbf{z}_k - \mathbf{H}_k\hat{\mathbf{x}}_k(-)] \\ &= \Phi_{k-1}\hat{\mathbf{x}}_{k-1}(+) + \bar{\mathbf{K}}_k[\mathbf{z}_k - \mathbf{H}_k\Phi_{k-1}\hat{\mathbf{x}}_{k-1}(+)]\end{aligned}\quad (3.15)$$

6. Compute  $\hat{\mathbf{x}}_k(-)$ , predicted estimate, using  $\hat{\mathbf{x}}_k(+)$ . That is,

$$\hat{\mathbf{x}}_{k+1}(-) = \Phi_k\hat{\mathbf{x}}_k(+)\quad (3.16)$$

7. Go to step 2 for recursive filtered estimate and predicted estimate. The parameters,  $\Phi$ ,  $\mathbf{H}$ ,  $\mathbf{Q}$ , and  $\mathbf{R}$ , can be updated if they are time-varying.

These equations are called Kalman filter recursive equations. Steps 3, 4, and 5 describe the observational update (i.e., filtered estimate) after obtaining the corresponding measurements. Steps 6, 7, and 2 describe the temporal update (i.e., predicted estimates) before the next measurements are obtained. They can be seen in the flow chart in Figure 3.1.

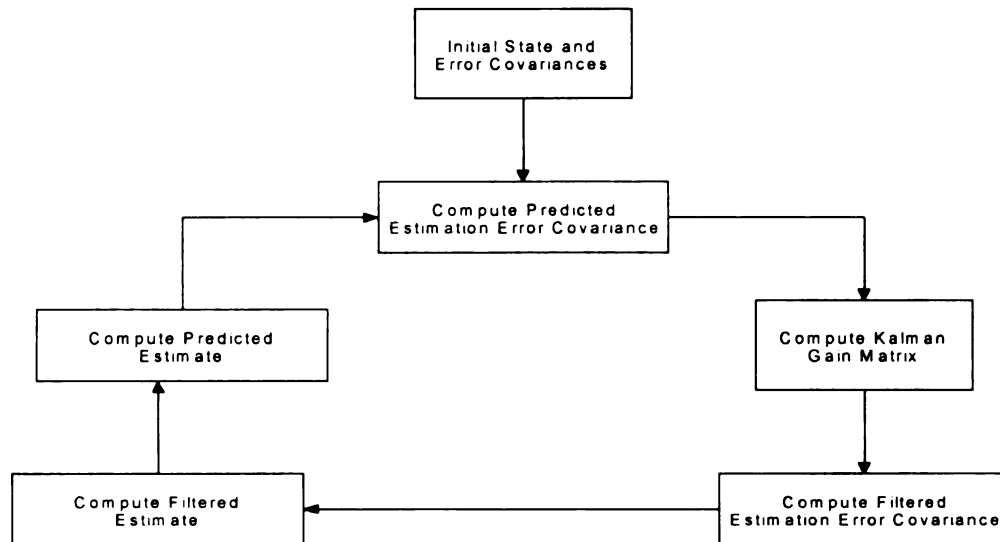


**Figure 3.1: Recursive Kalman Filtering Steps**

### 3.2 Incident Detection Algorithm Development using The Kalman Filtering

An incident detection algorithm can be developed based on the Kalman filtering algorithm. Since the Kalman filter is an algorithm, some modification of steps are made to determine an incident. Although, Kalman filtering was a basis for one of the freeway incident detection algorithms (Dailey 1993), there are some differences in the approach for arterial streets.

### 3.2.1 Considerations for Signalized Arterial Street Incident Detection

In the investigation in the literature review section, valuable lessons were learned. Some of the freeway studies present an approach that has potential arterial street applications. These studies were examined in terms of the historical data dependence, the transferability, the adaptability, and the availability.

Traffic flow is more dynamic and complex on arterial streets than on freeways. This complexity comes from various sources. Side street entrance and exits cause frequent lane changes of main street cars, slow vehicles such as buses, parking vehicles, and even bicycles and pedestrians are all external disturbing sources which interrupt the traffic stream on arterial streets that are rarely seen on freeways. A traffic signal system at an intersection is a major disturbance to main street traffic. There are, therefore, basic parameters that to be examined to consider these factors.

- **Data Sampling Time Interval:** In most freeway studies, it was possible to utilize a short time interval such as 30 seconds for collecting data. The HIOCC Algorithm uses 0.1-second data readings to track traffic flow dynamics. This was possible and useful owing to freeway traffic flow continuity. However, a fundamental problem exists in urban arterial streets. A signal system at an intersection prevents utilizing such a short sampling time interval. Since most detectors are located at intersections, the flow dynamics would appear as step functions due to the green, yellow, and red intervals. Theoretically, each interval could be used as a sampling time interval, but signal phases differ intersection by intersection, and even within the same intersection over time, thus this approach would not be generalizable. Other data aggregation time

intervals such as the seven minutes used in a previous study (Ivan 1995) minimizes the effect of flow variations through the cycle. However, seven minutes in incident detection can be too long, especially, for time series models, which usually compare predicted values and on-coming measurements. Therefore, the best and least data sampling time interval is the common cycle length over a controlled network since the network is usually optimized with the cycle length. This sampling time interval reduces data fluctuations due to different phases of a signal. Fluctuations that still come from a stop-and-go situation can be smoothed by some method, such as the moving average or the exponential smoothing method, etc.

- **Detector-Station Type:** As learned in the freeway comparative algorithms, the use of spatial information from adjacent detector stations for determining an incident is less effective where traffic flow is adversely affected by a geometric discontinuity between two consecutive detector stations. In urban arterial streets where there are many varying disturbing sources to traffic flow, point information from a single detector of a single station approach is essential. The correlation between upstream and downstream measurements in an arterial street may not be useful. For example, the number of vehicles counted at an upstream detector station would not be the same or close to the number of vehicles counted at downstream detector stations due to turning traffic in an intersection, traffic from side streets, and on-street parking, etc.

### 3.2.2 Linear State-Space Model

Since Kalman filtering uses steps to estimate the predicted and filtered parameter values, this procedure can be directly used to form an incident algorithm. Some

modifications for adaptive state-transition matrix ( $\Phi_k$ ) and variance matrix ( $\mathbf{Q}_k$ ) of the state-space model were made to obtain varying parameters in that procedure.

The state-space equation represents the dynamic (evolution) of the state variables with the additional noisy term. The state-transition matrix ( $\Phi_k$ ) is usually a known function but it is necessary to determine the relationships between traffic control variables at time  $k$  and  $k-1$  since there is no dynamic equation or relationships for the time evolution of the traffic control variables. Dailey (1993) constructed this relationship for raw measurements such as traffic flow, percent occupancy, and average speed. To obtain the state transition matrix,  $\Phi_k$ , first multiply the state equation by  $\mathbf{x}_{k-1}$  on both sides and take the expected values. Then,

$$\Phi_{k-1} = \mathbf{E}(\mathbf{x}_k \mathbf{x}_{k-1}^T) [\mathbf{E}(\mathbf{x}_{k-1} \mathbf{x}_{k-1}^T)]^{-1} \quad (3.17)$$

where  $\mathbf{E}(\mathbf{w}_{k-1} \mathbf{x}_{k-1}^T) = 0$  since  $\mathbf{w}_{k-1}$  and  $\mathbf{x}_{k-1}$  are uncorrelated. That is, the state transition matrix is represented by the multiplication of variance of  $\mathbf{x}$  with lag 1 and variance of  $\mathbf{x}$ . Therefore,  $\Phi_{k-1}$  is the matrix that represents the relationship of data from time  $k-1$  to  $k$ .

This was approximated by Dailey (1993) as:

$$\Phi_k \approx \left( \sum_{k=1}^{k=K} \mathbf{x}_k \mathbf{x}_{k-1}^T \right) \left[ \left( \sum_{k=1}^{k=K} \mathbf{x}_{k-1} \mathbf{x}_{k-1}^T \right) \right]^{-1} \quad (3.18)$$

since denominators  $K$  and  $K-1$  for expected values are approximately the same as time evolves. Also, to have the time-dependent noisy term,  $\mathbf{v}_{k-1} \approx N(0, \mathbf{Q}_{k-1})$ , the matrix  $\mathbf{Q}_{k-1}$  was also estimated. To obtain this matrix, first move  $\Phi_{k-1} \mathbf{x}_{k-1}$  from the right to the left, square both sides of the state equation and take its expected value. Then

$$\begin{aligned} \mathbf{Q}_{k-1} = & \mathbf{E}(\mathbf{x}_k \mathbf{x}_k^T) - \mathbf{E}(\mathbf{x}_k \mathbf{x}_{k-1}^T) \Phi_{k-1}^T \\ & - [\mathbf{E}(\mathbf{x}_k \mathbf{x}_{k-1}^T) \Phi_{k-1}^T]^T + \Phi_{k-1} \mathbf{E}(\mathbf{x}_{k-1} \mathbf{x}_{k-1}^T) \Phi_{k-1}^T \end{aligned} \quad (3.19)$$

since  $\mathbf{E}(\mathbf{w}_{k-1} \mathbf{w}_{k-1}^T) = \mathbf{Q}_{k-1}$ .

### 3.2.3 A Recursive Incident Detection Algorithm

As the regular Kalman filtering algorithm begins, a recursive process is started by initializing state variables and their error covariances from pre-obtained data. The temporal update to obtain predicted estimates then follows. The transition matrix ( $\Phi$ ) is estimated. This transition matrix estimate is used to estimate next-time predicted estimates of control variables. The corresponding variance matrix ( $\mathbf{Q}$ ) is then obtained for that time step. Predicted error covariance at this time step is then estimated. The Kalman gain matrix and filtered error covariance for the oncoming new noisy measurements follow. Then filtered estimates are obtained using the just obtained Kalman gain matrix and new noisy measurements. This process shows the observation update after obtaining new noisy measurements from detector stations. An incident state is indicated by comparing the corresponding traffic control variable thresholds computed from predicted error covariance and filtered estimates. False alarms due to inhomogeneous fluctuations can be reduced by smoothing raw aggregated data.

In this algorithm, the prediction model is implemented at each detector station separately. This feature is beneficial since there is no need to consider various exogenous factors between adjacent stations, resulting in no control variable functions associated with these factors and adjacent detector stations. This algorithm is self-learning using data from detectors which already reflect oncoming traffic dynamics.

### **3.2.4 Incident State Determination**

Traffic control variables show different patterns when an incident occurs. These patterns are similar to those shown in Figure 1.1 although this figure is from a freeway system. The patterns are dependent on traffic flow, geometry, detector configuration, incident conditions, and incident location. However, if detectors that are separately placed and operated in each lane of a roadway provide separate information, not aggregated information from adjacent detectors, different patterns for the same traffic control variables can be seen. For example, a partial-blocking incident (e.g., one-lane blockage in a multiple lane-road) that occurs immediately behind a detector station (i.e., downstream detector station) will soon show lower occupancy, lower flow rate, and higher speed (or normal speed) for the detector in that lane. A detector (or detectors) in adjacent lanes then shows higher occupancy, higher flow, and lower speed (or normal speed) due to the lane-switching behavior of vehicles. These are different patterns of the same control variables for the same incident and the same detector location (except lane). This knowledge can be used to develop an incident detection strategy for this type of detector configuration. Instead of using a particular criteria-combination such as higher occupancy, lower flow, and lower speed; or lower occupancy, lower flow, and higher speed for a particular detector station, any of these control variables which is detected to be out-of-intervals is an indication of an incident state. This eliminates the chance of missing incidents due to a combined criteria of each control variable. Also, the time requested to combine these control variables can be reduced. For example, a higher flow indication may not be

obtained at the same time a lower occupancy is obtained. Higher flows may occur several time steps later.

Determining an incident is implemented by constructing the upper and the lower intervals obtained from the predicted error covariance and comparing them with filtered estimates of traffic control variables. These intervals are not fixed, but change over time since updated predicted variances and estimates are made as soon as new measurements are obtained. These intervals can be written as

$$\begin{aligned} \text{Upper Limit at time } k: \hat{\mathbf{x}}_k(-) + n\sigma_{\hat{\mathbf{x}}}, \\ \text{Lower Limit at time } k: \hat{\mathbf{x}}_k(-) - n\sigma_{\hat{\mathbf{x}}}, \end{aligned} \tag{3.20}$$

where  $\sigma_{\hat{\mathbf{x}}}$  is  $\sqrt{\mathbf{P}_k(-)}$ , and  $n$  is the number of  $\sigma_{\hat{\mathbf{x}}}$  (standard deviations).

The procedure for determining an incident can be seen in Figure 3.2.

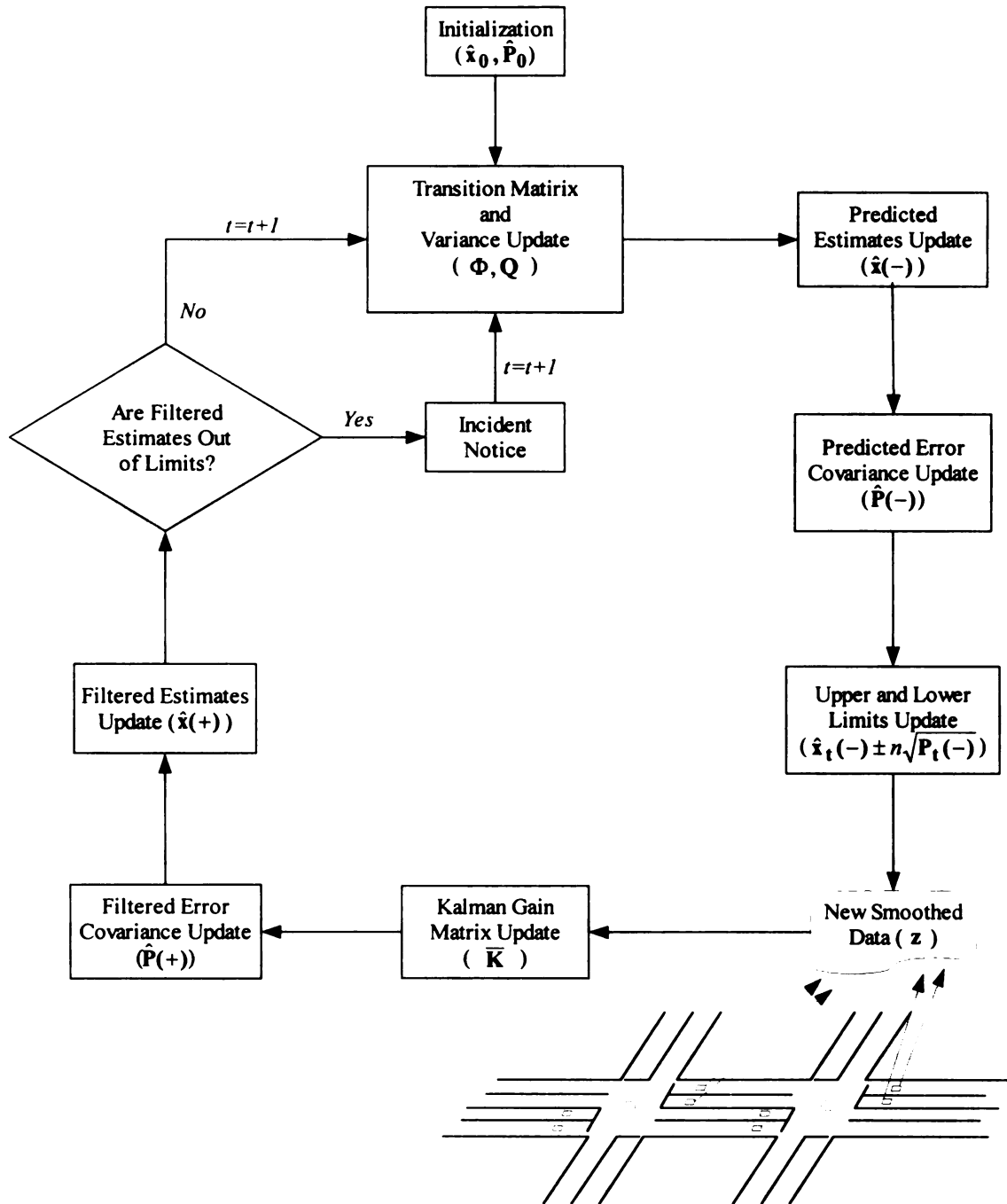


**Figure 3.2 Incident Detection Algorithm using the Kalman Filtering Recursive Procedure**

**Chapter 4**

**INCIDENT DETECTION ALGORITHM TESTS**

**ON ARTERIAL STREET FIELD DATA**

The Kalman filtering technique is not new in the transportation field. Gazis, and Knapp (1971) applied the technique to the estimation of traffic densities at the Lincoln Tunnel. Some freeway incident detection models adopted this model for real-time operation.

It is possible to use Kalman filtering if the situation can be expressed as a state-space model. Actually, Kalman filtering is beneficial because it can run variable models, variable parameters, and variable variances simultaneously. Also, this filtering method considers the correlation between data series, so that the predicted and filtered estimates are more realistic. For instance, the traffic flow and speed are correlated. The data show that the flow increases while the corresponding speed drops in peak hours and the contrary phenomena occurs in off-peak hours. Also, the flow in one lane affects the flow in adjacent lanes (e.g., lane changes from the congested to the non-congested). On freeways, the upstream traffic condition affects the downstream condition, but this is not always true on arterial streets. Kalman filtering can be used to estimate these interactive traffic variable changes adaptively.

#### **4.1 Application to Incident-Free Field Data**

The incident-free field data were obtained from a two-lane approach along Hagadorn Road where it meets Grand River Avenue in East Lansing, Michigan in July 1995. Detectors (HI-STAR from NU-METRICS, Model NC-90A) were placed in each lane about 500 feet upstream from the stop bar of the intersection. The detector senses a vehicle, the speed of the vehicle, and provides the length of that particular vehicle. Since the detector provides microscopic information on traffic, it was necessary to aggregate the data in a certain time interval. The best and least time interval to use as a unit time for time series data in this case was the signal cycle length. In this test, however, the signal system is an actuated type, therefore, it was necessary to select an appropriate, but constant analysis period. The time interval of 3 minutes was used for the data set.

The available data is the traffic flow (counts) in a given time unit, and the time mean speed. Data were obtained from 12:00 P.M. to 8:00 P.M. The data shows that in off-peak hours (12:00 - 4:00 P.M.) a relatively consistent pattern of traffic flow and speed evolves over time in each lane. However, in peak hours (4:00 - 6:00 P.M.), speed drops over time while traffic flow increases until the off-peak period (after 6:00 P.M.) This phenomenon is expected in normal days.

##### **4.1.1 Linear State-Space Model for the Data**

To implement the Kalman filtering algorithm, it is necessary to construct the state-space model and measurement model. The state vector in the state space model is represented as

$$\mathbf{x}_k = [x_1^f, x_1^s, \dots, x_n^f, x_n^s]^T \quad (4.1)$$

where superscripts  $f$  and  $s$  represent traffic flow and speed. The subscript represents the lane numbers where detectors are placed. These are (unknown) true flow and speed values that we are interested in estimating. Then, the linear state-space model (equation 3.7) for these measurements can be constructed by the equations 3.17 or 3.18 and 3.19.

#### 4.1.2 Linear Measurement Model for the Data

In the stochastic process system in this study, the observation at time  $k$  is assumed to be linearly related to the state of the system at the corresponding time as given in the measurement equation. The measurement vector for this data set is represented

$$\mathbf{z}_k = [z_1^f, z_1^s, \dots, z_l^f, z_l^s]^T \quad (4.2)$$

where the subscript and the superscript represent the same as in the state vector. These measurements are noisy observations from detectors.

It is also necessary to obtain the relationship between detector observations and true observations for the measurement equation. For this particular detector, two tests were conducted.

To obtain the measurement sensitivity for traffic flow, detectors were placed on Harrison Road in East Lansing, Michigan, in February 1996. Traffic flow then was videotaped for A.M., P.M. and off-peak periods. The usable data set was from 7:00 A.M. on February 6, 1996 to 8:00 P.M. the next day, resulting in a total of 116 records when aggregated in 3 minutes. This data set was then smoothed by moving average of order of

3 to eliminate impulsive noises. Detector measurements and the video-tape measurements were compared.

The measurement sensitivity test for speed was also performed. Since it was difficult to obtain true speed of random vehicles, a field driving test was conducted. The test was conducted in a large parking lot. A detector was placed in the middle location of the longest driving path. The driving path was long enough to increase the speed to more than 40 mph. This speed was high enough because most of arterial streets are posted around 30 to 35 mph, at most 45 mph. A total of 45 tests were conducted. Then, detector speed measurements and recorded speedometer measurements were compared. Since there are errors in reading the speedometer, detector measurements were assumed to be the equal to the recorded measurements if they were in the range of recorded measurements  $\pm 3$  mph.

The linear data fitting for flow and speed for this particular detector are as follows.

$$\begin{aligned}\hat{x}_f &= \frac{1}{0.987767} y_f - 0.441608 \\ \hat{x}_s &= \frac{1}{0.907173} y_s - 2.0364170\end{aligned}\tag{4.3}$$

where

$\hat{x}_f$  = true traffic flow estimates

$y_f$  = observed traffic flow

$\hat{x}_s$  = true speed estimates

$y_s$  = observed speed

These are plotted in Figure 4.1. The slopes and the intercepts explain the noisy factors for detector performance. Then, the measurement equation can be shown as follows.

$$\begin{bmatrix} z_1^f \\ z_1^s \\ z_2^f \\ z_2^s \end{bmatrix} = \begin{bmatrix} 0.987767 & 0 & 0 & 0 \\ 0 & 0.907173 & 0 & 0 \\ 0 & 0 & 0.987767 & 0 \\ 0 & 0 & 0 & 0.907173 \end{bmatrix} \begin{bmatrix} \hat{x}_1^f \\ \hat{x}_1^s \\ \hat{x}_2^f \\ \hat{x}_2^s \end{bmatrix} + \begin{bmatrix} 0.441608 \\ 2.364170 \\ 0.441608 \\ 2.364170 \end{bmatrix} \quad (4.4)$$

#### 4.1.3 Initialization

To implement Kalman filtering, it is necessary to have initial  $\hat{\mathbf{x}}_0$  and  $\hat{\mathbf{P}}_0$  values. To obtain  $\hat{\mathbf{x}}_0$ , the averages of the first 30 minute data were used for traffic flow and speed. The corresponding variance of the flow and speed are obtained and used as an initial error covariance matrix. The 30 minute-data contains 10 data records. Therefore,

$$\hat{\mathbf{x}}_0 = \begin{bmatrix} \bar{x}_{1,0}^f \\ \bar{x}_{1,0}^s \\ \bar{x}_{2,0}^f \\ \bar{x}_{2,0}^s \end{bmatrix} = \frac{1}{10} \begin{bmatrix} \sum_{k=1}^{10} x_{1,0,k}^f \\ \sum_{k=1}^{10} x_{1,0,k}^s \\ \sum_{k=1}^{10} x_{2,0,k}^f \\ \sum_{k=1}^{10} x_{2,0,k}^s \end{bmatrix} \quad (4.5)$$

and

$$\hat{\mathbf{P}}_0 = \begin{bmatrix} Var(x_{1,0}^f) & 0 & 0 & 0 \\ 0 & Var(x_{1,0}^s) & 0 & 0 \\ 0 & 0 & Var(x_{2,0}^f) & 0 \\ 0 & 0 & 0 & Var(x_{2,0}^s) \end{bmatrix} \quad (4.6)$$

#### 4.1.4 Results of Incident-Free Field Data Application

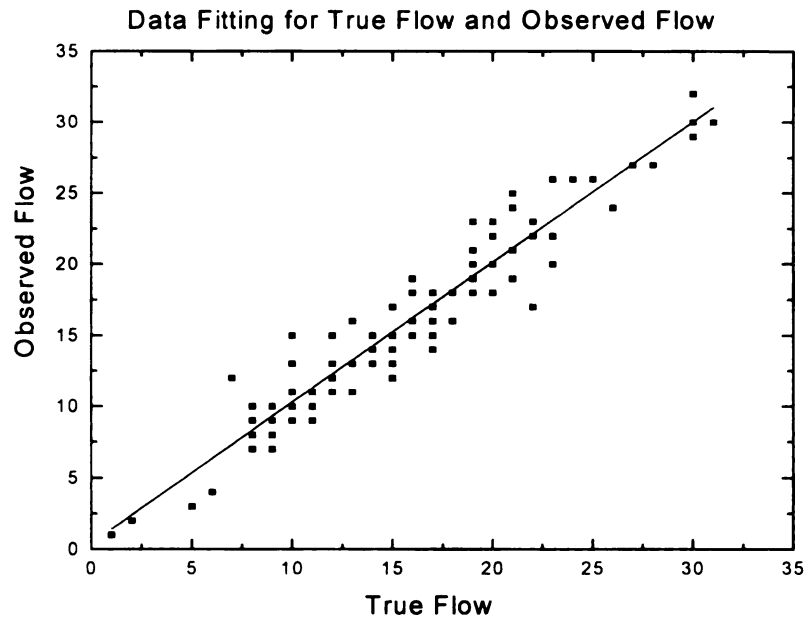
A prediction of obtained data was conducted by the linear Kalman filtering algorithm. The typical filtered and predicted values of traffic flow and speed for each lane are shown in Figure 4.2. Good tracking can be seen in the plots. Filtered estimates are also in the 95 percent upper and lower intervals for the time period from 4:00 P.M. to 8:00 P.M. Corresponding scatter plots for residuals of respective traffic flow and average speed are in Figure 4.3. These scatter plots show good randomness around zero. The resulting mean squared error (MSE) values, obtained from the discrepancy of predicted and filtered estimates, for flow and speed in lane 1 and lane 2 are in Table 4.1.

**Table 4.1 MSEs for Flow and Speed in Lane 1 and Lane 2**

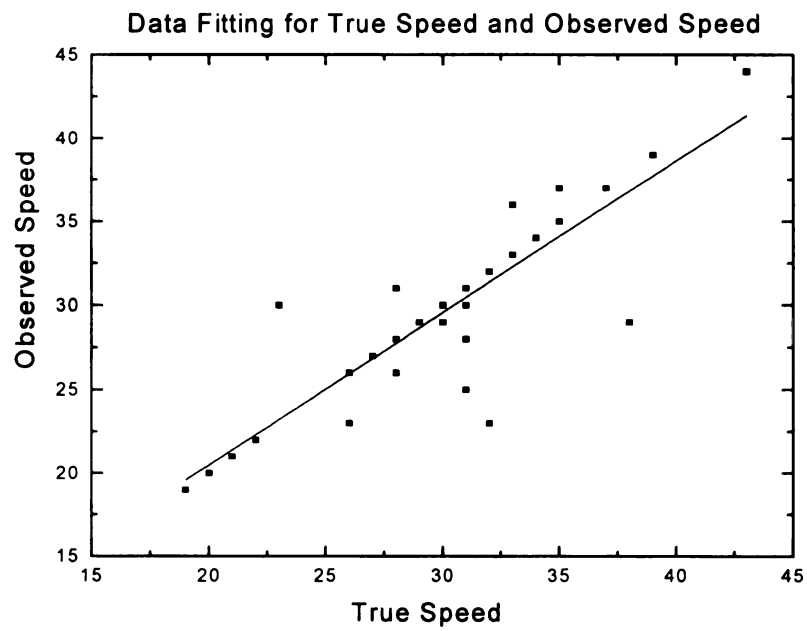
	<b>Flow</b>	<b>Speed</b>
Lane 1	6.278	3.968
Lane 2	5.887	5.166

Figure 4.4 shows the changing pattern of parameter  $\Phi$  over time. These are parameters of flow in lane 1 ( $\Phi(1,1)$ ), average speed in lane 1 ( $\Phi(2,2)$ ), flow in lane 2 ( $\Phi(3,3)$ ), and average speed in lane 2 ( $\Phi(4,4)$ ). These  $\Phi$  values concentrate after initial fluctuation. After about three fourth of time period (about 6 P.M.) these values begin to stabilize. Figure 4.5 shows the changing pattern of variance ( $\mathbf{Q}$ ) of the Gaussian noise term in the state-space equation. Values of  $\mathbf{Q}$  decrease as new data is obtained over time.

A priori error covariance changes over time is also shown in Figure 4.6. As time goes by, these error covariances concentrate.

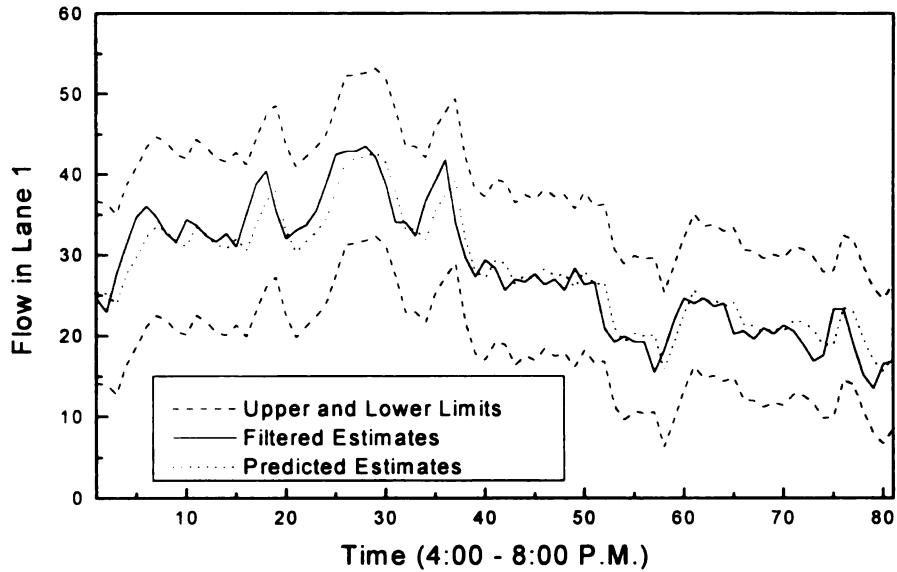


(a)

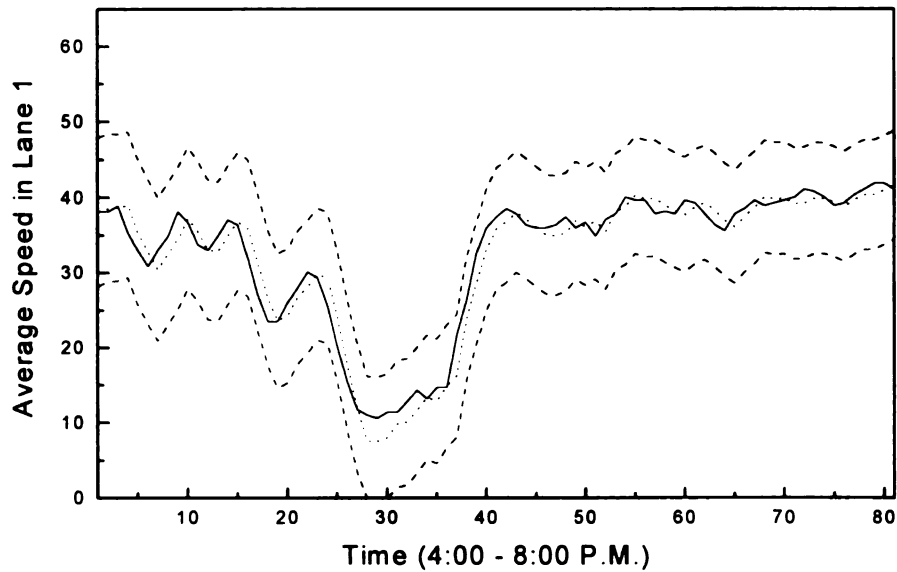


(b)

**Figure 4.1 Data Fitting for True and Observed Flow and Speed**

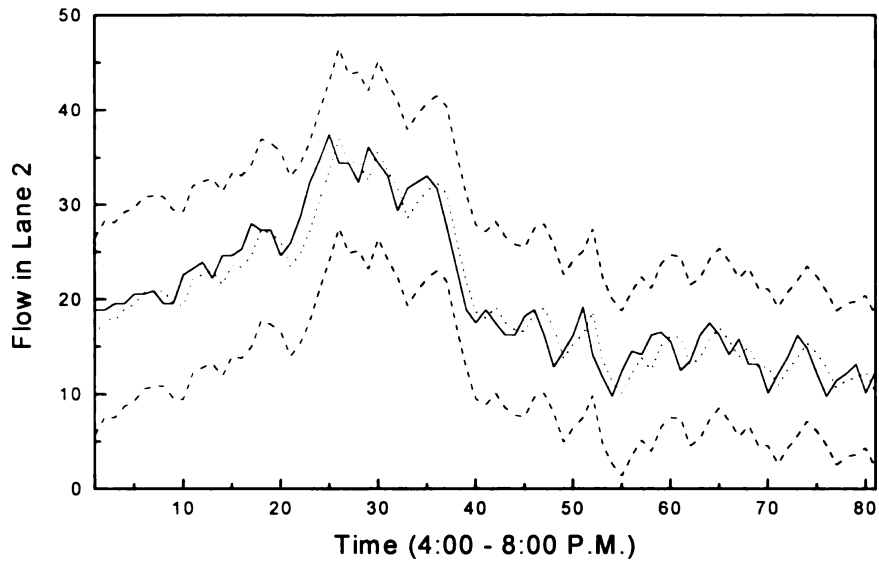


(a) Flow in Lane 1

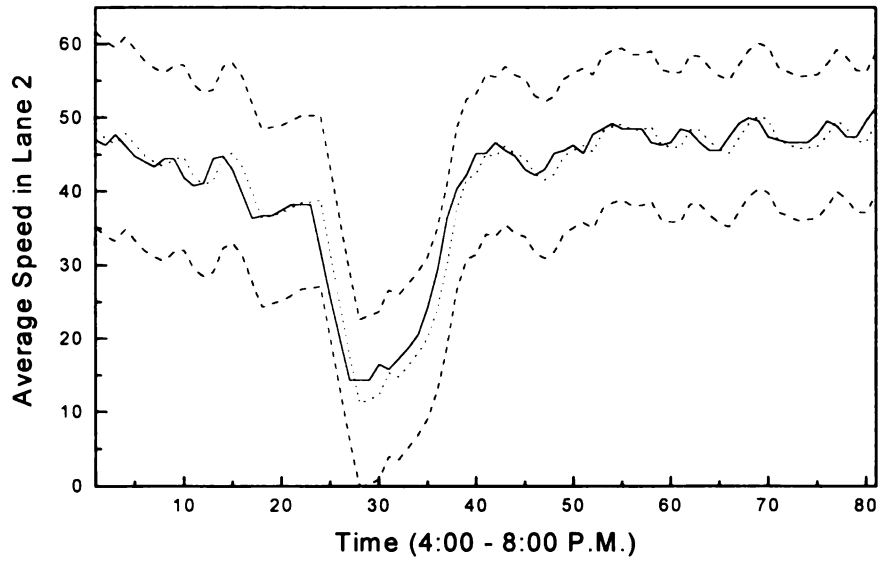


(b) Average Speed in Lane 1

**Figure 4.2 Predicted and Filtered Estimates of Flow and Speed in Lane 1 and 2 and 95 Prediction Interval**

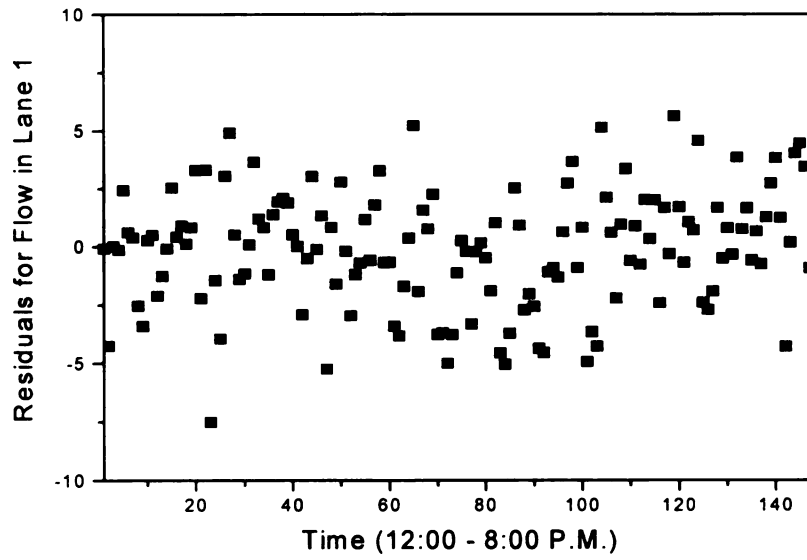


(c) Flow in Lane 2

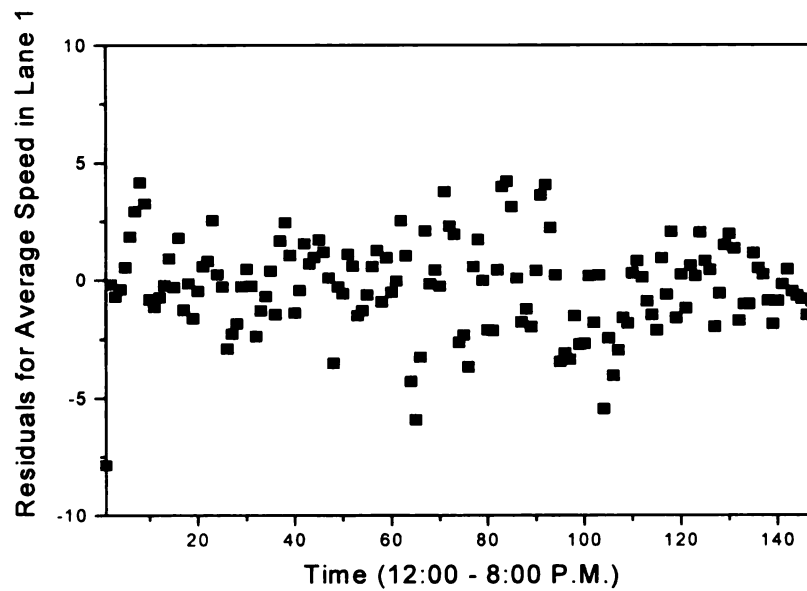


(d) Average Speed in Lane 2

**Figure 4.2 (cont'd)**

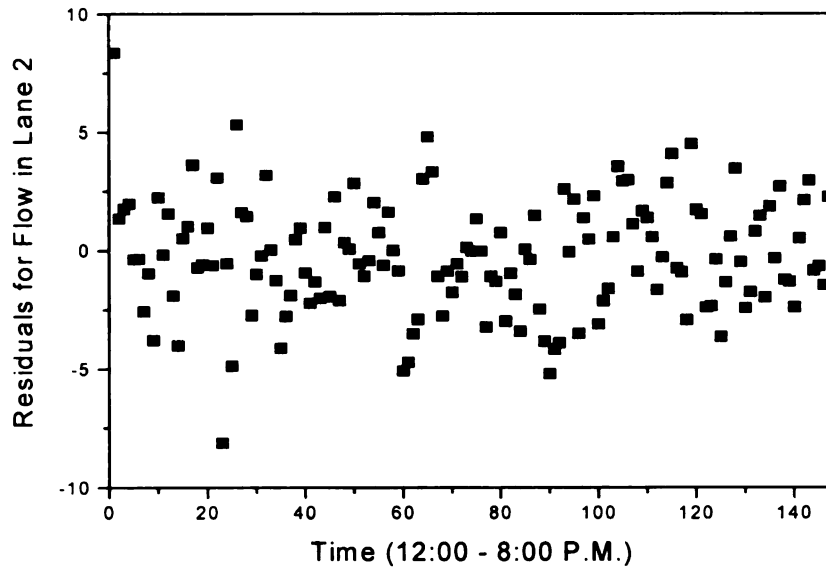


(a) Residuals of Flow in Lane 1

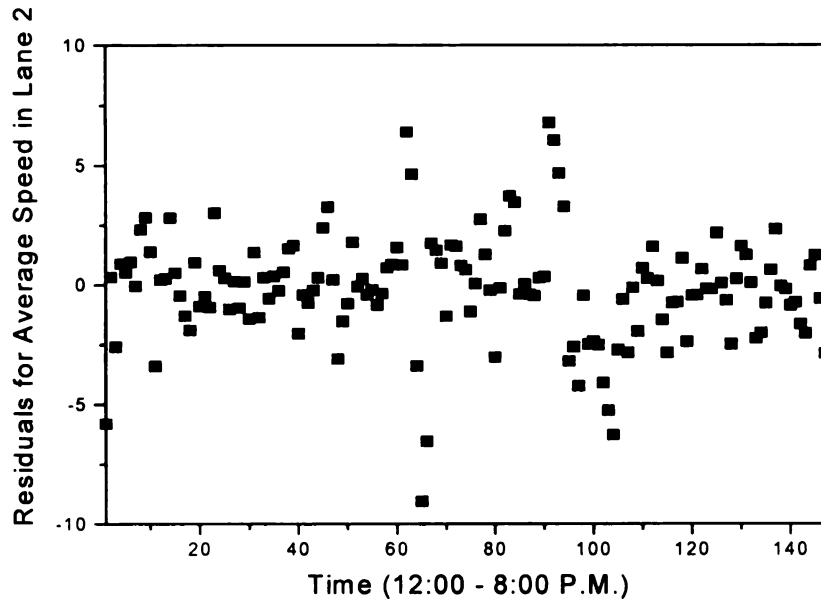


(b) Residuals of Average Speed in Lane 1

**Figure 4.3 Scatter Plots of Residuals for Traffic Flow and Average Speed in Lane 1 and Lane 2**



(c) Residuals of Flow in Lane 2



(d) Residuals of Average Speed in Lane 2

**Figure 4.3 (cont'd)**

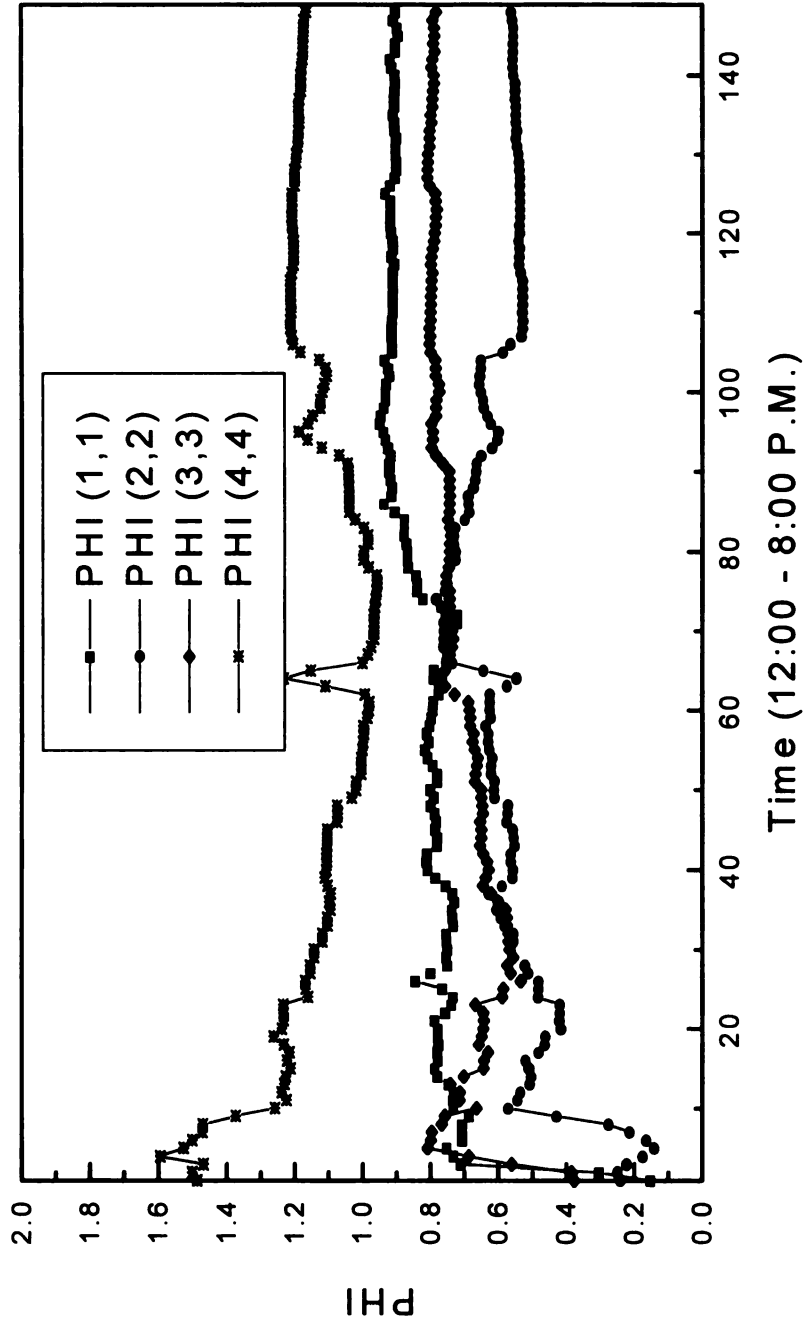


**Figure 4.4  $\Phi(i,i)$  Changes over Time**

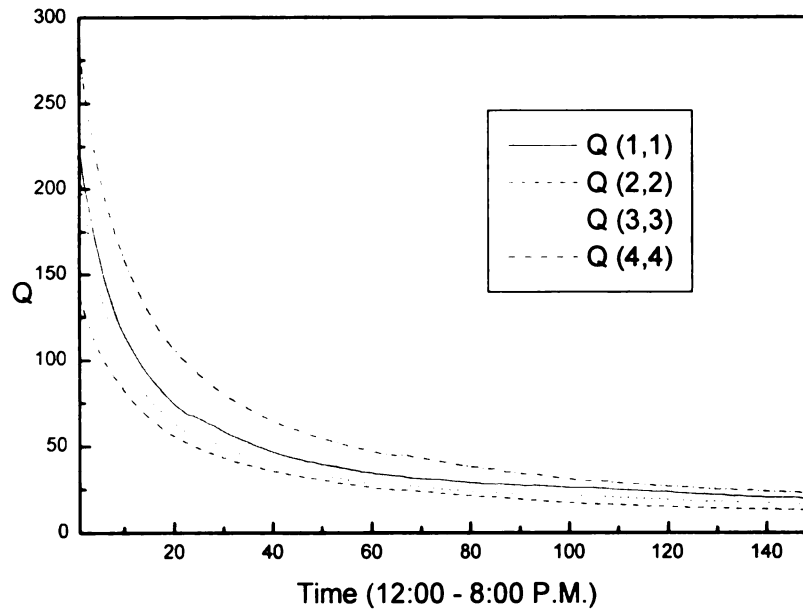


**Figure 4.5  $Q(i,i)$  Changes over Time**

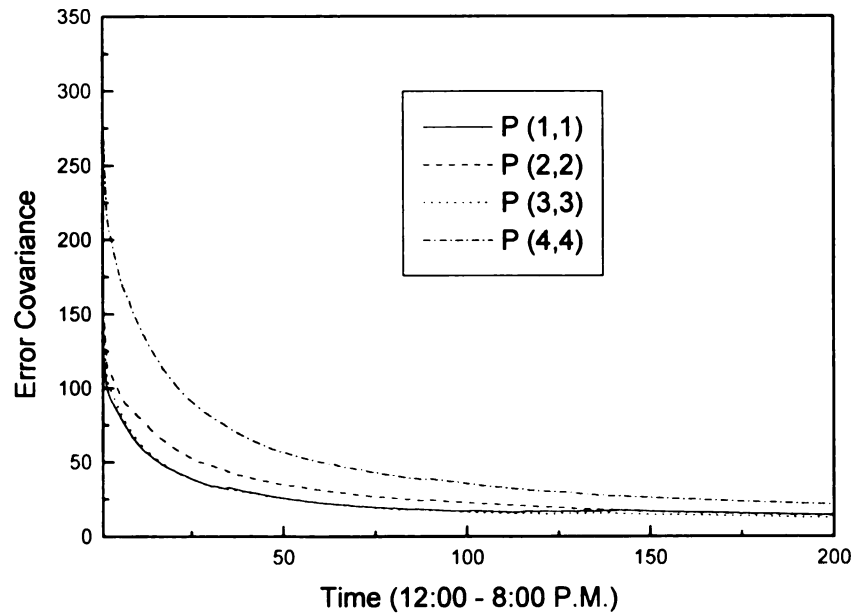


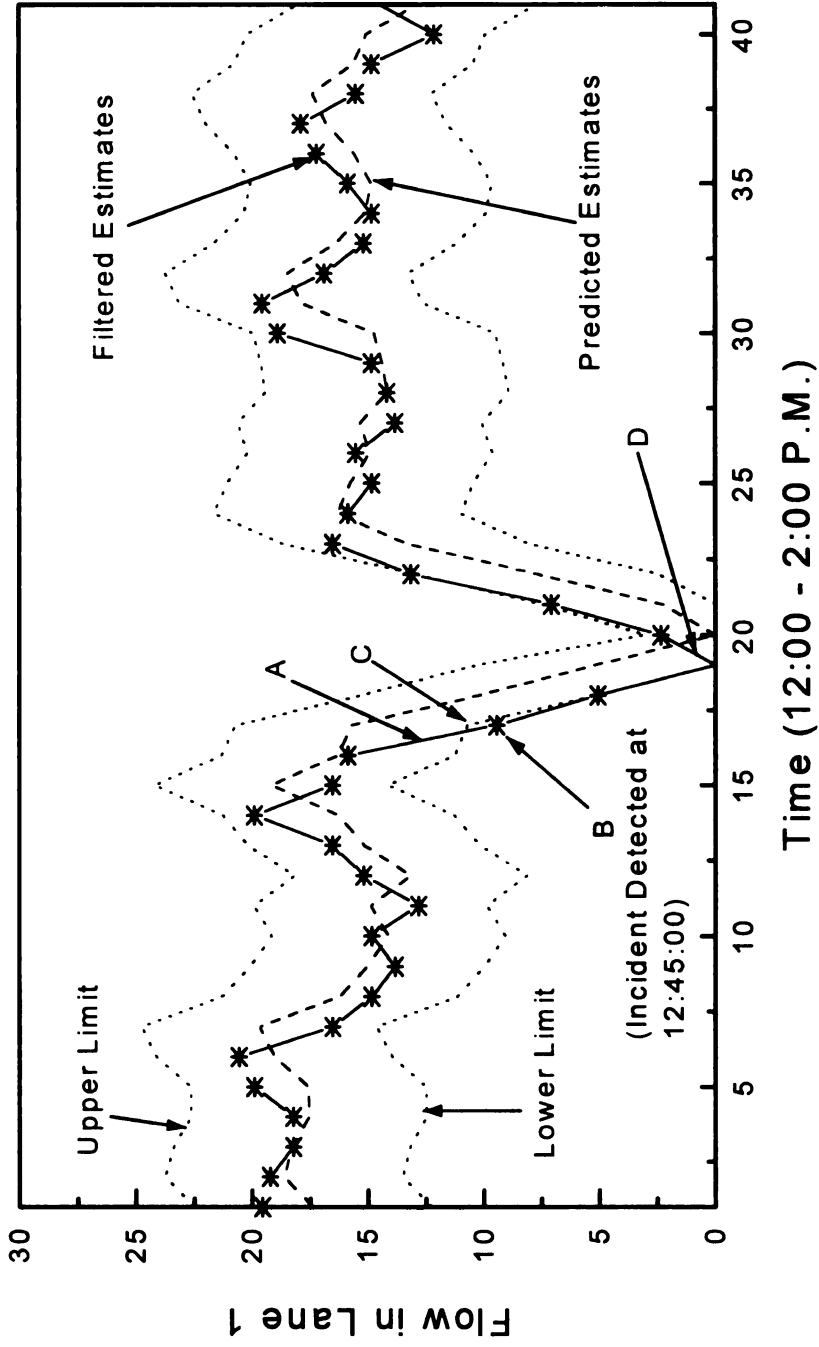
**Figure 4.6 A Priori Error Covariance Changes over Time**

## 4.2 Application to the Incident Data Set

A test was conducted to apply the incident detection algorithm on an arterial street. Incident data were included as part of the Harrison Road data set. An incident was found by analyzing the data set. In lane 1 (outer lane) a large headway (662 seconds) was found between consecutive passing vehicles. The cumulative headway of the last vehicle before that headway was 20476 seconds from 7:00 A.M. on the first day of data collection (i.e., 12:41.4 P.M.) The cumulative headway of the first vehicle after that headway was 21138 seconds (i.e., 12:52.2 P.M.) It was assumed that an incident occurred in that lane. In analyzing traffic in lane 2 (inner lane), an abrupt increase of traffic flow was also found for that time period. Therefore, a lane blockage before the detector in lane 1 was inferred from this traffic flow pattern.

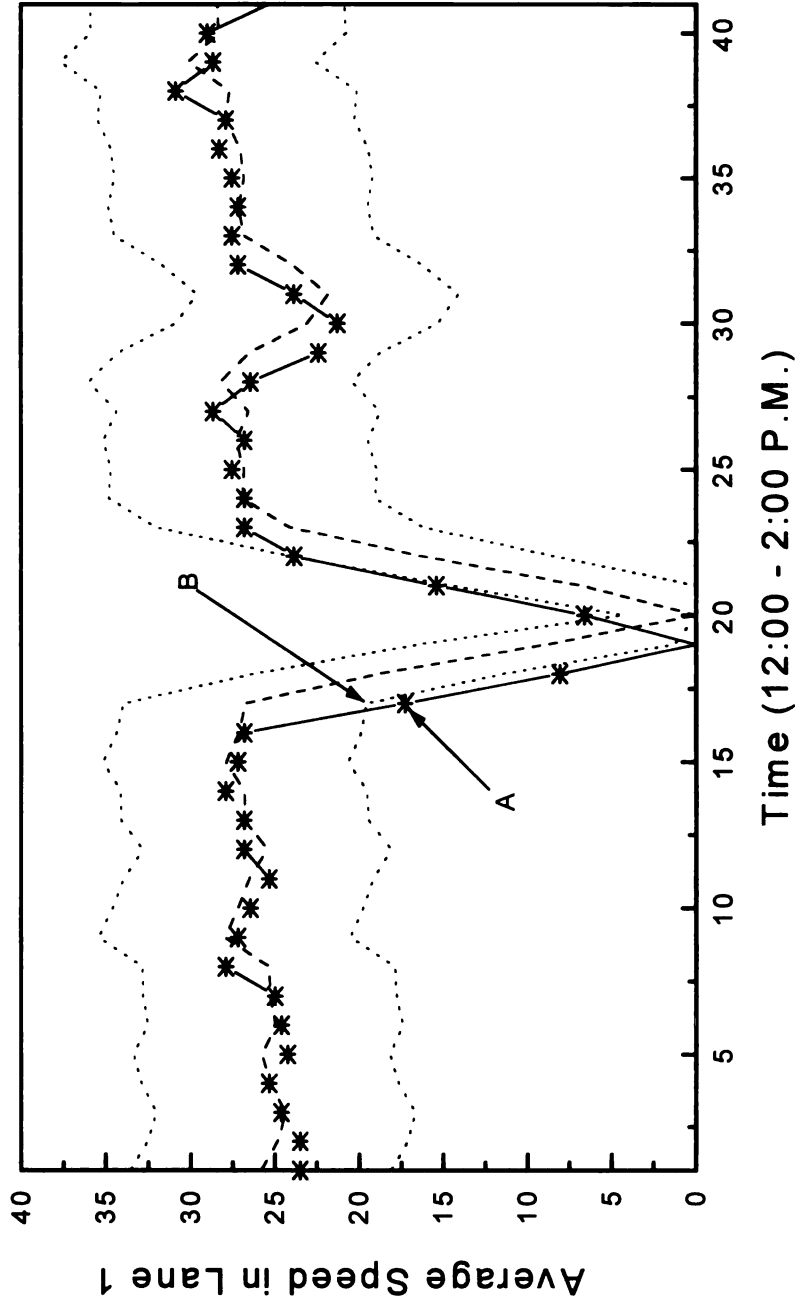
The incident detection algorithm was applied to this data set and  $\pm 2$  standard deviations of predicted error covariance were used as the upper and lower intervals. An incident is indicated if a filtered estimate is out of intervals. Figure 4.7 shows the traffic flow change in lane 1 and lane 2. These figures show the time when the incident occurred and how that was detected. In Figure 4.7a, the incident occurred at time step between 12:42:00 and 12:45:00 (arrow A). Using the incident detection algorithm, this incident was detected at time 12:45:00 with a filtered flow estimate of 9.446 (arrow B) and the lower interval value of 10.724 (arrow C) for the predicted flow estimate. The incident was terminated in the time period between 12:51:00 and 12:54:00 (arrow D). The speed change in lane 1 also showed the same pattern with a filtered speed estimate of 17.273 (arrow A) and lower interval of 19.579 (arrow B) for the predicted speed estimate (Figure 4.7b).

This incident also affected the traffic in lane 2 and was detected (Figure 4.7c). The sudden flow increase at time 12:42:00 was detected at 12:48:00. The filtered flow estimate was 39.817 (arrow A) with the upper interval of 33.677 (arrow B). However, the speed in lane 2 was not affected enough to be out of intervals (Figure 4.7d). Therefore, it took less than 3 minutes to detect the incident in lane 1 and less than 6 minutes in lane 2.



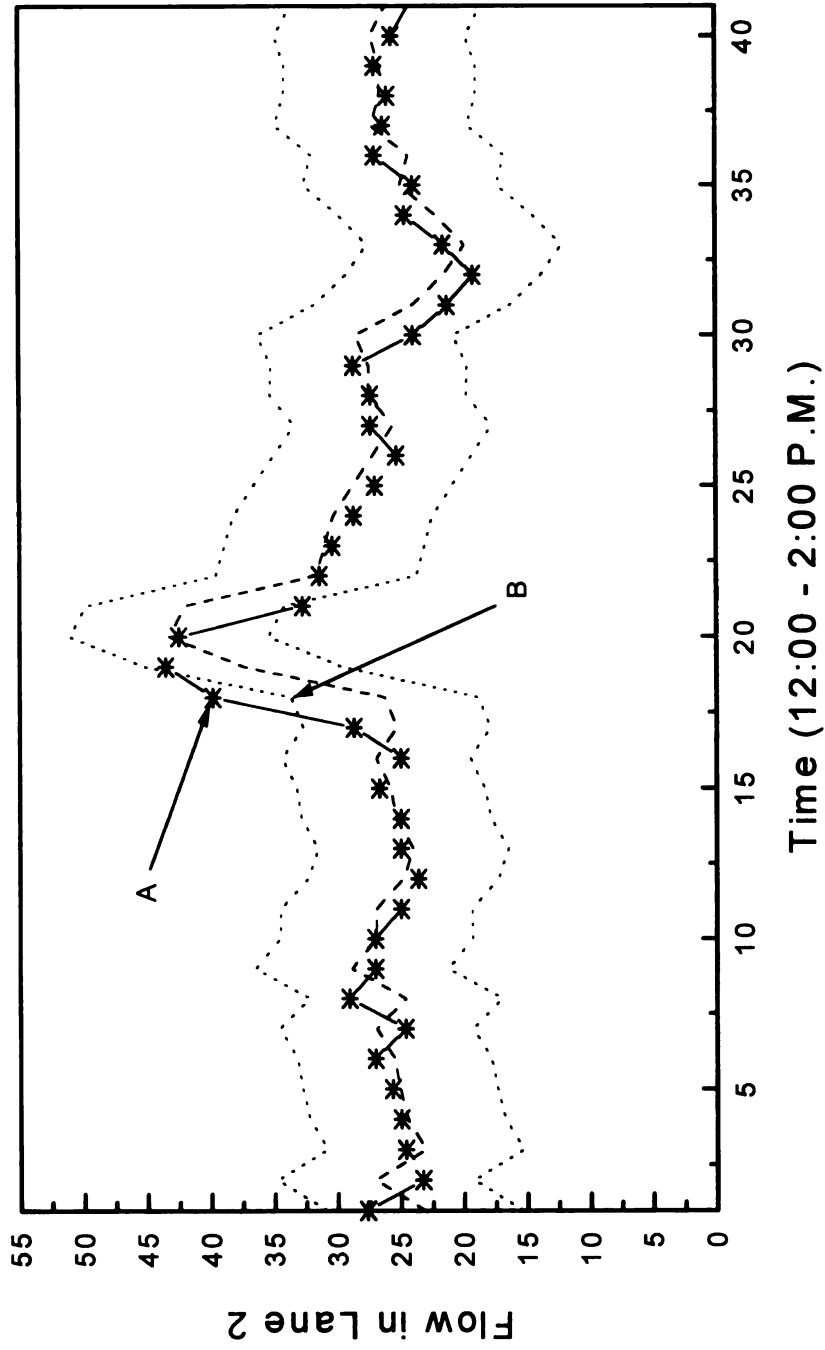
(a) Flow in Lane 1

Figure 4.7 Incident Detection Procedure on Field Data



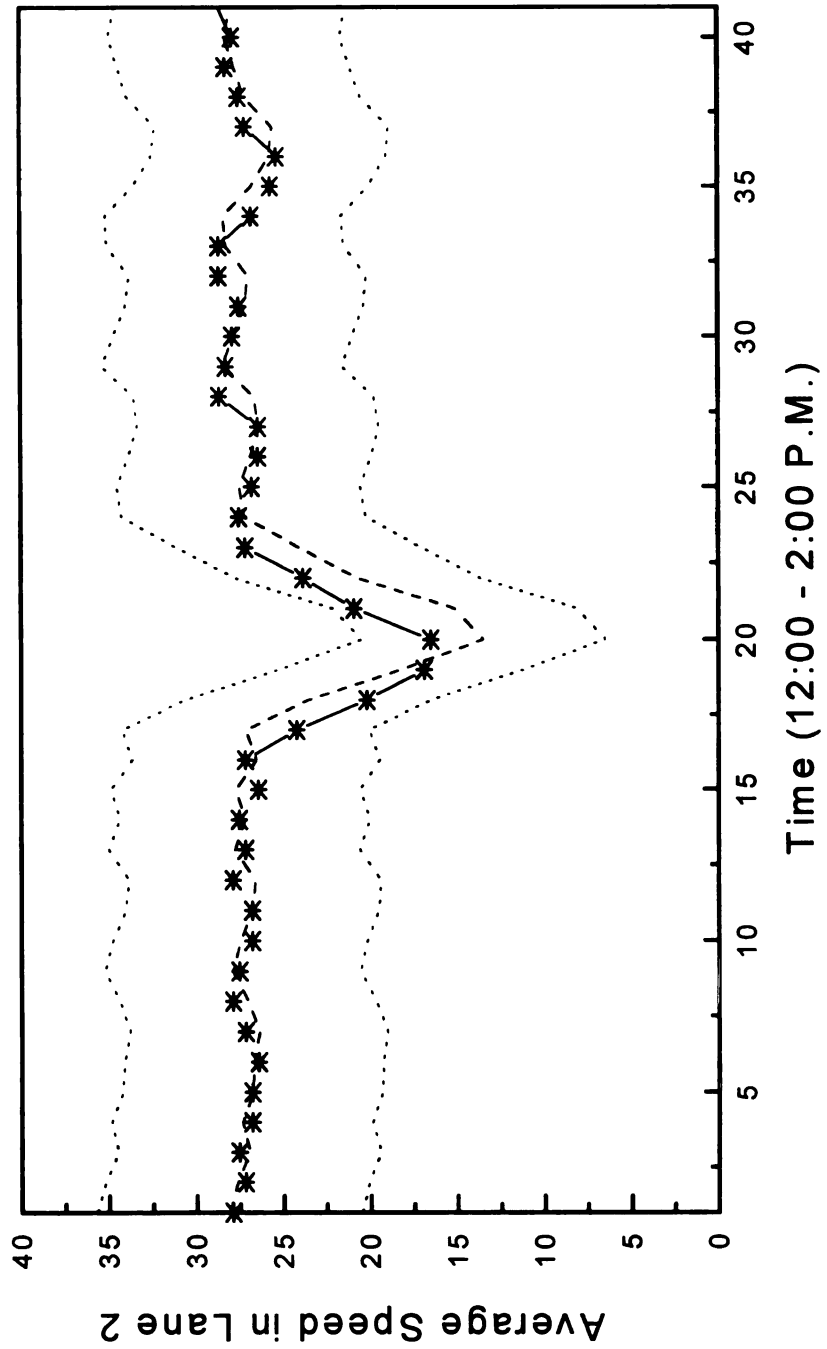
(b) Average Speed in Lane 1

Figure 4.7 (cont'd)



(c) Flow in Lane 2

Figure 4.7 (cont'd)



(d) Average Speed in Lane 2

Figure 4.7 (cont'd)

## **Chapter 5**

### **TRAF-NETSIM SIMULATION TEST**

#### **5.1 Simulation Test for the Algorithm**

The incident detection algorithm was tested with simulated data sets. The TRAF-NETSIM, Version 5 was selected for simulating incident-free and incident data sets. The NETSIM (NETwork SIMulation) is one module of the TRAF family, and is a microscopic simulation model of urban traffic (FHWA 1995). This microscopic model is based on the behavior of individual vehicles, and provides many features. One of these features is the ability to generate incidents in the network. Partial blockages and full blockages in a link can be generated for various durations. In this section, incident-free data were generated and used to test the false alarm rates. Then, incident-data were generated to test incident detection rates and the mean detection time statistics.

#### **5.2 Description of the Arterial Street Network**

The network for the simulation was selected to represent a real-world situation. The urban arterial street for the simulation test was Washtenaw Avenue located in Ann Arbor, Michigan. This site was used in a previous bus-preemption signal study (Al-Sahili, and Taylor 1996). This arterial street contained 12 intersections and stretched from the west to the east. The lengths of links between intersections vary from 400 feet to 4000 feet.

Available network data included intersection geometry, and traffic volumes from 7:00 A.M. to 8:00 A.M.(i.e., A.M. peak hour volume). The traffic flow from the east to the west was high in the A.M. peak hour period so this direction was selected for the test. The traffic signal timing was optimized by using TRANSYT-7F, Release 7. The TRANSYT-7F minimizes an objective function called the performance index (PI) to optimize the signal timing (Wallace, Courage and Hadi 1991). The PI is a linear combination of delay and stops, fuel consumption and excessive maximum length of queue. The best common cycle length was 120 seconds over the network. Each direction of the street had bus stations. A total of 34 bus stations were located along the street for both directions. The type of bus stop location was protected, which was pull out and no-parking bus stop. The average time the bus spends stopped at each bus station to load and unload passengers was assumed to be 30 seconds. The mean headway between buses was also assumed to be 900 seconds. The network is represented as a link and node diagram in Figure 5.1.

### **5.3 Measures of Effectiveness**

In evaluating various incident detection methods, the most widely used metrics are the detection rate, the false alarm rate, and the mean detection time.

- **Detection Rate (DR)** - The ratio of incidents detected to all incidents that occur during a specified time period.

$$DR(\%) = \frac{\text{Number of Incidents Detected}}{\text{All Incidents}} \times 100 \quad (5.1)$$

- **False Alarm Rate (FAR)** - The ratio of false alarms to all time intervals tested during a specified time period. There are two ways to express the false alarm rate: on-line definition and off-line definition. The on-line definition is the percentage of false incident messages out of the total incident messages generated by the algorithm. The off-line definition is the percentage of incident messages generated by the algorithm using representative incident-free data (Levin and Krause 1978). In this study, the false alarm rate (%) per detector station is calibrated as the ratio of the number of false alarms per hour per station to 30 records per hour because the data is aggregated in 2 minute slices (common best cycle length). In mathematical form, it is

$$\text{False Alarm Rate (\%)} = \frac{\text{Number of False Alarms / Hour / Station}}{30 \text{ Records / Hours}} \times 100 \quad (5.2)$$

- **Mean Detection Time (MDT)** - The average amount of time to detect an incident. This is defined as the difference between the detection time by the algorithm and the earliest possible detection time determined by examining both the upstream and downstream station data of the incident location. The process of estimating the earliest possible detection time requires subjective judgment.

These metrics are related with each other. For example, a lower false alarm rate is achieved at the cost of a lower detection rate. There are no definite standards for selecting the best combination of these metrics. The performance comparisons of various historical detection methods is also hard to make on an absolute scale, because the definition of incidents has varied study by study. For instance, some studies include stalled vehicles on the shoulder as incidents, although this vehicle may not impact traffic flow (Hughes Aircraft and JHK & Associates 1992).

#### **5.4 Incident-Free Data Set Description**

Incident-free data were generated for a false alarm check. A false alarm check was conducted for both directions of all 13 links of Washtenaw Avenue. One-hour simulations representing a weekday peak hour were conducted for generating normal A.M. peak hour condition. The first day was used for the initializations of filtered and corresponding error covariance estimates. The next two days were used to stabilize parameters and predicted error covariances for constructing upper and lower intervals. Then, ten days of data were generated to test the incident free condition.

This data is obtained by placing surveillance detectors at the downstream end of each links in the network. A total of 24 detector stations were placed for each direction. They are presence detectors and placed in through moving lanes because our interest is the detection of blockages for the through traffic. The detector provides traffic measurements of vehicle counts, average speeds, and percent occupancy. These measurements are collected every 120 seconds (best common cycle length in the network). Therefore, 30

records were created each hour (i.e., a day). For the ten-day incident free data set, a total of 300 records were created at each detector station. Therefore, a total of 7,200 records of data were generated for the 24 detector stations in the network. A record contained traffic measurements of each through lane. For example, six traffic measurements were in a record for a two-through lane link (i.e., vehicle counts, average speed, and percent occupancy in each through lane, respectively).

### **5.5 Incident Data Set Description**

As in the incident-free data generation, one-hour simulation representing a day was conducted for generating incidents in the A.M. peak hour. As in the incident-free data set, the first day was used for initialization, and the second and the third days for stabilization were conducted with incident-free data. The fourth day incident data was generated. The fifth day was incident-free and represented a recovery to normal traffic flow after an incident in the fourth day. Therefore, the predicted error covariance for the upper interval and the lower interval in the third day was used for the incident-check on the fourth day data set.

#### **5.5.1 Link Selection for Incident Generation**

There are a total of 13 links on Washtenaw Avenue in the network. Two links were selected for incident detection tests. This selection was based on traffic flow and geometric conditions. The link 34 was selected because it represented high traffic and a long link length. A bus station was located 700 feet away from a stop bar of the

downstream intersection. Link 45 was selected because it represented high traffic and a short link length. A bus stop was located 100 feet away from a stop bar of the downstream intersection. Intersections associated with these links are node 3, node 4, and node 5. Level of Service (LOS) of these intersections are in Table 5.1. These LOSs are obtained from the Highway Capacity Software (McTrans Center 1995). Their geometry and traffic conditions are shown in Figure 5.1-5.3.

**Table 5.1 LOS in Node 3, 4, and 5**

Direction	Lane Movement	Node 3		Node 4		Node 5	
EB	Left	D	D	A	A	A	A
	Through	C		A		A	
	Right	C		A*		A*	
WB	Left	D	C	C	B	B	B
	Through	C		B		B	
	Right	C*		B		B*	
NB	Left	F	E	N/A	E	E	E
	Through	D		E		D	
	Right	C		E*		D*	
SB	Left	D	D	N/A	D	D	D
	Through	D		E		D	
	Right	D*		D*		D*	

\* Shared Movement with Through Movement



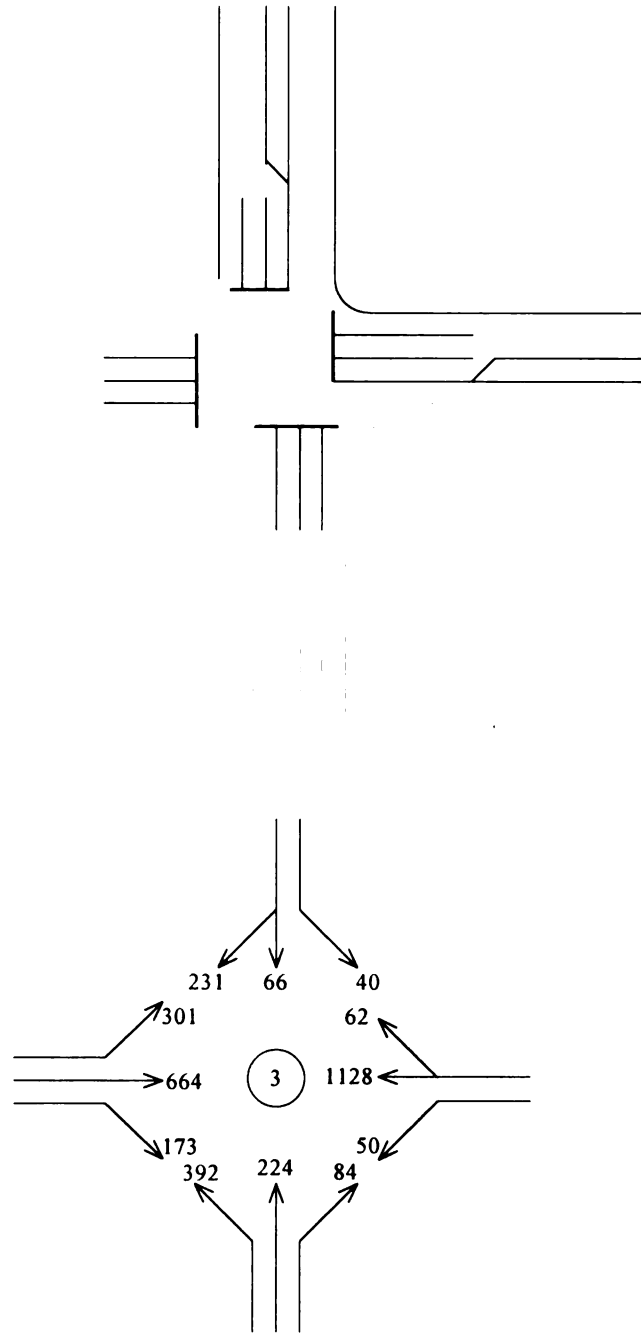


**Figure 5.2 Node 3 Geometric and Hourly Traffic Volume**

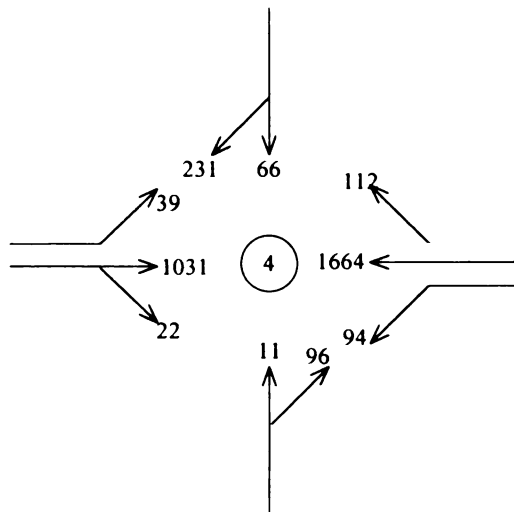
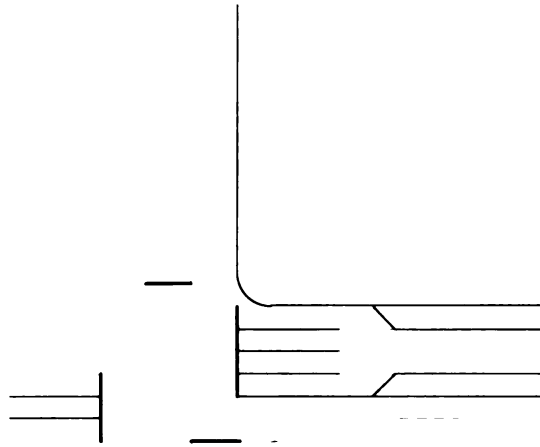


**Figure 5.3 Node 4 Geometric and Hourly Traffic Volume**

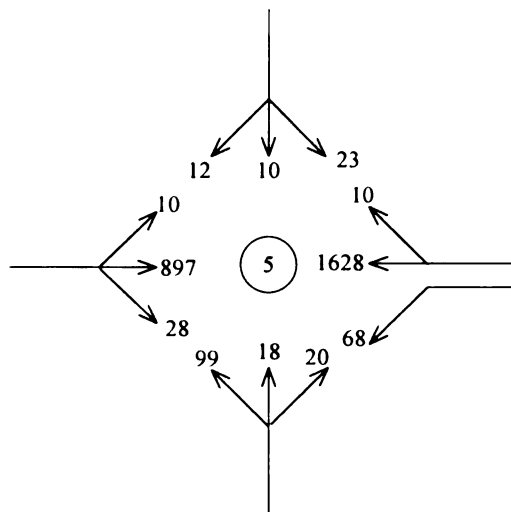
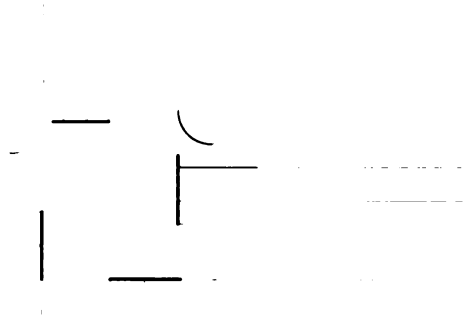


**Figure 5.4 Node 5 Geometric and Hourly Traffic Volume**

### 5.5.2 Incident Generation in TRAF-NETSIM

In TRAF-NETSIM, Version 5, an incident can be generated either in a link or an intersection. An incident in this simulation program represents long-term blockages due to illegal parking or vehicle breakdown. A limitation on an incidents generation in this simulation program is that they represent only one-lane blockages instead of full-link blockages (e.g., two lane blockages for two lane roadways). Another limitation is the randomness of the incident location along a subject link. For example, if a user specifies an incident on a certain link, an incident can occur at either end of the downstream link or the middle of the link. Since these incident types and incident location are important factors for an incident detection algorithm test some techniques were applied to generate realistic incidents.

- **Full-Link Blockages Generation** - A full-link blockage was created by using a signalized dummy node in a link. For normal traffic flow, the signal was given all green for the interested direction. When an incident occurs, the signal was given 5 seconds of green and 115 seconds of red phases. This 5-second green time represented the time period for metered vehicles to pass the incident location in a 120-second cycle length. The 115 seconds represent an incident event that blocks oncoming vehicles.
- **Incident Location Specification** - A one-lane blockage in a multi-lane roadway can be made using the microintersection feature in NETSIM. A dummy node for a

microintersection in the interested link was made. Since this was a microintersection, it was possible to specify a blockage in the intersection that was a particular incident location by specifying the distance between adjacent nodes. For example, a blockage in lane number 1 in an approach link (interested link) and lane number 0 on a cross street represents the incident in lane 1 of the approach link. By moving this dummy node (microintersection) along the interested link, an incident can be placed in various locations.

### **5.5.3 Various Incident Generation**

Mid-block incidents can be represented by the type, and duration, as well as the location on a link.

**Incident Type:** For two-lane streets, there are two types of incidents. An incident blocking one lane, lane 1 (outer lane) or a lane 2 (inner lane), is a partial blockage which reduces the capacity of the roadway. These incidents allow drivers to switch their driving lane to the non-incident lane. The other incident type is a full-link blockage.

**Incident Duration:** The duration of incidents is variable. That is, there is no time duration common to all incidents. In this study, the duration of an incident was studied in 10 minute increments. For one-lane blocks, incidents were assumed to last 10, 20, 30, 40, and 50 minutes. For full-link blocks, incidents were assumed to last 10, 20, and 30 minutes.

**Incident Location:** The location is an important factor for incident detection techniques. It is easy for an algorithm to detect an incident occurring near a detector since the impact of the incident will be sensed quickly. The closer an incident occurs to a detector, the faster the incident is detected. For link 34, three locations were selected for incident. They were an upstream location (100 feet away from an upstream intersection), a downstream location (100 feet away from a detector station), and a middle location (1050 feet away from both the upstream intersection and the downstream intersection). For link 45, two locations were determined since the link was short. They were the upstream (100 feet away from the upstream intersection) and the middle location (256 feet away from both the upstream and the downstream intersections). These locations were applied to the one-lane blockages and the full-link blockages.

As a result, a total of 65 incidents were generated for the incident test. For link 34, a total of 30 and 9 incidents were simulated for the one-lane blockage and full-link blockage, respectively. For link 45, a total of 20 and 6 incidents were simulated for one-lane blockage and full-link blockage, respectively. The characteristics of these incidents are shown in Table 5.2 and Table 5.3.

**Table 5.2 Incidents in Link 34 Descriptions**

Incident Type	Lane Blocked	Incident Location	Duration
One-Lane Blockage	1	Middle	10 minutes
One-Lane Blockage	1	Middle	20 minutes
One-Lane Blockage	1	Middle	30 minutes
One-Lane Blockage	1	Middle	40 minutes
One-Lane Blockage	1	Middle	50 minutes
One-Lane Blockage	2	Middle	10 minutes
One-Lane Blockage	2	Middle	20 minutes
One-Lane Blockage	2	Middle	30 minutes
One-Lane Blockage	2	Middle	40 minutes
One-Lane Blockage	2	Middle	50 minutes
One-Lane Blockage	1	Downstream	10 minutes
One-Lane Blockage	1	Downstream	20 minutes
One-Lane Blockage	1	Downstream	30 minutes
One-Lane Blockage	1	Downstream	40 minutes
One-Lane Blockage	1	Downstream	50 minutes
One-Lane Blockage	2	Downstream	10 minutes
One-Lane Blockage	2	Downstream	20 minutes
One-Lane Blockage	2	Downstream	30 minutes
One-Lane Blockage	2	Downstream	40 minutes
One-Lane Blockage	2	Downstream	50 minutes
One-Lane Blockage	1	Upstream	10 minutes
One-Lane Blockage	1	Upstream	20 minutes
One-Lane Blockage	1	Upstream	30 minutes
One-Lane Blockage	1	Upstream	40 minutes
One-Lane Blockage	1	Upstream	50 minutes
One-Lane Blockage	2	Upstream	10 minutes
One-Lane Blockage	2	Upstream	20 minutes
One-Lane Blockage	2	Upstream	30 minutes
One-Lane Blockage	2	Upstream	40 minutes
One-Lane Blockage	2	Upstream	50 minutes

**Table 5.2 (cont'd)**

<b>Incident Type</b>	<b>Lane Blocked</b>	<b>Incident Location</b>	<b>Duration</b>
Full-Link Blockage	1,2	Middle	10 minutes
Full-Link Blockage	1,2	Middle	20 minutes
Full-Link Blockage	1,2	Middle	30 minutes
Full-Link Blockage	1,2	Downstream	10 minutes
Full-Link Blockage	1,2	Downstream	20 minutes
Full-Link Blockage	1,2	Downstream	30 minutes
Full-Link Blockage	1,2	Upstream	10 minutes
Full-Link Blockage	1,2	Upstream	20 minutes
Full-Link Blockage	1,2	Upstream	30 minutes

**Table 5.3 Incidents in Link 45 Descriptions**

Incident Type	Lane Blocked	Incident Location	Duration
One-Lane Blockage	1	Middle	10 minutes
One-Lane Blockage	1	Middle	20 minutes
One-Lane Blockage	1	Middle	30 minutes
One-Lane Blockage	1	Middle	40 minutes
One-Lane Blockage	1	Middle	50 minutes
One-Lane Blockage	2	Middle	10 minutes
One-Lane Blockage	2	Middle	20 minutes
One-Lane Blockage	2	Middle	30 minutes
One-Lane Blockage	2	Middle	40 minutes
One-Lane Blockage	2	Middle	50 minutes
One-Lane Blockage	1	Upstream	10 minutes
One-Lane Blockage	1	Upstream	20 minutes
One-Lane Blockage	1	Upstream	30 minutes
One-Lane Blockage	1	Upstream	40 minutes
One-Lane Blockage	1	Upstream	50 minutes
One-Lane Blockage	2	Upstream	10 minutes
One-Lane Blockage	2	Upstream	20 minutes
One-Lane Blockage	2	Upstream	30 minutes
One-Lane Blockage	2	Upstream	40 minutes
One-Lane Blockage	2	Upstream	50 minutes
Full-Link Blockage	1,2	Middle	10 minutes
Full-Link Blockage	1,2	Middle	20 minutes
Full-Link Blockage	1,2	Middle	30 minutes
Full-Link Blockage	1,2	Upstream	10 minutes
Full-Link Blockage	1,2	Upstream	20 minutes
Full-Link Blockage	1,2	Upstream	30 minutes

## 5.6 Results of the Incident-Free Test

The incident free condition was tested to check the false alarm rate. An incident indication was made by comparing the filtered estimates and the prediction intervals of the predicted estimate in each time increment. If any filtered estimate is out of intervals, then an incident alarm is recorded. For the upper and the lower intervals, 95 percent (e.g.,  $\pm 2\sqrt{P(-)}$ ) prediction intervals were used. Raw traffic counts, percent occupancy, and the average speed in each lane were smoothed by the moving average of 3 time intervals.

Results showed that a total of 36 false alarms were indicated in the network. These false alarms were accumulated from 24 detector stations over 10 hours. This is 0.15 false alarms per hour per station. If the system was operated for 2 hours a day, then there could be 0.3 false alarms per day per station. For the network, a total of 7.2 false alarms would occur in a day. Since 0.15 false alarms were made in an hour (30 records of data an hour) per station, the false alarm rate is 0.5 percent. For the direction of high traffic (e.g., from east to west), a total of 4 false alarms were indicated. This is 0.033 false alarms per hour per station. If the system were operated for 2 hours a day, then there would be 0.067 false alarms per day per station. For the high traffic direction, this is 0.800 false alarms per day per station. The false alarm rate is 0.111 per hour per station. They are shown in Table 5.4.

**Table 5.4 Results of Incident Free Test for 95 Percent Prediction Intervals**

<b>Statistics</b>	<b>Network (Both Directions)</b>	<b>High Traffic Direction (from east to west)</b>
Total # of FA/10 Hr/ Total # of Stations	36	4
FA/Hr/Station	0.150	0.033
FA/2Hr/Station	0.300	0.067
FA/2Hr/Total # of Station	7.200	0.800
FAR/Hr/Station (%)	0.500	0.111

By analyzing the result, a distribution of false alarms with the associated traffic control variables are shown in Table 5.5.

**Table 5.5 Distribution of False Alarms over Detector Stations**

<b>Station No.</b>	<b>No. of FA</b>	<b>Traffic Control Variables*</b>
2	1	1(4)
4	1	2
5	1	2
8	3	2(5), 2
9	2	2(4)
10	1	2
18	1	5
19	1	5
20	20	2(2), 18(5)
22	2	2(5)
24	4	4(5)
<b>Total</b>	<b>36</b>	<b>5(2), 3(4), 28(5)</b>

\*The number in a parenthesis indicates a traffic control variable. The number before a parenthesis indicates the number of that traffic control variables in the parenthesis.

### **Traffic Control Variable Description**

- 1: traffic count in lane 1
- 2: percent occupancy in lane 1
- 3: average speed in lane 1
- 4: traffic count in lane 2
- 5: percent occupancy in lane 2
- 6: average speed in lane 2

A total of 11 detector stations showed false alarms. Eight of these stations were in the low traffic flow direction (i.e., from west to east). These are even-numbered stations. Three of these stations were in the direction of high traffic flow (i.e., from east to west). These are odd-numbered stations. This result suggests that the incident detection algorithm is more effective in the high traffic direction. This is illustrated by comparing

the stations with the most false alarm and the station with no false alarm. Station 20 and station 5 one-hour traffic statistics are shown in Table 5.6, and 5.7, respectively.

**Table 5.6 One-Hour Traffic Statistics at Detector Station 20**

	Traffic Control Variables					
	1	2	3	4	5	6
Average	7.433	14.660	25.033	7.033	15.570	25.457
Std. Dev.*	0.971	4.220	1.948	1.426	6.385	2.804

\*Standard Deviations

By looking at the statistics for station 20, the average time interval between consecutive vehicles can be calculated. Assuming a 2 second discharge interval, the effective green time for the signal is 100 seconds (i.e., 98 seconds for green, 4 seconds for yellow, and 2 second for the lost time). The average number of vehicles per lane is 7.233 for that phase. Therefore,

$$\frac{100}{7.233} = 13.826 \text{ seconds is the average time interval} \quad (5.3)$$

A measure of the variations in the percent occupancy in lane 1 and lane 2 can be seen by taking the ratio of the standard deviation to the average, respectively.

$$\frac{4.220}{14.66} \times 100 = 28.79\% \text{ in lane 1} \quad (5.4)$$

$$\frac{6.385}{15.570} \times 100 = 41.04\% \text{ in lane 2} \quad (5.5)$$

As seen in Table 5.5, the most sensitive false alarm variable is the percent occupancy in lane 2. It is probable that the high variation in percent occupancy in lane 2 caused many false alarms. This high variation in percent occupancy might be attributable to low traffic with a high average time interval between consecutive vehicles. This hypothesis is confirmed with data from the no-false detector station.

Detector station 5 produced no false alarms in the test. Typical one-hour traffic statistics is shown in Table 5.7.

**Table 5.7 One-Hour Traffic Statistics at Detector Station 5**

	Traffic Control Variables					
	1	2	3	4	5	6
Average	26.133	24.783	33.960	27.167	24.507	33.750
Std. Dev.	2.389	4.639	1.561	1.683	5.697	1.143

The effective green time for the associated phase of the intersection (i.e., node 4) is 97 seconds (i.e., 95 seconds for green, 4 seconds for yellow, and 2 second for the lost time).

The average per lane volume is 26.650 vehicles for that phase. Therefore,

$$\frac{97}{26.650} = 3.640 \text{ seconds is the average time interval} \quad (5.6)$$

Variation in the percent occupancy in lane 1 and lane 2 as shown by the ratio of standard deviation to the average are:

$$\frac{4.639}{24.783} \times 100 = 18.718\% \text{ in lane 1} \quad (5.7)$$

$$\frac{5.697}{24.507} \times 100 = 23.246\% \text{ in lane 2} \quad (5.8)$$

By comparing these results to the detector station with the greatest number of false alarm confirmed that the high variation in percent occupancy due to low traffic be the cause of the high false alarm rate.

## **5.7 Results of the Incident Test**

Results of the incident tests are shown in four sub-sections. First, a partial-blockage in link 34 is shown, followed by a full-blockage in link 34. Next, a partial blockage and a full blockage in link 45 are discussed.

### **5.7.1 Results of One-Lane Blockage in Link 34**

An incident detection evaluation was conducted at both the upstream and the downstream stations. The upstream station (station 3) and the downstream station (station 5) showed the same number of incident detections. A total of 21 out of 30 incidents were detected in both stations. This is a 70 percent detection rate at either detector station. However, the mean detection time in these stations was different. The mean detection

time is 8.286 minutes with a standard deviation of 3.364 for the upstream station while the mean detection time is 4.476 minutes with a standard deviation of 1.250. This results implies that detection efficiency is higher in the downstream detector station.

There are incidents that were detected by the upstream detector station that were not detected by the downstream station, and vice versa. Considering both stations together, all the incidents were detected. The mean detection time for the combined data is 4.8 minutes with the standard deviation of 1.243.

### **5.7.2 Results of Full-Link Blockage in Link 34**

The incident detection algorithm for full-blockages in link 34 was evaluated in the same way. As expected, the impact of a full-blockage is very large. At both the upstream and the downstream detector stations, all 9 incidents were detected regardless of the incident location, respectively. The mean detection time for the upstream station is 6.667 minutes with the standard deviation of 1.414. The mean detection time for the downstream station is 4 minutes with a standard deviation of 1.000. By considering both stations together, the mean detection time is 3.778 minutes with a standard deviation of 0.667. While the incidents were eventually detected by the upstream detector station, all of them were more rapidly detected by the downstream detector station.

### **5.7.3 Results of One-Lane Blockage in Link 45**

Since this link is short (i.e., 530 feet), the impact of an incident is easily detected on either the upstream or the downstream station. All one-lane blockages occurring at the upstream or the middle location were detected by the upstream and downstream detector stations. The mean detection time for the upstream detector station is 2.9 minutes with a standard deviation of 1.373. For the downstream detector station, the mean detection time is 4 minutes with the standard deviation of 0.918. On this link, the overall performance of the upstream detector station was better than the downstream station because no incidents were assumed at the downstream location. By considering both stations, all the incidents were detected as well. The mean detection time is 2.7 minutes with a standard deviation of 1.174.

### **5.7.4 Results of Full-Link Blockage in Link 45**

As expected, all the incidents were detected by either detector station. The mean detector time for the upstream detector station is 2.333 minutes with a standard deviation of 0.817. For the downstream detector station, the mean detection time is 4 minutes with 0.000 standard deviation.

## **5.8 A Sensitivity Test for Various Prediction Intervals**

There is a trade-off among the detection rate, false alarm rate, and the mean detection time. For example, wider upper and lower intervals would be less sensitive in detecting an abnormality of the control variable, resulting in fewer false alarms, but also a lower

detection rate. Narrower intervals would be more sensitive providing more false alarms but better detection rate. If a confirmation check is used to reduce the number of false alarms, then the incident rate and the false alarm rate would be better, but they would require a longer mean detection time.

The previous results were from a test using 95 percent prediction intervals (i.e.,  $2 \sigma_{\hat{x}_k}$  of the predicted control variable estimates for the upper and the lower intervals). Wider intervals using  $2.1 \sigma_{\hat{x}_k}$ ,  $2.5 \sigma_{\hat{x}_k}$ , and for  $3.0 \sigma_{\hat{x}_k}$  were tested with the same incident-free and incident data sets to investigate how the false alarm rate, detection rate, and the mean detection time change.

### 5.8.1 False Alarm Changes over Different Intervals

False alarms were tested with 3 different intervals to see the overall change. These intervals were 2.0, 2.5, and 3.0  $\sigma_{\hat{x}_k}$ . The results are shown in Table 5.8.

**Table 5.8 False Alarm Statistics Changes for 2.0, 2.5, and 3.0  $\sigma_{\hat{x}_k}$**

	Interval (No. of $\sigma_{\hat{x}_k}$ ) Changes		
	2.0	2.5	3.0
FA/2Hr/Network	7.2	1.80	0.60
FA/2Hr/Station	0.3	0.08	0.03
FAR/Hr/Station (%)	0.5	0.08	0.04
FA/2Hr/High Traffic Direction	0.8	0.20	0.00

The number of false alarms decreases as the upper intervals and lower intervals increase. The ratio of the changes in the number of false alarms from 2.0 to 3.0  $\sigma_{\hat{x}_k}$  is significant and one to twelve. At 3.0  $\sigma_{\hat{x}_k}$ , there are no false alarms detected for the high traffic direction.

### **5.8.2 Detection Rate and Mean Detection Time Changes over Different Intervals**

The detection rates and mean detection time of one-lane blockages and full-link blockages in link 34 and link 45 are shown in Table 5.9, 5.10, and 5.11, 5.12, respectively, for the same interval changes.

**Table 5.9 Detection Rates of One-Lane Blockage over 2.0, 2.5, and 3.0  $\sigma_{\hat{x}_k}$  Changes (percent)**

	Detector Location	Interval Changes		
		2.0	2.5	3.0
Link 34	Upstream	70	53.3	46.7
	Downstream	70	56.7	6.7
	Both	100	83.3	46.7
Link 45	Upstream	100	100	100
	Downstream	100	70	5
	Both	100	100	100

**Table 5.10 Detection Rates of Full-Link Blockage over 2.0, 2.5, and 3.0  $\sigma_{\hat{x}_k}$  Changes (percent)**

	Detector Location	Interval (No. of $\sigma$ ) Changes		
		2.0	2.5	3.0
Link 34	Upstream	100	100	88.9
	Downstream	100	100	33.3
	Both	100	100	100
Link 45	Upstream	100	100	100
	Downstream	100	100	0
	Both	100	100	100

**Table 5.11 Mean Detection Time of One-Lane Blockage over 2.0, 2.5, and 3.0  $\sigma_{ik}$  Changes (minutes)**

	Detector Location		Interval Changes		
			2.0	2.5	3.0
Link 34	Upstream	Mean	8.29	9.13	10.71
		Std. Dev.	3.37	3.26	4.61
	Down-stream	Mean	4.48	5.29	5.00
		Std. Dev.	1.25	1.21	1.41
	Both	Mean	4.8	6.00	9.87
		Std. Dev.	1.24	2.38	4.87
Link 45	Upstream	Mean	2.9	9.13	10.71
		Std. Dev.	1.37	3.26	4.61
	Down-stream	Mean	4.00	5.29	5.00
		Std. Dev.	0.92	1.21	1.41
	Both	Mean	2.70	6.00	9.87
		Std. Dev.	1.17	2.38	4.87

**Table 5.12 Mean Detection Time of Full-Link Blockage over 2.0, 2.5, and 3.0  $\sigma_{ik}$  Changes (minutes)**

	Detector Location		Interval Changes		
			2.0	2.5	3.0
Link 34	Upstream	Mean	6.67	7.78	7.75
		Std. Dev.	1.41	2.11	2.25
	Down-stream	Mean	4.00	4.67	6.00
		Std. Dev.	1.00	1.00	0.00
	Both	Mean	3.78	4.44	7.11
		Std. Dev.	0.67	0.88	2.03
Link 45	Upstream	Mean	2.33	2.33	2.67
		Std. Dev.	0.82	0.82	1.03
	Down-stream	Mean	4.00	5.00	N/A*
		Std. Dev.	0.00	1.67	N/A*
	Both**	Mean	2.33	2.33	2.67
		Std. Dev.	0.82	0.82	1.03

\*No detection is made.

\*\*This statistics are the same as that of the upstream station because the upstream station is faster than the downstream station.

For the incident tests, the detection rates and mean detection times were as expected. The detection rate at a  $2.0 \sigma_{\hat{x}_k}$  decreases about 50 percent at a  $3.0 \sigma_{\hat{x}_k}$  on both detector stations for a one-lane blockages in link 34,. The detection time increases about two times from the  $2.0 \sigma_{\hat{x}_k}$  to the  $3.0 \sigma_{\hat{x}_k}$ . The link 45, all the blockages were detected at both stations even at the  $3.0 \sigma_{\hat{x}_k}$  since this link is short. The mean detection time in this link increases about 4 times at the  $3.0 \sigma_{\hat{x}_k}$ . Full-link blockages are much more critical and they were all detected on both stations earlier than one-lane blockages.

### 5.8.3 A Detailed Sensitivity Test for Link 34

Since the statistical changes in the false alarm test and one-lane blockage test in link 34 are relatively change, more detailed interval tests were made using 2.1 to 2.9  $\sigma_{\hat{x}_k}$ . For the network itself, the number of false alarms decreases as the intervals are increased. For the high traffic direction, no false alarms were detected after reaching a  $2.7 \sigma_{\hat{x}_k}$ , as shown in Table 5.13. The results are also shown in Figures 5.5-5.10.

Detection rates for the one-lane blockage in link 34 shows a consistent decrease at both detector stations. These results are shown in Table 5.14, and Table 5.15, respectively. At the upstream detector station the detection rate slowly decreases while the detection rate at the downstream detector station drops sharply after the  $2.5 \sigma_{\hat{x}_k}$  as in Figure 5.11.

Generally the mean detection time at either station increases as intervals go higher. But as seen in Figure 5.12, and Figure 5.13, respectively, the mean detection time fluctuates after the  $2.5 \sigma_{\hat{x}_k}$ . This is due to the reduction in the number of detections. That is, when an incident that was detected at one time step is not detected at the next time step, the number of recorded detections is reduced. The mean detection time computed with the lower number of detections may also be reduced. For example, at the  $2.5 \sigma_{\hat{x}_k}$ , the detection rate for the downstream detector station is 56.7 percent (17 detections out of 30 incidents) while the detection rate at the  $2.6 \sigma_{\hat{x}_k}$  is 46.7 percent (14 detections out of 30 incidents). The simple mean detection time at the  $2.5 \sigma_{\hat{x}_k}$  is 5.25 minutes while it is 5.14 minutes at the  $2.6 \sigma_{\hat{x}_k}$  because one of detections (i.e. 8 minutes of detection time) was missed, resulting in a lower mean detection time. Overall, the detection time, when considering both stations together, consistent increases as the  $\sigma_{\hat{x}_k}$  increase as seen in Figure 5.14.

The detection rate and the mean detection time of the full-link blockages in link 34 are shown in Table 5.16, and Table 5.17, respectively. Since the impact of these blockages are large, all the blockages are eventually detected at all intervals at both stations. The detection rate at the downstream detector station shows drops suddenly after  $2.5 \sigma_{\hat{x}_k}$  while the upstream station shows a nearly constant rate until  $2.8 \sigma_{\hat{x}_k}$ . These results are shown in Figure 5.15.

The mean detection time at the upstream station shows a rather consistent pattern after  $2.4 \sigma_{\hat{x}_k}$  while this value consistently increases at the downstream station. However, the

mean detection time is still shorter at the downstream station. By considering both stations together, the mean detection time consistently increases. They are shown in Figures 5.16-5.18. The standard deviation of the mean detection time at each generally increases as the  $\sigma_{\dot{x}_k}$  increases.

Table 5.13 False Alarm Changes over Different Intervals

	Unit	Interval Changes										
		2.0	2.1	2.2	2.3	2.4	2.5	2.6	2.7	2.8	2.9	3.0
Network	FA/10Hr/ Network	36	23	21	15	12	9	8	7	5	4	3
	FA/2Hr/ Network	7.2	4.6	4.2	3.0	2.4	1.8	1.6	1.4	1	0.8	0.6
	FA/Hr/ Station	0.150	0.096	0.088	0.063	0.050	0.038	0.033	0.029	0.021	0.017	0.013
	FA/2Hr/ Station	0.3	0.192	0.175	0.125	0.100	0.075	0.067	0.058	0.042	0.033	0.025
High Traffic Direction	FAR(%) /Hr/ Station	0.5	0.319	0.292	0.208	0.167	0.125	0.111	0.097	0.070	0.057	0.042
	FA/10Hr/ Direction	4	4	3	2	1	1	1	0	0	0	0
	FA/2Hr/ Direction	0.800	0.800	0.6	0.4	0.2	0.2	0.2	0.0	0.0	0.0	0.0
	FA/Hr/ Station	0.033	0.033	0.025	0.017	0.008	0.008	0.008	0.000	0.000	0.000	0.000
Direction	FA/2Hr/ Station	0.067	0.067	0.050	0.033	0.017	0.017	0.017	0.000	0.000	0.000	0.000
	FAR(%) /Hr/ Station	0.111	0.111	0.083	0.056	0.028	0.028	0.028	0.000	0.000	0.000	0.000

**Table 5.14 Detection Rate Changes for One-Lane Blockage in Link 34 over Different Intervals (percent)**

Detector Location	Interval Changes										
	2.0	2.1	2.2	2.3	2.4	2.5	2.6	2.7	2.8	2.9	3.0
Upstream	70	63.3	63.3	56.7	53.3	53.3	50.0	46.7	46.7	46.7	46.7
Downstream	70	66.7	63.3	60.0	60.0	56.7	46.7	36.7	20.0	10.0	6.7
Both	100	100	96.7	86.7	83.3	83.3	76.7	70.0	60.0	50.0	46.7

**Table 5.15 Mean Detection Time Change for One-Lane Blockage in Link 34 over Different Intervals (minutes)**

	Interval Changes										
	2.0	2.1	2.2	2.3	2.4	2.5	2.6	2.7	2.8	2.9	3.0
Upstream	7.78	7.79	8.32	8.82	8.88	9.13	9.2	9.43	9.71	10.71	10.71
Downstream	2.90	2.82	3.35	3.17	3.26	3.26	3.36	3.37	3.31	4.61	4.61
Both	4.48	4.5	4.53	5	5.11	5.25	5.14	5.09	5.67	5.33	5.0
Std. Dev.	1.25	1.28	1.31	1.41	1.23	1.24	1.03	1.04	0.82	1.15	1.41
Mean	4.8	4.93	5.31	5.77	5.76	6.0	6.35	6.85	8.11	9.47	9.87
Std. Dev.	1.24	1.36	2.47	2.49	2.40	2.38	2.93	3.20	3.32	4.93	4.87

**Table 5.16 Detection Rate Change for Full-Link Blockage in Link 34 over Different Intervals (percent)**

Detector Location	Interval Changes										
	2.0	2.1	2.2	2.3	2.4	2.5	2.6	2.7	2.8	2.9	3.0
Upstream	100	100	100	100	100	100	100	100	100	88.89	88.89
Downstream	100	100	100	100	100	100	77.78	66.67	66.67	55.56	33.33
Both	100	100	100	100	100	100	100	100	100	100	100

**Table 5.17 Mean Detection Time Change for Full-Link Blockage in Link 34 over Different Intervals (minutes)**

	Interval Changes										
	2.0	2.1	2.2	2.3	2.4	2.5	2.6	2.7	2.8	2.9	3.0
Upstream	Mean	6.67	6.89	6.89	7.11	7.78	7.78	7.78	7.78	7.75	7.75
	Std. Dev.	1.41	1.45	1.45	1.45	2.11	2.11	2.11	2.11	2.25	2.25
Downstream	Mean	4.00	4.00	4.22	4.44	4.67	4.57	4.67	5.67	5.6	6.00
	Std. Dev.	1.00	1.00	1.22	0.88	1.00	0.98	1.03	0.82	0.89	0.00
Both	Mean	3.78	3.78	4.00	4.22	4.44	4.44	4.89	6.22	6.67	7.11
	Std. Dev.	0.67	0.67	1.00	0.67	0.88	1.45	2.19	1.86	2.24	2.03

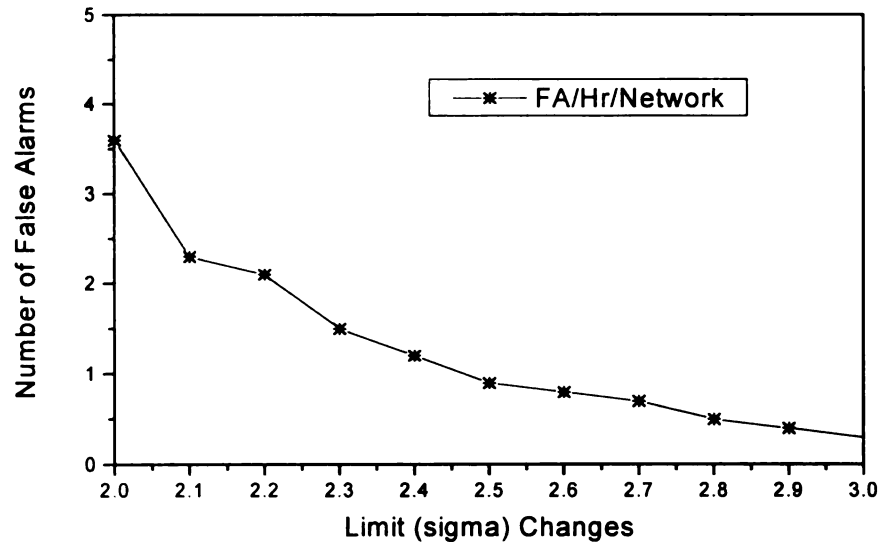


**Figure 5.5 Number of False Alarms for the Network over  $\sigma_{\hat{x}_k}$  Changes**

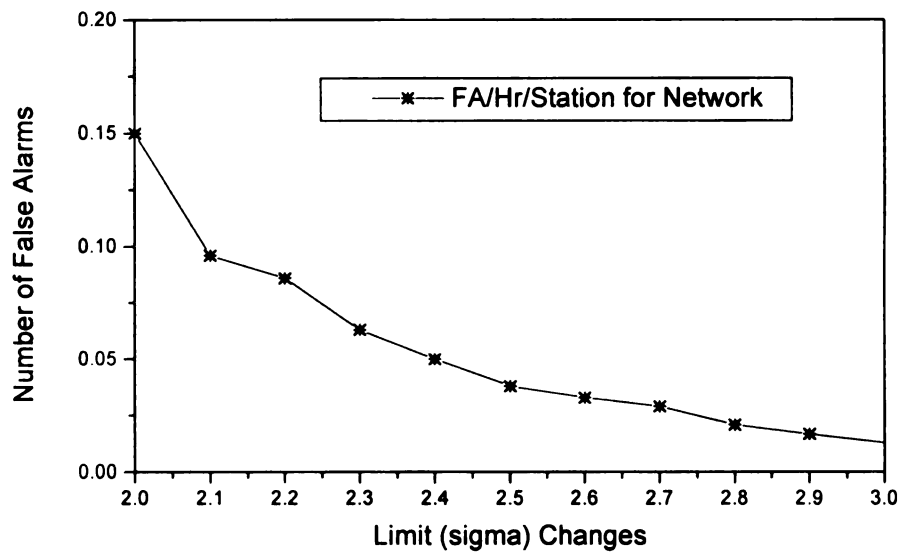


**Figure 5.6 Number of False Alarms per Station for the Network over  $\sigma_{\hat{x}_k}$  Changes**

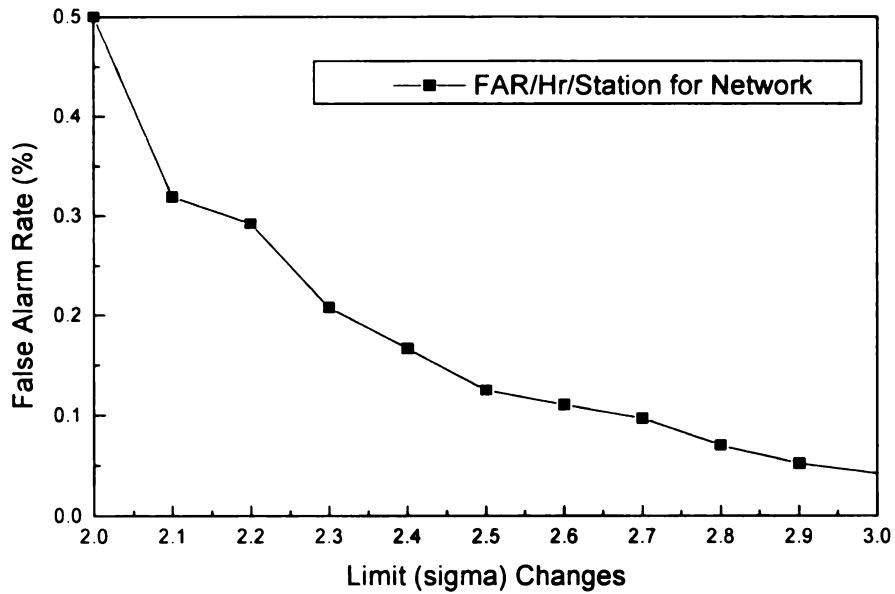


**Figure 5.7 False Alarm Rate per Station for the Network over  $\sigma_{\hat{x}_k}$  Changes**

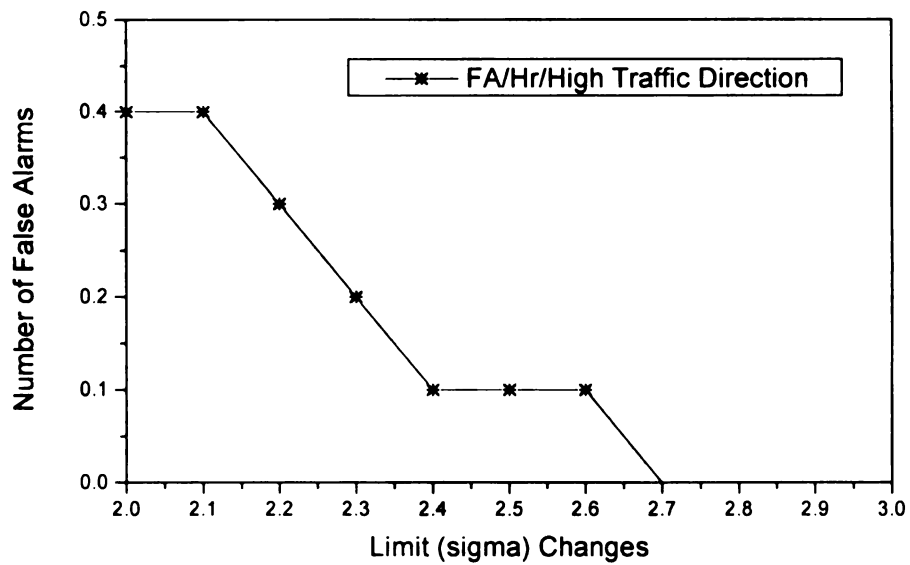


**Figure 5.8 Number of False Alarms for High Traffic Direction over  $\sigma_{\hat{x}_k}$  Changes**

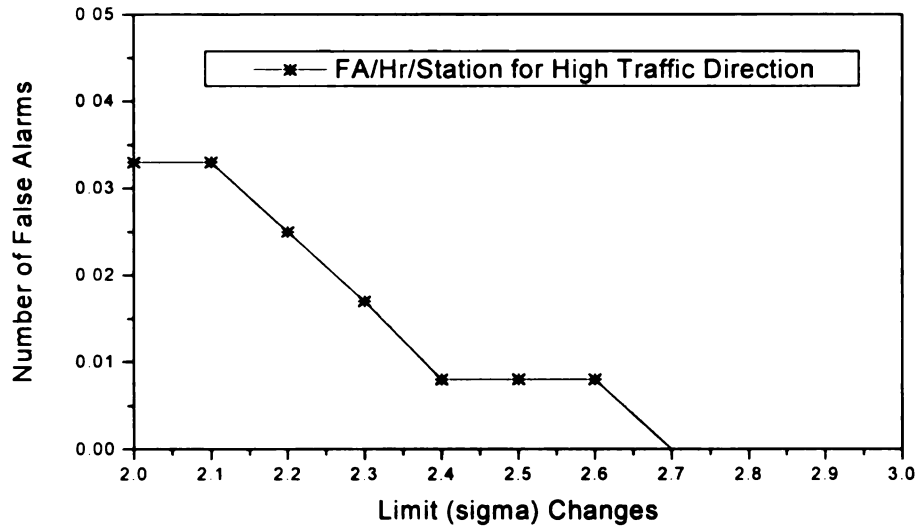


**Figure 5.9 Number of False Alarms per Station for High Traffic Direction over  $\sigma_{\hat{x}_k}$  Changes**

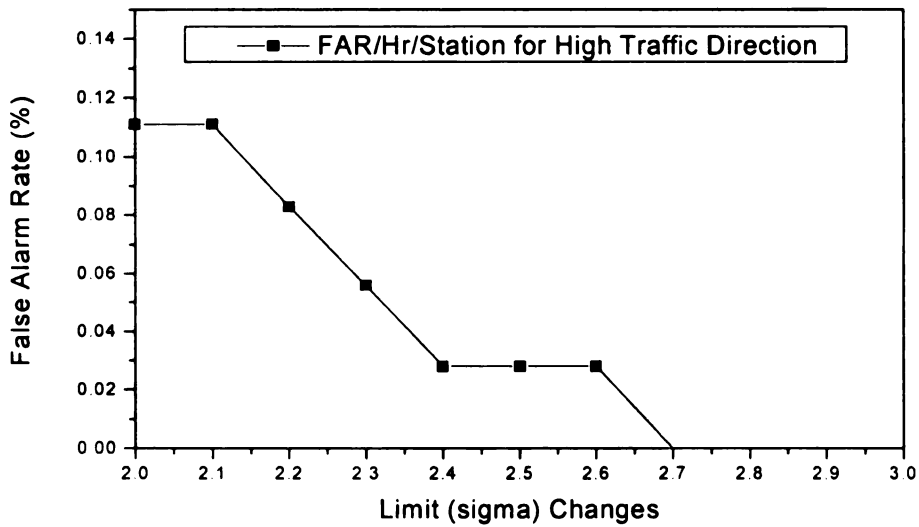


**Figure 5.10 False Alarm Rate per Station for High Traffic Direction over  $\sigma_{\hat{x}_k}$  Changes**

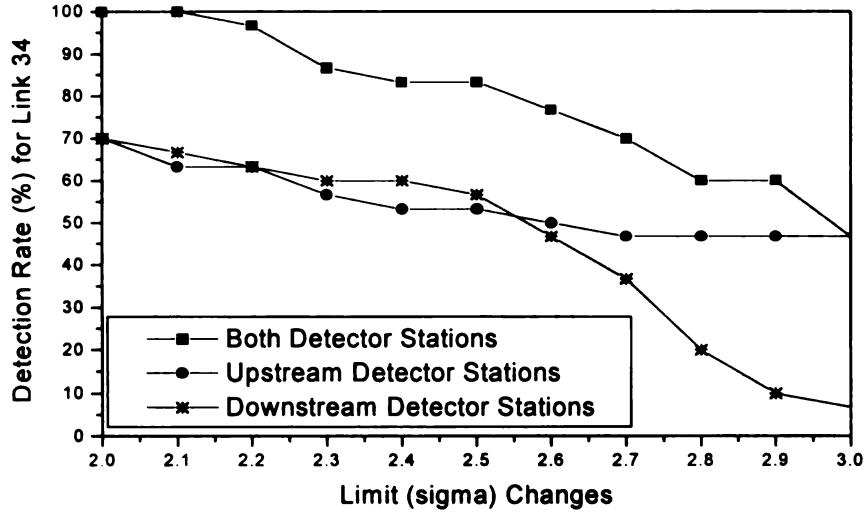


**Figure 5.11 Detection Rate Changes for One-Lane Blockage in Link 34 over Interval Changes**

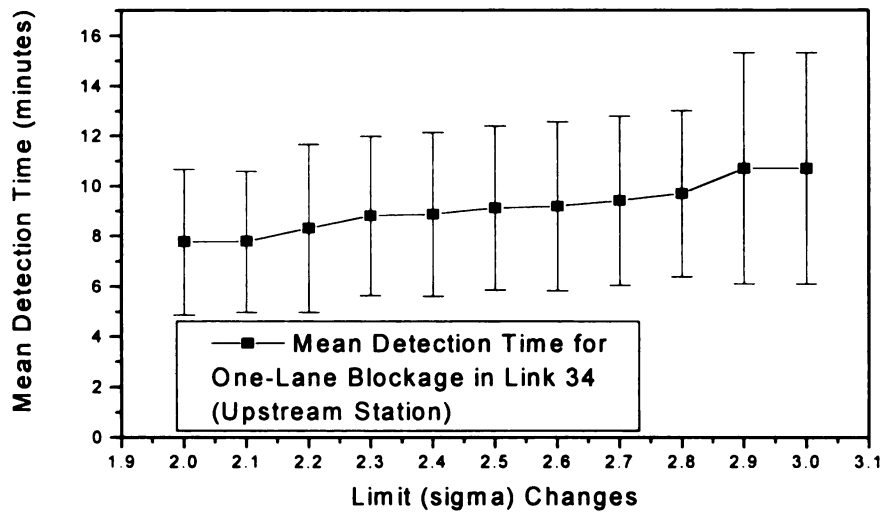


**Figure 5.12 Mean Detection Time (minutes) for One-Lane Blockage in Link 34 with Bars of One Standard Deviation (Upstream Station)**

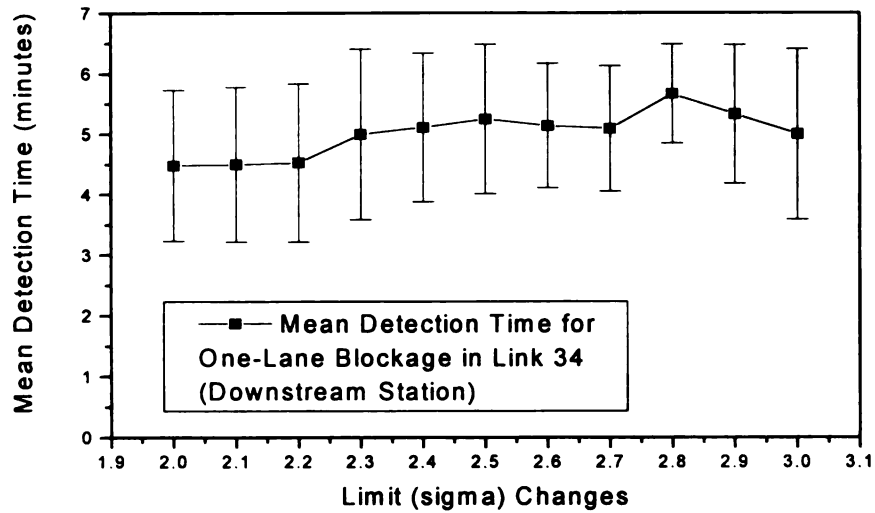


**Figure 5.13 Mean Detection Time (minutes) for One-Lane Blockage in Link 34 with Bars of One Standard Deviation (Downstream Station)**

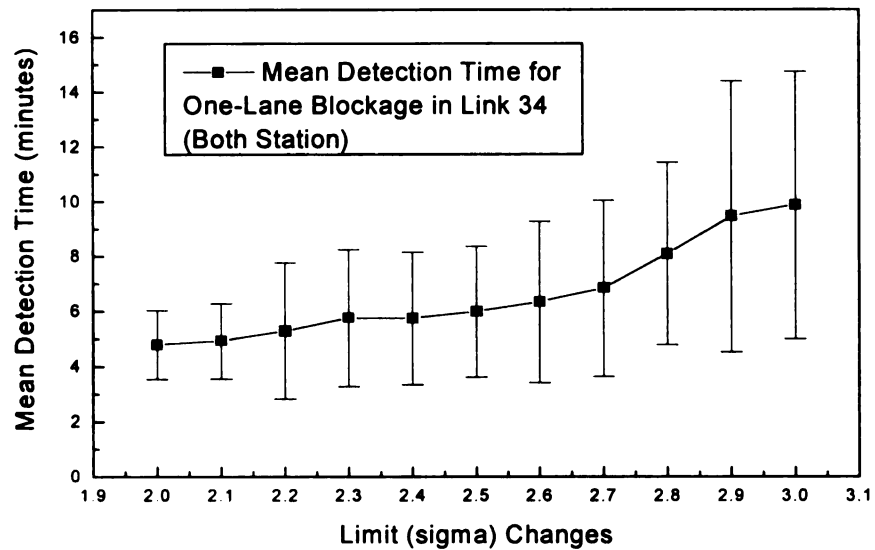


**Figure 5.14 Mean Detection Time (minutes) for One-Lane Blockage in Link 34 with Bars of One Standard Deviation (Both Upstream and Downstream Stations)**

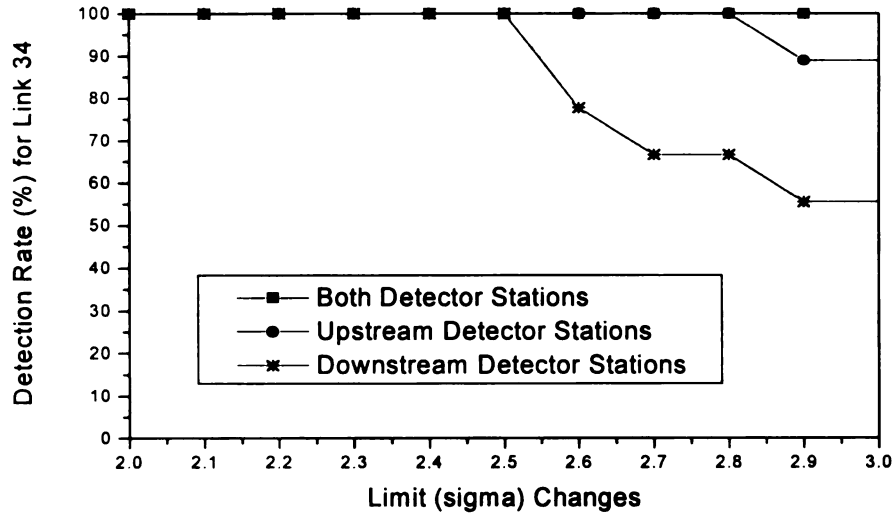


**Figure 5.15 Detection Rate Changes for Full-Link Blockage in Link 34 over Interval Changes**

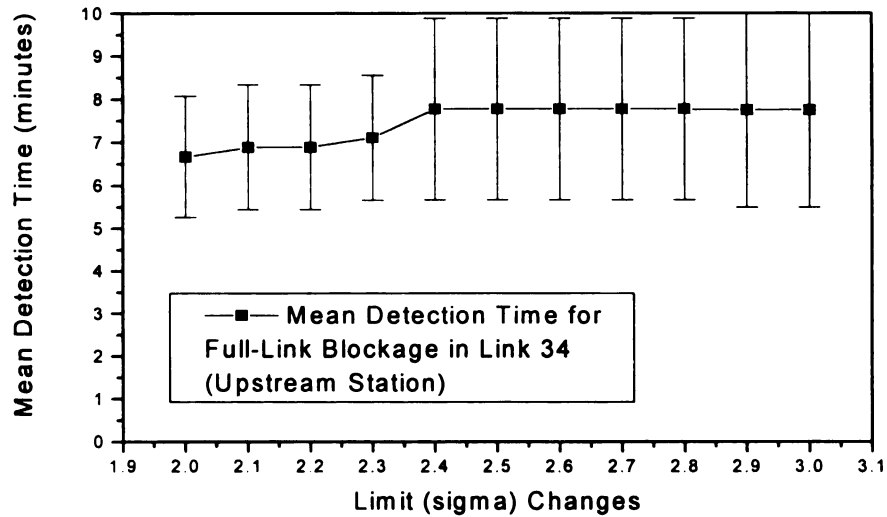


**Figure 5.16 Mean Detection Time (minutes) for Full-Link Blockage in Link 34 with Bars of One Standard Deviation (Upstream Station)**

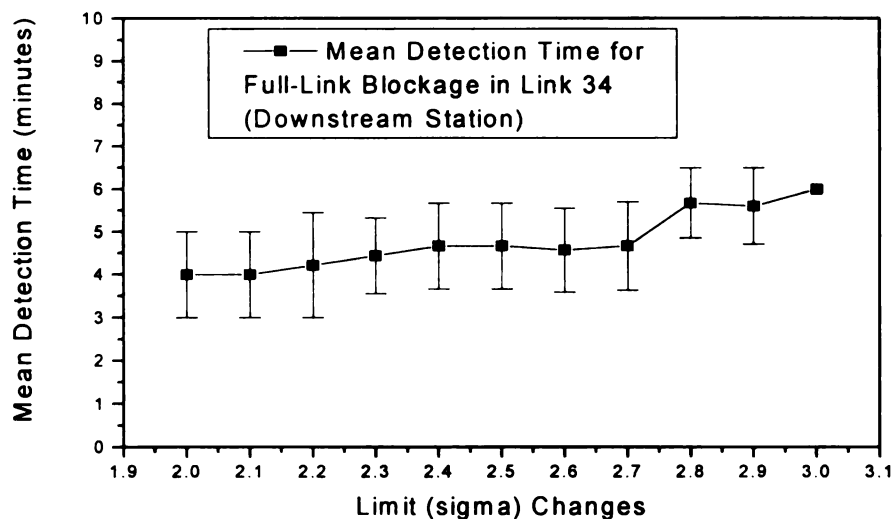


**Figure 5.17 Mean Detection Time (minutes) for Full-Link Blockage in Link 34 with Bars of One Standard Deviation (Downstream Station)**

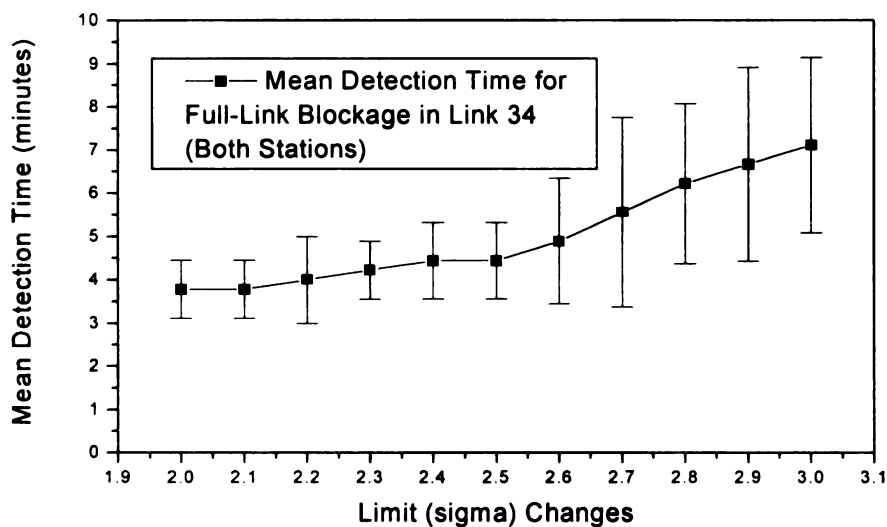


**Figure 5.18 Mean Detection Time (minutes) for Full-Link Blockage in Link 34 with Bars of One Standard Deviation (Both Stations)**

#### 5.8.4 Determination of Recommended Intervals

As seen in Tables 5.13-5.17 and Figures 5.5-5.18, the false alarm rate has an inverse relationship with the detection rate as  $\sigma_{\hat{x}_k}$  increases. Generally the mean detection time also increases as  $\sigma_{\hat{x}_k}$  increases. These changes in the false alarm rate, the detection rate, and the mean detection time can be expressed by the change in the slope of the relationship. These slope changes are shown in Table 5.18-5.20. The detection rate and the mean detection time were investigated only for link 34 and 45. Therefore, the relationship between false alarms, detection rate and corresponding mean detection time does not necessarily precisely represent the relationship for all links in a network.

The recommended  $\sigma_{\hat{x}_k}$  values were found by analyzing the results for both the network as a whole, and for the high traffic direction. These values are found by analyzing the false alarm rate and the mean detection time for intervals where the detection rate is 100 percent for both one-lane blockages and full-link blockages.

For the network as a whole, a 100 percent detection rate was found at 2.0 and 2.1  $\sigma_{\hat{x}_k}$  for the one-lane blockage and full-link blockage in link 34, respectively. The corresponding number of false alarms are 7.2 and 4.6, respectively, if the system were operated for 2 hours a day. The mean detection time for the one-lane blockages is 4.80 and 4.93 minutes at these respective intervals. The mean detection time for a full-link blockage is identical (3.78 minutes) at these respective intervals. As can be seen in Table 5.18-5.20, the slope change for false alarms is the largest, and the slope change for mean

detection time is the smallest at  $2.1 \sigma_{\hat{x}_k}$  for the one-lane blockage. The slope change of the mean detection time for full-link blockages is not changed.

For the high traffic direction (from east to west), the detection rate is 100 percent for values up to  $2.1 \sigma_{\hat{x}_k}$ . The corresponding false alarms in this direction showed no slope changes from  $2.0$  to  $2.1 \sigma_{\hat{x}_k}$ . The corresponding slope of the mean detection time for a one-lane blockage is 0.13 (from 4.80 minutes to 4.93 minutes) at  $2.1 \sigma_{\hat{x}_k}$ . The full-link blockage again show no change. From these results, it is recommended that a value of  $2.0 \sigma_{\hat{x}_k}$  defines the best interval, because there are no changes in false alarms and the mean detection time and the gain in the mean detection time is greatest in this interval for  $2.0 \sigma_{\hat{x}_k}$  to  $2.1 \sigma_{\hat{x}_k}$ .

These results are summarized in Table 5.21. It should be noted that if the cycle length were less than 120 seconds, then the mean detection time would be lower. For example, the 4.93 minutes to detect a one-lane blockage in link 34 would be reduced to 2.47 minutes if the cycle length were 60 seconds.

**Table 5.18 Change in False Alarms over Different Intervals**

	Unit	Interval Changes										
		2.0	2.1	2.2	2.3	2.4	2.5	2.6	2.7	2.8	2.9	3.0
Network	FA/2Hr/ Network	7.2	4.6	4.2	3.0	2.4	1.8	1.6	1.4	1	0.8	0.6
	SC (-)*	0.0	2.6	0.4	1.2	0.6	0.6	0.2	0.2	0.4	0.2	0.2
High Traffic Volume Direction	FA/2Hr/ Direction	0.8	0.8	0.6	0.4	0.2	0.2	0.2	0	0	0	0
	SC (-)*	0.0	0.0	0.2	0.2	0.2	0.0	0.0	0.2	0.0	0.0	0.0

\*Slope Change: (-) indicates a negative slope change and (+) a positive slope change

**Table 5.19 Change in DR and MDT for One-Lane Blockages over Different Intervals (Both Stations)**

Unit	Interval Changes										
	2.0	2.1	2.2	2.3	2.4	2.5	2.6	2.7	2.8	2.9	3.0
DR	100	100	96.7	86.7	83.3	83.3	76.7	70.0	60.0	50.0	46.7
SC(-)	0.0	0.0	3.3	10.0	3.4	0.0	6.6	6.7	10.0	10.0	3.3
MDT	4.8	4.93	5.31	5.77	5.76	6.0	6.35	6.85	8.11	9.47	9.87
SC(+)	0.0	0.13	0.38	0.46	-0.01	0.24	0.35	0.5	1.26	1.36	0.40

**Table 5.20 Change in DR and MDT for Full-Link Blockages over Different Intervals (Both Stations)**

Unit	Interval Changes										
	2.0	2.1	2.2	2.3	2.4	2.5	2.6	2.7	2.8	2.9	3.0
DR	100	100	100	100	100	100	100	100	100	100	100
SC(-)	0.0	0.0	0.0	0.0	0.0	0.0	0.0	0.0	0.0	0.0	0.0
MDT	3.78	3.78	4.00	4.22	4.44	4.44	4.89	5.56	6.22	6.67	7.11
SC(+)	0.00	0.00	0.22	0.22	0.22	0.00	0.45	0.67	0.66	0.45	0.44

**Table 5.21 Results of Incident Detection Performance at Recommended Intervals**

			Network ( $2.1 \sigma_{ik}$ )	High Traffic Direction ( $2.0 \sigma_{ik}$ )
False Alarm		FA/10 Hr/Network	23	4
		FA/Hr/Station	0.096	0.033
		FAR/Hr/Station (%)	0.319	0.111
Link 34	One-Lane Blockage	DR (%)	100	100
		MDT (minute)	4.93 (1.36*)	4.8 (1.24*)
	Full-Link Blockage	DR (%)	100	100
		MDT (minutes)	3.78 (0.67*)	3.78 (0.67*)

\*Standard Deviation

### 5.9 Parameter Estimation for Different Conditions

In this section, the state-space model for different geometric and traffic conditions are varied. The values of  $\Phi$  for these different conditions are plotted to see how they change over time and under different conditions.

Test locations were selected based on geometry and traffic volumes. Four links in the network were selected for the test. They were link 34, link 45, link 89, and link 910. Link 34 represents high traffic and long distance, while link 45 is high traffic and short distance. Link 89 is low traffic and long distance, and link 910 is low traffic and short distance. The characteristics of these links are shown in Table 5.22.

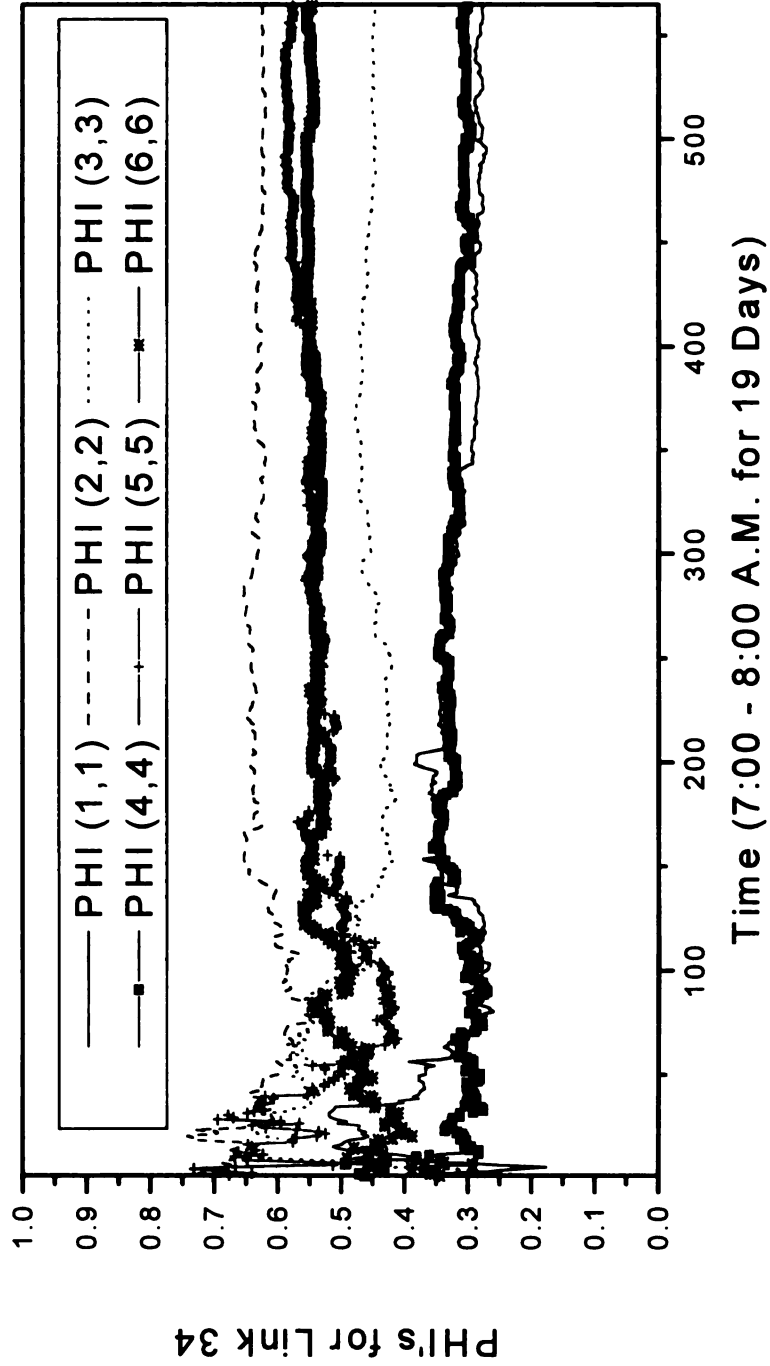
**Table 5.22 Characteristics of Selected Links**

<b>Selected Links</b>	<b>Link Length (feet)</b>	<b>Entering Traffic Volume for the Link (vph)</b>
34	2100	1870
45	530	1696
89	2900	890
910	925	940

Simulations were run for 20 days, with one hour of simulation representing one day. The first day was used for initialization, with the remaining 19 days were used to obtain parameter stabilization.

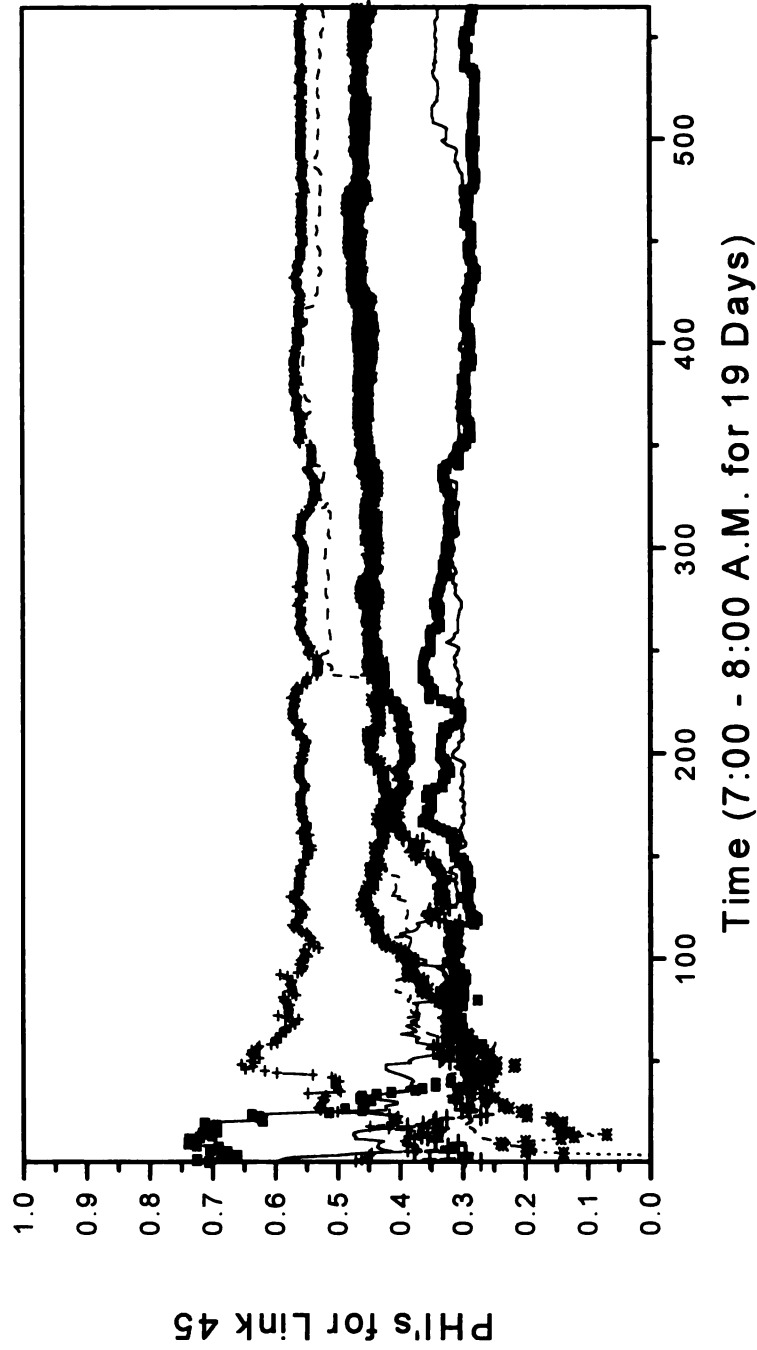
Plots of these parameters for various conditions are shown in Figure 5.19.  $\Phi(1,1)$  represents the error covariance of the flow,  $\Phi(2,2)$  the error covariance of the percent

occupancy,  $\Phi(3,3)$  the error covariance of the average speed in lane 1 while  $\Phi(4,4)$ ,  $\Phi(5,5)$ , and  $\Phi(6,6)$  represent the error covariance of the flow, percent occupancy, and average speed in lane 2, respectively. In these figures, the parameters fluctuate for the first part of the time period, and then become stable. These fluctuations are different under different conditions. For example,  $\Phi(1,1)$  at link 34 begins to concentrate at about one-fourth of the time period to around 0.27 while  $\Phi(1,1)$  at link 89 begins to concentrate about one-third of the time period to around 0.1. Other  $\Phi$ 's show different patterns under different conditions as well.



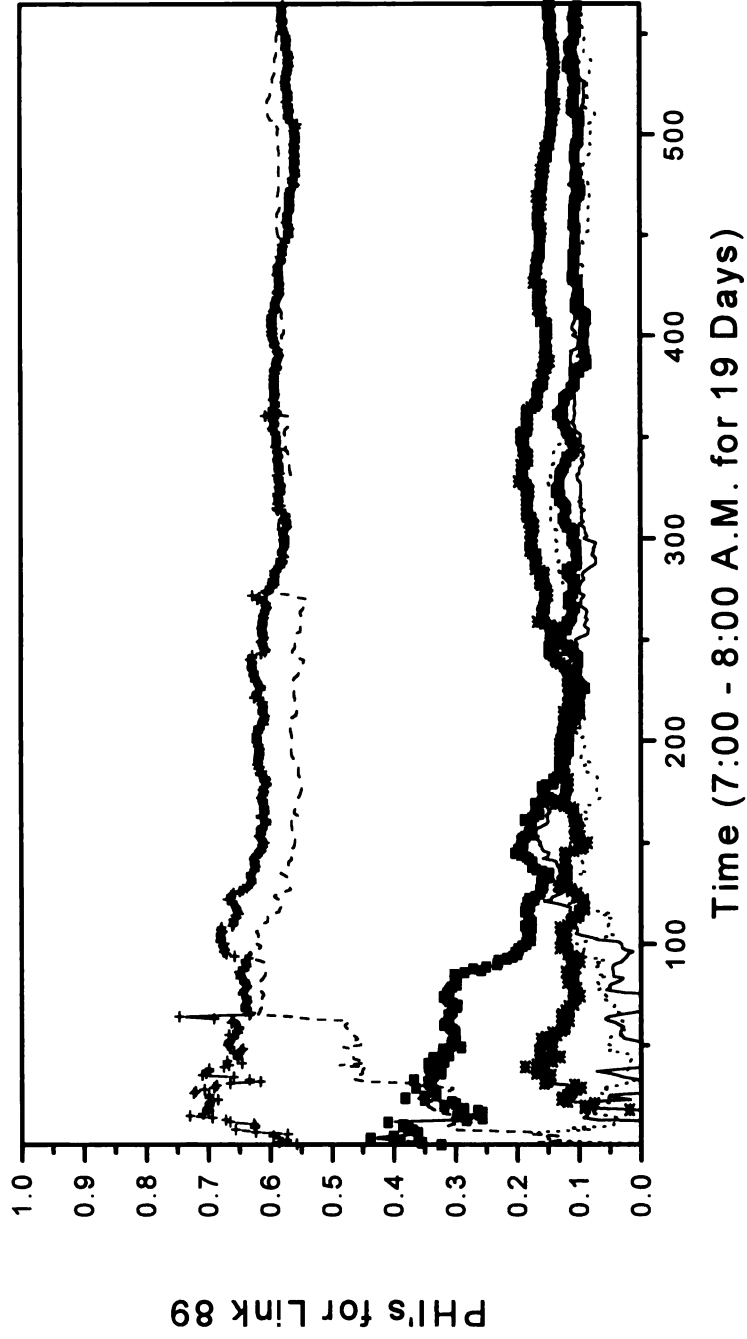
(a) PHI Changes at link 34

Figure 5.19 Parameter ( $\Phi$ ) Patterns in Different Geometric and Traffic Conditions



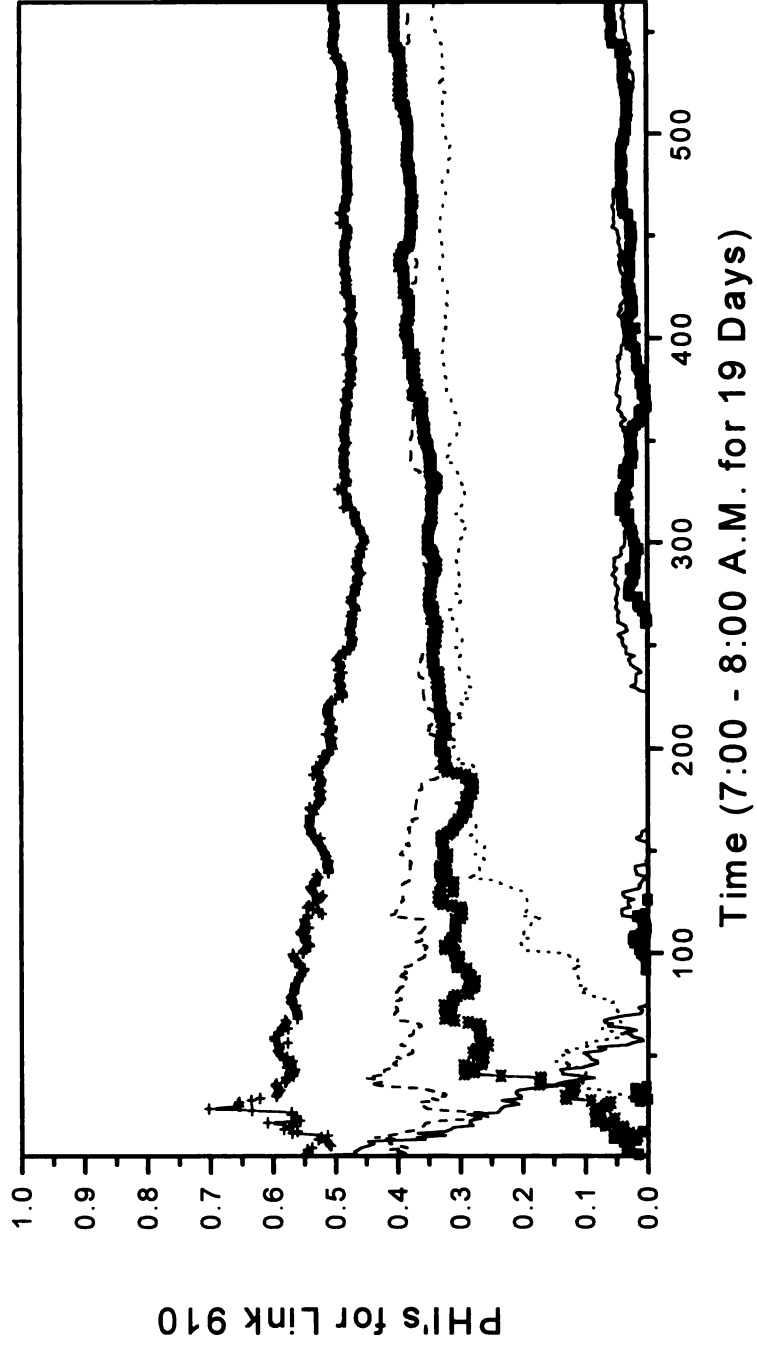
(b) PHI Changes at link 45

Figure 5.19 (cont'd)



(c) PHI Changes at link 89

Figure 5.19 (cont'd)



(d) PHI Changes at link 910

Figure 5.19 (cont'd)

## 5.10 Summary of TRAF-NETSIM Simulation Results

Simulations using the TRAF-NETSIM program were made to generate incident-free and incident data in order to evaluate the incident detection algorithm. The network simulated was Washtenaw Avenue located in Ann Arbor, Michigan. The traffic variables obtained from the simulation for the algorithm were traffic counts, percent occupancy, and average speed in each lane.

### 5.10.1 A Test at 95 Prediction Intervals ( $2.0 \sigma_{ik}$ )

Two tests were conducted: an incident-free test, and an incident test.

Incident-free data sets were generated for a false alarm check. One-hour of simulation representing a weekday peak hour were conducted for generating the normal A.M. peak hour condition. A total of ten-days of incident-free data were generated. The raw data from detectors were smoothed using a moving average with 3 time intervals. The records were then aggregated in 2 minute time slice for analysis. Incidents were indicated by checking the upper and the lower intervals constructed with 2 standard deviations of the predicted error covariance.

Results of this test show a total of 7.2 false alarms for the network if the system were operated 2 hours per weekday. This converts to 0.15 false alarms per hour per station. For the high volume traffic direction (from east to west), a total of 0.8 false alarms occurred when the system was simulated for 2 hours a weekday. This is 0.033 false alarms per hour per station.

Incident data sets were also generated to test the performance of the algorithm. Link 34 and 45 were selected to represent different geometric characteristics under high volume traffic conditions (i.e., long distance and short distance, respectively). A total of 65 incidents were generated. For link 34, a total of 39 incidents were simulated at different locations. For link 45, a total of 26 incidents were simulated.

By considering the upstream and the downstream detector stations together, the detection rate of one-lane blockages was 100 percent for both link 34 and link 45. The mean detection time for each link is 4.8 minutes and 2.7 minutes, respectively. The detection rate of full-link blockages showed 100 percent for each link, with a mean detection time of 3.78 and 2.33 minutes, respectively.

### **5.10.2 A Sensitivity Test for Various Prediction intervals**

Various prediction intervals from 2.0 to 3.0  $\sigma_{\hat{x}_k}$  were applied to test a trade-off between false alarms and detection rate on link 34. The corresponding mean detection time was also investigated. As expected the false alarms decreased as the intervals became wider and the detection rate was decreased. The mean detection time shows a consistent increase as the interval became wider.

For the network, if the system were operated for 2 hours a day, there would be reasonable number of false alarms (4.6), perfect detection rate, and reasonable mean detection time (4.93, and 3.78 minutes, respectively) using a 2.1  $\sigma_{\hat{x}_k}$ . Wider prediction intervals result in the algorithm failing to detect incidents and long mean detection time.

For the high volume traffic direction, there is less than one false alarm per day using a  $2.0 \sigma_{\hat{x}_k}$ . Detection rate at this interval was 100 percent with a mean detection time of 4.8 minutes and 3.78 minutes for one-lane blockages and full-link blockages. Therefore,  $2.0 \sigma_{\hat{x}_k}$  prediction intervals are appropriate for the high volume traffic direction.

### 5.10.3 Parameter Estimation for Different Conditions

The parameter ( $\Phi$ ) in the state-space model was investigated under different geometric and traffic volume conditions. Links 34, link 45, link 89, and link 910 were selected to represent high traffic and long distance, high traffic and short distance, low traffic and long distance, and low traffic and short distance, respectively. Plots of  $\Phi$  on these different links show different patterns. These parameters concentrate on and change as new measurements from different geometry and temporal traffic flow are obtained.

Conventional incident detection algorithms, such as the California algorithm, the Bayesian approach, the Exponential Smoothing algorithm, and the Box-Jenkins Technique-based algorithm are not advantageous in this aspect because they utilize fixed parameters. However, an adaptive model-based algorithm as used in this study is advantageous by utilizing flexible parameters to represent different spatial and temporal conditions, reducing the disadvantage of the fixed-parameter model.

## **Chapter 6**

### **CONCLUSIONS AND DISCUSSION**

#### **6.1 Conclusions**

In this section, the findings of this research are summarized. Also, the comparison with previous incident detection algorithms for arterial streets is discussed.

##### **6.1.1 Summary of the Research**

This section briefly summarizes the research results.

1. In the literature reviewed, the theoretical background and limitation of various freeway and arterial street algorithms were examined. No algorithm could be defined as the best for all applications since no direct comparisons were available for all the different conditions. Commonly found issues were: data dependency, transferability, adaptability, and availability.
2. An incident detection algorithm was developed based on the Kalman filtering algorithm. Some modifications were made to the algorithm to assist in defining an incident. The common cycle length over a controlled network was determined to be the best data sampling time interval. This aggregation reduces data fluctuations due to different phases of a signal. Also, it was determined that point information from a



single detector at an intersection approach was essential since there are many forces that disturb the traffic flow between successive detectors on an urban arterial street.

3. A state-space model and a measurement model were constructed. Traffic flow dynamics on an urban arterial street was represented by a transition matrix. The time-dependent noisy term in the state-space model was also determined. An incident was identified by using the upper and lower intervals obtained from the predicted error covariance, compared with filtered estimates of the traffic control variables.
4. The incident detection algorithm was applied to field incident-free and incident data sets. The purpose of the test was to fit the obtained data into the state-space model and estimate states with the noisy flow and speed data. The field data were collected by using experimental detectors on Hagadorn Road in East Lansing, Michigan. Raw data (traffic flow and speed) were then aggregated in 3 minute time slices and smoothed by a moving average over 3 time intervals to eliminate impulsive noises. Field data which included an incident were obtained from Harrison Road in East Lansing, Michigan. Raw data were aggregated and smoothed in the same way as the Hagadorn Road data. Results showed good tracking of predicted and filtered estimates in the incident-free data, as there were no filtered estimates beyond the 95 percent prediction intervals. The corresponding scatter plots for residuals of traffic flow and average speed showed good randomness around zero.

Results from the incident-data showed the potential for detecting abnormality in arterial street traffic flow. The plots of these variables versus time (Figure 4.7) show how traffic flow and speed change when there is an incident. These figures showed good potential in detecting incidents.

5. The incident detection algorithm was also tested with simulated data. The TRAF-NETSIM, Version 5 was used to simulate incident-free and incident data sets. Washtenaw Avenue located in Ann Arbor, Michigan was selected as the network to represent a real-world situation. The arterial street was optimized using a 120 second signal cycle length. This signal cycle length was also used as the data sampling time interval. Raw data (traffic flow, percent occupancy, and average speed) for the A.M. peak hour was obtained and smoothed by the moving average of three orders.

Ten hours (one hour represents one-day) of incident-free data was simulated, resulting in 300 records at each detector station. A total of 7,200 records of data were generated for the 24 detector stations in the network. To generate incident data, two links were selected to represent various geometry (a long and short link length) with high traffic volume. Various incidents were generated. They included partial blockages and full-link blockages at various locations with various duration. As a result, a total of 65 incidents were generated. Both the incident-free and incident data were tested using the 95 percent prediction interval (i.e.,  $2 \sigma_{\hat{x}_k}$ ).

Results for the incident-free data showed that a total of 36 false alarms over 10 hours were indicated in the network. This is 0.15 false alarms per hour per station. The corresponding false alarm rate is 0.5 percent per hour per station for the network. For the direction of the high volume traffic (e.g., from east to west), a total of 4 false alarms were indicated over 10 hours. This is 0.033 false alarms per hour per station. The corresponding false alarm rate is 0.111 percent per hour per station. As expected, the incident detection algorithm showed better performance in the high traffic flow direction than light traffic flow direction.

Results for the incident data showed a detection rate of 100 percent at both the upstream and the downstream stations for one-lane blockages and full-link blockages in the two links tested, link 34 and link 45. The mean detection time for a one-lane blockage was 4.8 minutes with a standard deviation of 1.24 for both stations on link 34. On link 45, the mean detection time was 2.7 minutes with a standard deviation of 1.17. For full-blockages, the mean detection time was 3.78 minutes with a standard deviation of 0.67 for link 34 and 2.33 minutes with a standard deviation of 0.82 for link 45. The analysis showed that the downstream detector station had a lower mean detection time.

A sensitivity test for prediction intervals was conducted to search for a recommended criterion. For the network, a reasonable false alarm rate (0.319 percent) with a perfect detection rate (100 percent for one-lane blockages and full-link blockages) and a reasonable mean detection time (4.93 minutes with a standard deviation of 1.24 for one-lane blockages and 3.78 minutes with a standard deviation of 0.67 for full-link blockages, respectively) were found when using a  $2.1 \sigma_{\hat{x}_k}$ . For the high traffic volume direction, the algorithm showed good performance at  $2.0 \sigma_{\hat{x}_k}$ . That is, 0.111 percent false alarm rate, 100 percent detection rate for one-lane blockages and full-blockages and 4.8 minutes for the mean detection time with a standard deviation of 1.24 for one-lane blockages and 3.78 minutes for the mean detection time with a standard deviation of 0.67 for full-link blockages, respectively.

### **6.1.2 Comparison with Previous Studies**

This section discusses the performance results of existing incident detection algorithms on arterial streets. Their test conditions are also mentioned. Then, the performance of these algorithms are compared with the algorithm developed in this research. It should be noted that the comparison of the algorithms do not represent absolute superiority and inferiority, because the condition under which these algorithms have been tested is different.

The incident detection system developed by Chen (1994) used a 750 foot long three lane link to test the algorithm. This link contained two detector stations located at both the upstream and downstream ends. The cycle length was 60 seconds. TRAF-NETSIM was used to generate incidents. A total 72 observations were generated for normal traffic conditions, and 60 cases were simulated for incidents with one-lane blockages and two-lane blockages on the link. These cases were evenly divided for peak and off-peak periods (18 cases for one-lane closures and 12 cases for two-lane closures). Incidents were located in the center of the link. The three control variables were used: downstream speed, flow and occupancy. The time unit for data aggregation was 30 seconds. The results of the incident detection system were a 96.7 percent detection rate, a 12.8 percent false alarm rate, and a 240.0 seconds for the mean detection time when traffic flow is less than 900 vehicles per hour per lane. For traffic flow greater than or equal to 900 vehicle per hour per lane, the algorithm resulted in a 100 percent detection rate, a 13.1 percent false alarm rate, and 60 seconds of mean detection time.

The detection rate and the mean detection time in Chen's study are good in the congested condition. Compared to the results in this research, the detection rate is the

same and the mean detection time is better (60 seconds). For the algorithm developed in this research, a simple mean of the mean detection time would be 3.4 minutes for all the incidents in link 34 and link 45 using a  $2.0 \sigma_{\hat{x}_k}$  for A.M. peak hours. However, the data aggregation methodology is different, and the detector configuration in Chen's study is not practical due to the requirement for multiple detectors in a link. The false alarm rate in Chen's study is much higher (13.1 percent) than that of this algorithm (0.111 percent per hour per station for the high traffic volume direction). If the incident detection algorithm is to be used to trigger a response, a false alarm rate of over 13 percent would be unacceptable.

Martinez et al. (1994) conducted field trials of an Urban AID system based on computer vision techniques. Field tests included a field trial that contained one complex junction, and field trials that covered four adjacent large junctions and the most important adjacent links. Eight cameras were installed at these locations. A total of 951 incidents were logged in the period from October 93 to March 94. Their duration was less than one minutes for 86 percent of the cases. These incidents were stopped vehicles in one lane disturbing traffic in the same lane, or stopped vehicles in two lanes at the same position, or a stopped vehicle in one lane disturbing the adjacent lane in an entry zone near the junction. Overall detection rate was 92.74 percent with the false alarm rate 24.23 percent. No mean detection time was discussed.

The Urban AID system shows potential for detecting incidents on signalized streets by using different sensor systems. However, the high false alarm rate compared with the algorithm in this research suggested improvement is required in this technology. Also, the mean detection time should be discussed.

Ivan et al. (1995) used the data fusion approach in detecting an incident on urban arterial streets. The data fusion approach obtains data, such as traffic volume, occupancy, and speed from fixed detectors, and observed travel times collected from probe vehicles traveling the street network. These observed data are processed in uniquely developed algorithms for each link to determine the likelihood of an incident. Then the Algorithm Output Fusion Network combines these algorithm outputs using neural network logic. By using INTRAS, a microscopic freeway corridor traffic simulation model, more than 100 simulations were run to generate the training data for a variety of incident and corresponding non-incident conditions. The simulation network was a 5-km section of major arterial streets that contained 8 intersections and 39 loop detectors. A data aggregation interval of 7 minutes (all signals had cycle length of 140 seconds). Incidents were simulated on six different links, at three or four locations on each link, for duration of from 5 to 10 aggregation intervals. These are major incidents of 35 to 70 minute duration. Ten percent of the training data files were selected randomly and set aside for testing the algorithm. The Algorithm Output Fusion Network (the Two Input Network) detected all of the incidents in the testing data with no false alarms. The algorithm misclassified 0.11 percent of the non-incident observations in the training data set.

An additional study by Ivan (1996) with network alternatives was conducted. The alternatives included an Output Memory Network and a Full Network which added input from previous time periods to the current input. These alternatives showed better performance. The Output Memory Network showed a detection rate of 86.11 percent in the training data and 100 percent in the test data with a 0 percent false alarm rate in both data sets. The Full Network showed a 92.59 percent detection rate in the training data and

100 percent in the test data, and a 0 percent false alarm rate in both data sets, respectively.

The mean detection time was not discussed in both studies.

This approach showed good detection and a better false alarm rate (0 percent) in the test data compared to the algorithm in this research. However, the performance should also be evaluated by the mean detection time. The data aggregation time interval of 5 or 7 minutes from fixed detectors is too long to allow an incident detection system to be useful. Also, this algorithm is data intensive. That is, this test used 90 percent of total data as training data to produce the 100 percent detection rate in the other 10 percent of the test data. In comparison, the algorithm in this research used only three hours of data to initialize and stabilize the parameters, resulting in less data dependency.

### **6.1.3 Conclusions of the Research**

The incident detection algorithm in this research shows good potential for use on signalized arterial streets. With less data dependency, this real-time algorithm will be simple and efficient to apply to existing arterial conditions using raw data from existing sensors such as loop detectors. This algorithm does not require special equipment and can be applied to existing arterial conditions, although it is still in the experimental stage. The comparison with other incident detection systems on arterial streets shows good detection rate, good false alarm rate, and reasonable mean detection time for this algorithm.

### **6.2 Discussion on Further Research**

In this section some factors that would improve this incident detection algorithm are discussed. Also, further arterial street incident detection research is discussed.

### **Limitation of a Simulation**

Although the incident detection algorithm in this research shows potential, it is based on simulation. A simulation may be a good alternative when the real field data is not available. However, there are always limitations in the ability of simulation to represent a real world situation. For example, driver's response to a stalled vehicle in a lane would be varying individually. Some drivers may change their route to avoid the incident by taking alternative roadways or some may still drive in that roadway by changing lanes. The rate of diverting drivers may affect the performance of an incident detection system.

One of the variables in the simulation is the "seed number" to generate different traffic patterns. For the same incident conditions, a different seed number will generate a different traffic pattern for that incident scenario. This may result in various incident detection results.

### **An Incident Detection Treatment after an Incident**

In this study, the incident detection algorithm was developed mainly to identify the beginning of an incident for efficient incident management. The pattern of traffic control variables during an incident state are unstable and fluctuate due to the stop and go status. Using these measurements to estimate the flow after termination of the incident (i.e., normal traffic flow) may increase the chance of a false alarm shortly after the incident termination. Therefore, it is probably advantageous to use measurements from a time period prior to the incident to eliminate false alarm chances after the incident termination. This would be implemented by storing the prior measurements and corresponding

parameter values in memory, and using them after the incident termination as the new process begins.

### **Detector Location, the Number of Detectors, and New Detectors**

It is well known that the location of detectors is very important to an incident detection algorithm, especially on long links. Existing detector location is usually at the downstream end of a link, resulting in full occupancy during the red phase of a signal. Alternative detector locations are at the upstream end of a link as used in Europe, or at the middle of a link.

The best location for any link could be found by simulating various incidents against various detector locations. That is, the relationship among mean detection time, detection rate, and false alarm rate could be found from the simulated data. The best locations would be dependent on various traffic conditions such as A.M. peak hour, P.M. peak hour, and off-peak hour volumes.

The more detectors available the better the performance of an incident detection system. Some of incident detection systems on arterial streets, such as Chen's (1994) and Ivan's (1995), obtain traffic measurements from multiple detectors and various sources. Using information from multiple sensors enhances an incident detection system. If the cost is justified by the benefits, it is worth considering this approach.

Martinez et al. (1994), and by Parkany, and Bernstein (1993) have demonstrated that new technology-based sensors may improve an incident detection system. A video-image process or a VRC (or "tags") technology can provide a detailed information on the traffic state or an individual vehicle that can not be obtained from conventional detectors. This

type of information suggests different approaches to an incident detection system. To use a new-technology based sensor, the cost and benefit should be justified as well.

### **Efficient On-Line Implementation**

The algorithm in this research was tested with field collected and simulated data. In implementing an on-line detection system for an urban network, it will be necessary to construct a computing structure to run the algorithm in multitasking because the algorithm is run for all-detector stations at the same time. A suitable computing system will require a fast and efficient computer.

### **Emergency Hot-Lines**

Nothing is more accurate and faster than a driver who witnesses an incident occur describing the incident. Many drivers now use a cellular phone or a car phone. Reports from drivers may soon be quicker than an incident detection system. Further research should include the possible use of this alternative.

## **APPENDICES**

## **APPENDIX A**

## APPENDIX A

### DESCRIPTION OF TRAFFIC VOLUME FOR EACH NODE IN THE NETWORK

**Table A Descriptions of Traffic Volume for Each Node in the Network**

Node No.	East Bound			West Bound			North Bound			South Bound		
	T	R	L	T	R	L	T	R	L	T	R	L
2	576	33*	152	920	37*	22	36	203*	85	143	235	126
3	664	311	301	1128	62*	50	224	84	392	90	350*	60
4	1031	22*	39	1664	112	94	11	96	N/A	10	32*	N/A
5	897	28*	10*	1628	10*	68	18	20*	99*	10	12*	23
6	750	40*	157	1165	174*	226	303	89*	181	253	126*	79
7	975	706	35	1284	10*	44	62	107*	32	28	24*	47*
8	311	10	N/A	890	N/A	594*	N/A	617	N/A	N/A	N/A	N/A
9	382	33*	N/A	863	N/A	27	N/A	35*	77*	N/A	N/A	N/A
10	391	12*	17*	912	19*	10*	21	10*	15*	14	28*	11*
11	340	30*	11*	926	19*	10*	70	57*	71*	108*	29*	12
12	304	20*	10*	842	10*	174*	16	51*	18*	34	35*	13*

T: Through Traffic

R: Right Turn Traffic

L: Left Turn Traffic

\*: Shared Lane Traffic with Through Traffic

## **APPENDIX B**

**APPENDIX B****DESCRIPTION OF GEOMETRIC CONFIGURATIONS FOR NETWORK LINKS****Table B Description of Geometric Configurations for Network Links**

Link	Length (ft)	No. of Through Lanes*	East to West		West to East	
			Length of Left Turn Bay (ft)	Length of Right Turn Bay (ft)	Length of Left Turn Bay (ft)	Length of Right Turn Bay (ft)
1,2	3000	2	800	N/A	N/A	N/A
2,3	4000	2	800	N/A	800	N/A
3,4	2100	2	200	200	200	200
4,5	530	2	200	200	200	N/A
5,6	1450	2	600	N/A	N/A	N/A
6,7	3960	3	400	N/A	600	N/A
7,8	400	3	200	N/A	150	150
8,9	2900	2	N/A	N/A	N/A	400
9,10	926	2	N/A	N/A	N/A	N/A
10,11	2776	2	N/A	N/A	N/A	N/A
11,12	1200	2	N/A	N/A	N/A	N/A

\*The number of turning bay lanes is one.

## **APPENDIX C**

## APPENDIX C

## DESCRIPTION OF SURFACE STREET TURNING MOVEMENTS

Table C Description of Surface Street Turning Movements

Upstream Node	Downstream Node	% of Traffic Turning Left	% of Traffic Going Thru	% of Traffic Turning Right
1	2	3	92	5
2	1	0	100	0
32	3	4	91	5
32	2	20	76	4
43	4	5	89	6
43	3	26	59	15
54	5	4	96	0
54	4	4	94	2
65	6	13	67	10
65	5	0	97	3
76	7	3	97	0
76	6	17	79	4
87	8	40	60	0
87	7	1	95	4
98	9	3	97	0
98	8	0	97	3
509	10	1	97	2
509	9	0	92	8
510	11	1	97	2
510	10	4	93	3
521	12	17	82	1
521	11	3	89	8

**Table C (cont'd)**

Upstream Node	Downstream Node	% of Traffic Turning Left	% of Traffic Going Through	% of Traffic Turning Right
12	13	0	100	0
13	12	3	91	6
52	2	25	28	47
22	2	26	11	63
53	3	12	18	70
23	3	70	18	12
14	4	0	10	90
24	4	0	10	90
15	5	62	14	24
25	5	72	13	15
16	6	17	55	28
26	6	31	53	16
17	7	48	28	24
27	7	16	31	53
28	8	0	0	100
29	9	69	0	31
110	10	21	26	53
30	10	33	46	21
111	11	8	72	20
31	11	36	36	28
112	12	16	41	46
62	12	21	19	60

## **APPENDIX D**

**APPENDIX D****DESCRIPTION OF PRETIMED SIGNAL INTERVAL FOR EACH NODE****Table D Description of Pretimed Signal Interval for Each Node**

Node	Offset	Interval 1	Interval 2	Interval 3	Interval 4	Interval 5	Interval 6	Interval 7	Interval 8
2	119	17	4	44	4	24	4	19	4
3	49	21	4	41	4	26	4	16	4
4	110	97	4	1	13	4	1		
5	108	99	4	1	11	5			
6	60	20	4	50	4	16	4	18	4
7	4	91	4	1	19	5			
8	7	92	4	20	4				
9	36	16	4	2	94	4			
10	53	12	4	2	98	4			
11	108	19	4	93	4				
12	14	13	4	99	4				

## **LIST OF REFERENCES**

## LIST OF REFERENCES

- Abdulhai, Baher, and S. G. Ritchie. 1995 Performance of Artificial Neural Networks for Incident Detection in ITS. *Transportation Congress, Volume 1, Civil Engineers-Key to the World's Infrastructure*, Proceedings of the Conference, American Society of Civil Engineers, New York. pp. 227-238.
- Ahmed, Samir A. 1983. Stochastic Processes in Freeway Traffic, I. Robust Prediction Models, *Traffic Engineering & Control*, June/July, pp. 306-310, 314.
- Ahmed, Mohamed S., and Allen R. Cook. 1979. Analysis of Freeway Traffic Time-Series Data by Using Box-Jenkins Techniques. *Transportation Research Record 722*, TRB, National Research Council, Washington, D. C., pp. 1-9.
- Ahmed, Samir. A., and Allen R. Cook. 1980. Time Series Models for Freeway Incident. *Transportation Engineering Journal of ASCE*, ASCE, November, pp. 731-745.
- Ahmed, Samir A., and Allen R. Cook. 1982. Discrete Dynamic Models for Freeway Incident Detection Systems. *Transportation Planning and Technology*, Vol. 7. Pp. 231-242.
- Al-Sahili, Khaled A., and William C. Taylor. 1996. Bus Preemption Signal (BPS) - An Application of an Advanced Public Transportation System (APTS), *Michigan State University*, East Lansing.
- Balke, Kevin N. 1993. An Evaluation of Existing Incident Detection Algorithms. *Research Report 1232-20. Texas Transportation Institute*, College Station, TX. November.
- Barbaresso, James C. 1993. Overview of the FAST-TRAC IVHS Program. *Pacific Rim TransTech Conference*, Proceedings Vol. I, American Society of Civil Engineers, New York, July 25-28, pp. 134-137.
- Bell, M. G. H., Dr., and B. Thancanamootoo, Dr. 1988. Automatic Incident Detection within Urban Traffic Control Systems. *Roads and Traffic 2000*, Vol. 4/2, Proceedings, Berlin 6-9, page 35-39.

Bhandari, Nikhil, Frank S. Koppelman, Joseph L. Schofer, Vaneet Sethi, and John N. Ivan. 1995. Arterial Incident Detection Integrating Data from Multiple Sources. *Transportation Research Record 1510*, Washington, D. C., pp 60-69.

Bretherton, R. D., and G. T. Bowen. 1991. Incident Detection and Traffic Monitoring in Urban Areas. Drive Conference, Brussels, Belgium, *Advanced Telematics in Road Transport*, Vol. I., pp 740-751.

Chang, Edmond Chin-Ping. 1992. A Neural Network Approach to Freeway Incident Detection. *Vehicle Navigation & Information Systems*, Oslo, Norway. September 2-4. pp. 641-647.

Chang, Edmond Chin-Ping and Kunhuang Huarng. 1993. Incident Detection Using Advanced Technologies. Preprint 930943, *The 72nd Annual Meeting Transportation Research Board*, Washington, D. C. January.

Chassiakos, Athanasios P. 1992. Spatial-Temporal Filtering and Correlation Techniques for Detection of Incidents and Traffic Disturbances. *Doctoral Dissertation*, December, University of Minnesota,

Chassiakos, Athanasios P., and Yorgos J. Stephanedes. 1993. Smoothing Algorithms for Incident Detection. *Transportation Research Record 1394*, TRB, National Research Council, Washington, D. C., pp. 8-16.

Chen, Chao-Hua. 1994. A Dynamic Real-Time Incident Detection System for Urban Arterials. *Doctoral Dissertation*, University of Maryland. College Park. Maryland.

Chen, Chao-Hua, and Gang-Leng Chang. 1992. A Review of Recent Freeway Incident Detection Algorithms. *Report No. DTFH61-92-R-00122*, Department of Civil Engineering, University of Maryland, June 5, College Park, MD 20742.

\_\_\_\_\_. 1993. A Dynamic Real-Time Incident Detection System for Urban Arterials-System Architecture and Preliminary Results. *Proceedings of Pacific Rim TransTech Conference*, Vol. 1, American Society of Civil Engineers, July 25-28, Seattle, Washington, pp. 98-104.

Cheu, R. L., S. G. Ritchie, and W. W. Recker. 1991. Investigation of a Neural Network Model for Freeway Incident Detection. *The Second International Conference on the Application of Artificial Intelligence Techniques to Civil and Structural Engineering*, Oxford. England, September.

Cohen, S. 1994. Comparative Assessment of Conventional and New Incident Detection Algorithms. *Road Traffic Monitoring and Control. Conference*, Publication No. 391, April 26-28, pp. 156-159.

Cohen, S, and Z. Ketselidou. Unknown Date. DAISI: A Calibration Tool for Automatic Incident Detection Algorithms. Application on the Paris Ringway. *Unknown Source*.

Collins, J. F. 1977. Incident Detection Experiments on the Boulevard Peripherique in Paris. TRRL Supplementary Report 362.

Collins, J. F. 1983. Automatic Incident -Experience with TRRL Algorithm-HIOCC. TRRL Supplementary Report 775.

Collins, J. F., C. M. Hopkins, and J. A. Martin. 1979. Automatic Incident Detection-TRRL Algorithm HIOCC and PATREG. TRRL Supplementary Report 526.

Cook, Allen R., and Donald E. Cleveland. 1974. Detection of Freeway Capacity-Reducing Incidents by Traffic-Stream Measurements. *Highway Research Record 495*, Highway Research Board, National Research Council, Washington, D. C., pp. 1-11.

Dailey, Daniel J. 1993. Improved Error Detection for Inductive Loop Sensors. Report Number WA-RD 300.1, Washington State Transportation Center. May.

Dudek, Conrad L., and Carroll J. Messer. 1973. Detecting Stoppage Waves for Freeway Control. *Highway Research Record 469*, Highway Research Board, National Research Council, Washington, D. C., pp. 1-15.

Dudek, Conrad L., Carroll J. Messer, and Nelson B. Nuckles. 1974. Incident Detection on Urban Freeways. *Highway Research Record 495*, Highway Research Board, National Research Council, Washington, D. C., pp. 12-24.

Dudek, Conrad L., and Gerald L. Ullman. 1992. Freeway Corridor Management. *National Cooperative Highway Research Program Synthesis of Highway Practice 177*, March, Washington, D. C.

Federal Highway Administration. 1995. *TRAF User Reference Guide*, Version 5. March.

Gall, Ana I., and Fred L. Hall. 1989. Distinguishing between Incident Congestion and Recurrent Congestion: A Proposed Logic. *Transportation Research Record 1232*, TRB, National Research Council, Washington, D. C., pp. 1-8.

Giuliano, Genevieve. Incident Characteristics, Frequency, and Duration on a High Volume Urban Freeway. *Transportation Research*, Part A, Vol. 23A, No. 5, 1989, pp. 387-396.

Goolsby, M. E. 1971. Influence of Incidents on Freeway Quality of Service. *Highway Research Record 349*, pp. 41-46.

Grewal, Mohinder S., and Angus P. Andrews. 1993. *Kalman Filtering Theory and Practice*. Prentice Hall, New Jersey

Hall, Fred L. 1987. An Interpretation of Speed-Flow-Concentration Relationships using Catastrophe Theory. *Transportation Research*, Part A, Vol. 21A, No. 3, pp. 191-201.

Hall, F. L., Brian L. Allen, and Margot A. Gunter. 1986. Empirical Analysis of Freeway Flow-Density Relationships. *Transportation Research*, Part A, Vol. 20A, No. 3, pp. 197-210.

Hall, F. L., Yong Shi, and Gerge Atala. 1993. On-Line Testing of the McMaster Incident Detection Algorithm under Recurrent Congestion. *Transportation Research Record 1394*, TRB, National Research Council, Washington, D. C., pp. 1-7.

Hoose, Neil. 1994. Incident Detection and Traffic Surveillance using the IMPACTS Video Analysis System. *Traffic Technology International '94*. pp. 94-99.

Hoose, Neil, M.-A. Vicencio and X. Zhang. 1992. Incident Detection in Urban Roads Using Computer Image Processing. *Traffic Engineering and Control*, April, pp. 236-244.

Hughes Aircraft and JHK & Associates, Direct Project, Incident Detection Issues. 1992 *Report for Michigan Department of Transportation*, MDOT-92-0413, August, Washington, D. C.

Ivan, John N. 1996. Neural Network Representations for Arterial Street Incident Detection Data Fusion. Preprint 960096, *Transportation Research Board 75th Annual Meeting*, January 7-11, Washington, D. C.

Ivan, John N., Joseph L. Schofer, Chandra R. Bhat, Pen-Chi Liu, Frank S. Koppelman, and Alvin Rodriguez. 1993. Arterial Street Incident Detection Using Multiple Data Sources: Plans for ADVANCE. *Pacific Rim TransTech Conference*, July 25-28, Seattle, Washington, USA, Proceedings Vol. I, Advanced Technologies, pp. 429-435.

Ivan, John N., Joseph L. Schofer, Frank S. Koppelman, and Lina L. E. Massone. 1995. Real-Time Data Fusion for Arterial Street Incident Detection Using Neural Networks. *Transportation Research Record 1497*, Washington, D. C., pp 27-35.

Judycki, D. C., and J. Robinson. 1991. Freeway Incident Management. Technical Papers from ITE's 1990, 1989, and 1988 Conference, contained in *Massachusetts Incident Management Conference Proceeding*, DOT-T-92-05, June 6. pp. 359-368.

Kalman, R. E. 1960. A New Approach to Linear Filtering and Prediction Problems. *Journal of Basic Engineering*, March, pp. 35-45.

Kelly, David. 1991. Results of a Field Trial of the IMPACTS Image Processing System for Traffic Monitoring. *Vehicle Navigation & Information Systems Conference Proceedings*, P-253, Part 1. Society of Automotive Engineers, October, pp. 151- 167.

Knobel, H. C., and E. D. Helfenbein. 1976. Development and Testing of Incident Detection Algorithms. Final Report, Volume 4: Program Documentation for Calibration, Evaluation, and Implementation, FHWA-RD-76-22, *Technology Service Corporation*, Santa Monica, California, April.

Lam, Joseph K., and D. Bowen Tritter. 1994. Innovative Technologies in the COMPASS Advanced Traffic Management System. *Traffic Technology International '94*, pp. 44-49.

Lari, A., Christianson, D., and S. Porter. 1982. I-35W Incident Management and Impact of Incidents on Freeway Operations. *Minnesota Department of Transportation*, January.

Levin, Moshe, and Gerianne M. Krause. 1978. Incident Detection: A Bayesian Approach. *Transportation Research Record 682*, TRB, National Research Council, Washington, D. C., pp. 52-58.

\_\_\_\_\_. 1979a. Evaluation of Incident Detection Algorithms. *Report No. FHWA/IL/PR-085*, Illinois Department of Transportation, Bureaus of Materials and Physical Research, December, Springfield, Illinois.

\_\_\_\_\_. 1979b, Incident-Detection Algorithms, Part 1. Off-Line Evaluation. *Transportation Research Record 722*, TRB, National Research Council, Washington, D. C., pp. 49-58.

\_\_\_\_\_. 1979c. Incident-Detection Algorithms, Part 2. On-Line Evaluation. *Transportation Research Record 722*, TRB, National Research Council, Washington, D. C., pp. 58-64.

\_\_\_\_\_. 1979d. A Probabilistic Approach to Incident Detection on Urban Freeways. *Traffic Engineering and Control*, March, pp. 107-109.

Martinez, J. J., Guillen S., Sellam S., Boulmakoul A., Boilot F., Diaz E., Ferris R., and Cavero V. 1994. Evaluation of a Computer Vision Based Automatic Incident Detection System in an Urban Context. *World Congress on Application of Transport Telematics and Intelligent Vehicle-Highway Systems, Toward an Intelligent Transportation System*, Vol. 2.

Masters, Philip H., Joseph K. Lam, and Kam Wong. 1991. Incident Detection Algorithms for COMPASS - An Advanced Traffic Management System. *Vehicle Navigation and Information Systems Conference Proceedings*, Part 1, Society of Automotive Engineers, Inc., October, Warrendale, PA, pp. 295-310.

McTrans Center. 1995. *Highway Capacity Software*, Release 2.1b, University of Florida, Gainesville, FL.

Michalopoulos, Panos G. and Richard D. Jacobson. 1992. Field Implementation of the Minnesota Video Detection System. *The 3rd International Conference on Vehicle Navigation & Information Systems*, Oslo, Norway. September 2-4. pp. 105-111.

Michalopoulos, Panos G., Richard D. Jacobson, Craig A. Anderson, and Thomas B. DeBruycker. 1993. Automatic Incident Detection through Video Image Processing. *Traffic Engineering & Control*, February. pp. 66-75.

Montgomery, Douglas C., Lynwood A. Johnson, and John S. Gardiner. 1990. *Froecasting & Time Series Analysis*, Second Edition, McGraw-Hill, Inc. New York

Parkany, A. Emily, and David Bernstein. 1993. Using VRC Data for Incident Detection. *Pacific Rim. TransTech Conference*, Proceedings, Volume I. Advanced Technologies. ASCE Third International Conference on Applications of Advanced Technologies in Transportation Engineering. Seattle. Washington, USA. July 25-28. pp. 63-68.

\_\_\_\_\_. 1995. Design of Incident Detection Algorithms Using Vehicle-to-Roadside Communication Sensors. *Transportation Research Record 1494*, TRB, National Research Council, Washington, D. C., pp. 67-74.

Payne, H. J., E. D. Helfenbein, and H. C. Knobel. 1976. Development and Testing of Incident Algorithms, Research Methodology and Detailed Results, *Final Report*, FHWA-RD-76-20, Volume 2. April.

Payne, H. J., and S. C. Tigor. 1978. Freeway Incident-Detection Algorithms Based on Decision Trees with States. *Transportation Research Record 682*, TRB, National Research Council, Washington, D. C. pp. 30-37.

Persaud, Bhagwant N., and Fred L. Hall. 1989. Catastrophe Theory and Patterns in 30-Second Freeway Traffic Data. Implications for Incident Detection. *Transportation Research*, Part A: General, Vol. 23, No. 2, March, pp. 103-113

Persaud, Bhagwant N., F. L. Hall, and Lisa M. Hall. 1990. Congestion Identification Aspects of the McMaster Incident Detection Algorithm. *Transportation Research Record 1287*, TRB, National Research Council, Washington, D. C., pp. 167-175.

Ritchie, Stephen G., and Ruey L. Cheu. 1993. Simulation of Freeway Incident Detection using Artificial Neural Networks. *Transportation Research*, Part C, Volume 1., No. 3. pp. 203-217.

Roper, David H. Freeway Incident Management. *National Cooperative Highway Research Program Synthesis of Highway Practice 156*, National Research Council, December 1990, Washington, D. C.

Roseman, David, and Sean Skehan 1995, Automated Arterial Incident Detection Santa Monica Freeway Smart Corridor. *Institute of Transportation Engineers 65th Annual Meeting*, Compendium of Technical Papers, page 27-31.

Sakasita, Masami, De Leuw, Cather and Company, and Adolf D. May. 1975. Development and Evaluation of Incident-Detection Algorithms for Electronic-Detector Systems on Freeways. *Transportation Research Record 533*, TRB, National Research Council, Washington, D. C. pp. 48-63.

Sellam S. and A. Boulmakoul. 1994, Intelligent Intersection: Artificial Intelligence and Computer Vision Techniques for Automatic Incident Detection. *Artificial Intelligence Applications to Traffic Engineering*, pp. 189-200.

Stephanedes, Yorgos J., and Athanasios P. Chassiakos. 1993a. Application of Filtering Techniques for Incident Detection. *Journal of Transportation Engineering*, Vol. 119, No. 1, ASCE, Jan/Feb, pp. 13-26.

\_\_\_\_\_. 1993b. *Transportation Research*, Part C, Vol. 1, No. 3, pp. 219-233.

Stephanedes, Yorgos J., Athanasios P. Chassiakos, and Panos G. Michalopoulos. 1992. Comparative Performance Evaluation of Incident Detection Algorithms. *Transportation Research Record 1360*, TRB, National Research Council, Washington, D. C., pp. 50-57.

Stephanedes, Yorgos J., and George Vasilakis. 1995, Accident Detection at Intersections for ITS. *Transportation Congress*, Vol. I, Civil Engineers - Key to the World's Infrastructure, Proceedings of the 1995 Conference, San Diego, California, Oct 22-26, American Society of Civil Engineers, page 239-244.

Tarko, Andraej, Jeffrey Tsai, and Nagui M. Roupail. 1993. Detection of Traffic Congestion using Fuzzy Operator Logic in ADVANCE-like Systems. *Proceedings of the Intelligent Vehicles '93 Symposium*, IEEE Industrial Electronics Society, July 14-16, Tokyo, Japan, pp. 189-194.

Tignor, Samuel C., and H. J. Payne. 1977. Improved Freeway Incident Detection Algorithms. *Public Roads*, Vol. 41, No. 1, June, pp. 32-40.

Urbanek, G. L., and Rogers. Alternative Surveillance Concepts and Methods for Freeway Incident Management - Volume 1: Executive Summary. *Report No. FHWA RD-77-58*, March 1978

Wallace, Courage, and Hadi. 1991. *TRANSYT-7F, Users Guide*, Volume 4 in a Series: Methodology for Optimizing Signal Timing, Federal Highway Administration, December.

Willsky, A. S. 1976. A Survey of Design Methods for Failure Detection in Dynamic Systems. *Automatica*, Vol. 12, pp. 601-611.

Willsky, A. S., E. Y. Chow, S. B. Gershwin, C. S. Greene, P. K. Houpt, and A. L. Kurkjian. 1980. Dynamic Model-Based Techniques for the Detection of Incidents on Freeways. *IEEE Transaction on Automatic Control*, Vol. AC-25, No.3, June, pp. 347-359.

Wirasinghe, S. C. 1978. Determination of Traffic Delays from Shock-Wave Analysis. *Transportation Research*, Vol. 12, pp. 343-348.